Identification of immune-suppressors of Diamond-back Moth (DBM)

Dr Richard Glatz
South Australia Research &
Development Institute (SARDI)

Project Number: VG08048

VG08048

This report is published by Horticulture Australia Ltd to pass on information concerning horticultural research and development undertaken for the vegetables industry.

The research contained in this report was funded by Horticulture Australia Ltd with the financial support of the vegetables industry.

ISBN 0 7341 2704 9

Published and distributed by:
Horticulture Australia Ltd
Level 7
179 Elizabeth Street
Sydney NSW 2000
Telephone: (02) 8295 2300
Fax: (02) 8295 2399

Horticulture Australia

HAL Project VG08048

(completed July 2011)

Identification of immune suppressors of Diamondback Moth (DBM)

Glatz *et al.**

HAL
Horticulture Australia

The University Of Queensland

Government of South Australia

SARDI
SOUTH AUSTRALIAN RESEARCH AND DEVELOPMENT INSTITUTE

HAL Project No. VG08048

Project Leader: Richard Glatz
GPO Box 397 ADELAIDE SA 5001
Phone: 08 8303 9539
Fax: 08 8303 9542
richard.glatz@sa.gov.au

Chief Investigator: Tamara Cooper
Senior Collaborator: Sassan Asgari
Collaborator: Kayvan Etebari
Collaborator: Greg Baker
Collaborator Cate Paull

* For correct acknowledgement of authors, please cite this report as follows:
Cooper T, Glatz R, Asgari S & Etebari K. (2011) Horticulture Australia Ltd. Project VG08048 Final Report. *Investigation of Immune Suppressors of Diamondback moth (DBM)*; 114pp.

This report summarises all experiments and associated data arising from the HAL-funded project VG08048 *Identification of Immune Suppressors of Diamondback Moth (DBM).* The purpose of the work was to examine wasp-related proteins to find compounds that could potentially be developed as immune-suppressive controls targeting Diamondback moth and other brassica vegetable caterpillars. Ultimately, these compounds are expected to increase the sustainability and efficiency of integrated pest management practices within vegetable industries.

This project has been funded by HAL using the vegetable industry levy and matched funds from the Australian Government. The project was a collaboration between HAL, The South Australian Research and Development Institute (SARDI) and The University of Queensland.

HAL
Horticulture Australia

THE UNIVERSITY OF QUEENSLAND

Government of South Australia

SARDI
SOUTH AUSTRALIAN RESEARCH AND DEVELOPMENT INSTITUTE

Contents

Media Summary

In Australia, Diamondback moth (DBM) is the most serious pest of Brassica vegetables and significant resources are expended to manage it. However, the main approach of using insecticidal toxins is problematic in terms of expense, public perception and loss of efficacy through development of resistance in DBM. Therefore, there is a continual need to refine our development and use of commercial insecticides.

With this in mind, SARDI collaborated with University of Queensland to undertake HAL-funded research (through vegetable industries) investigasting new insecticidal compounds. Researchers proposed that parasitic wasps that attack DBM, effectively contained a range of novel insecticidal compounds in their venom, and in viruses within their venom. The wasp *Diadegma semiclausum*, was investigated as it causes immune-suppression and developmental problems in DBM larvae that it parasitises. The primary goal was to investigate the proteins that *Diadegma* uses to produce these effects, to identify new compounds for use in a commercial pest management context in vegetables.

We found that a range of wasp venom and virus proteins are active in attacking immune cells in pest caterpillars, and further, we now have a good understanding of the how the immune system of DBM responds to parasitisation. These pieces of information effectively identify a pool of novel immune-suppressive bioactive compounds, and a pool of molecular targets within larval DBM, respectively. We have disseminated much of this information throughout the scientific community through international peer-reviewed journals.*

This research suggests that immune-suppression could be utilised as part of integrated pest and resistance management strategies, for Brassica caterpillar pests. In addition, as the immune-suppressive compounds are not inherently "toxic" *per se*, they would have less environmental impact and be seen as a "greener" option compared to traditional insecticides and/or could be used synergistically with traditional insecticides and other exisiting management options. We estimate that a further 1-2 years research would be needed to provide the level of understanding (of the compounds) required to investigate commercial development with relevant partners such as agrichemical companies.

* Cooper, T., Bailey-Hill, K., Leifert, W.R., McMurchie, E.J., Asgari, S. and Glatz, R.V. (2011). Identification of an *in vitro* interaction between an insect immune-suppressor protein (CrV2) and Gα proteins. *The Journal of Biological Chemistry*, 286, 10466-10475.

* Etebari, K., Palfreyman, R., Schlipalius, D., Nielsen, L., Glatz, R. and Asgari, S. (2011). Deep sequencing-based transcriptome analysis of *Plutella xylostella* larvae parasitized by *Diadegma semiclausum*. *BMC Genomics* (in press).

Technical Summary

In Australia, *Plutella xylostella* (Linnaeus, 1758) or Diamondback moth (DBM), is the most serious pest of Brassica vegetables and significant resources are expended to manage it. However, the main approach of using insecticidal toxins, is problematic in terms of expense, public perception and loss of efficacy through development of resistance in DBM. Therefore, there is a continual need to refine the development and use of commercial insecticides.

With this in mind, The South Australian Research and Development Institute (SARDI) collaborated with University of Queensland to undertake HAL-funded research (through vegetable industries) to investigate new insecticidal compounds. Researchers proposed that parasitic wasps targeting DBM contained novel insecticidal compounds in their venom, and in viruses within the venom. The wasp *Diadegma semiclausum* (Hellen, 1949) was investigated as it causes immune-suppression and developmental problems in DBM larvae it parasitises. The primary goal was to investigate bioactives that *Diadegma* uses to produce these effects, as potential new compounds for commercial pest management in vegetables.

Main research priorities were:

- investigation of effect of total wasp venom on blood cells of DBM and *Pieris rapae* (Linnaeus, 1758), known as Cabbage white butterfly (CWB)
- production of a gene library of the wasp venom gland
- screening of the gene library for venom genes
- investigating the function of venom genes in suppressing caterpillar immunity
- identifying immune genes altered in DBM larvae, by parasitisation
- identifying *Diadegma* ichnovirus (*Ds*IV) genes suppressing DBM immunity
- continue investigating CrV2, a previously identified protein causing immune-suppression in DBM/CWB

Initial experiments confirmed that total wasp venom prevented spreading of blood cells (haemocytes) of DBM and CWB, which is a key immune function. Some venom components were entering cells and reduced nucleus size was also noted. Venom also reduced viability of cultured *Sf*9 insect cells. Total wasp venom was found to be a complex mixture of between 10-20 proteins.

Subsequently, a gene library was produced from the wasp venom gland, leading to identification of 9 putative venom genes/proteins. From these 9 proteins, a range of predicted active peptides were artificially synthesised for functional experiments. Attempts to manufacture the complete venom proteins in cell culture were problematic due to the unusual characteristics of the proteins, however, production and purification of two complete proteins was achieved.

The venom proteins showed features similar with other known toxins, however, they were sufficiently novel that their function was not able to be determined through similarities with known proteins. The synthesised peptides displayed effects such blood cell penetration, toxicity against caterpillar blood cells, and toxicity against cultured *Sf*9 insect cells. None of the peptides had antibacterial activity which is a common property of venoms. These data suggest that venom proteins of *Diadegma* are evolved from known venom proteins but have undergone changes to produce immune-suppression rather than acute effects such as paralysis. Thus, further research will be required to fully understand how the venoms work.

Deep sequencing experiments produced a list of DBM larval immune genes which are altered by *Diadegma* parasitisation. Additionally, a range *Ds*IV genes was identified in parasitised DBM larvae; some have assigned immune-suppressive functions and several are novel virus genes of unknown function. This fundamental information is in press with *BMC Genomics* and will improve the collective understanding of DBM immunity, and how we can modulate it for pest management.

We also confirmed an interaction between the previously discovered immune-suppressive CrV2 protein and an important cell-signalling molecule known as Gα. We also discovered that CrV2 enters a specific class of CBW blood cell (granulocytes). This is intriguing as it represents a novel mode of immune-suppression in insects and the data were published in *The Journal of Biological Chemistry*. The publication of scientific articles is important as they stimulate/inform research by various groups working on brassica pests globally.

This project generated fundamental information about how venom is composed, its broad effects on caterpillar blood cells, and DBM/*Ds*IV genes associated with immune regulation. The key output for Australian vegetable growers is the series of identified immune-related genes/compounds, which could potentially be developed for commercial use as field-ready insect controls. We recommend that a further 12-24 months research should be undertaken prior to consultation with a commercial partner for assessment and development of these compounds. Future research would focus on:

- screening for further undetected proteins
- isolating new virus proteins for analysis
- targeting partially characterised, promising proteins/peptides for detailed functional studies
- investigate CrV2 mode-of-action to assess development potential
- investigate other methods of DBM immune regulation based on deep sequencing data

Introduction

In Australia and globally, the Diamondback moth (DBM), *Plutella xylostella* (Lepidoptera: Plutellidae) is a destructive pest of the plant family Brassicaceae, which includes important crops such as cabbages, broccoli, cauliflower and canola (1). Historically, DBM has been controlled using synthetic and biological pesticides, however, instances of resistance to both classes of pesticide have been reported raising concerns over the sustainability of chemical control strategies for DBM and the impact on natural enemy populations (2-4).

Integrated pest management strategies have become increasingly important in controlling DBM, and *Diadegma semiclausum* (Hymenoptera: Ichneumonidae) is an important biological control agent in this regard (1,5). *D. semiclausum* is an endoparasitoid (developing inside its host) of the larval stage of DBM, depositing eggs into DBM larvae along with maternal secretions that include venom and a polydnavirus (PDV) known as the *D. semiclausum* ichnovirus (*Ds*IV) (6). *Diadegma* is a koinobiont and feeds on host hemolymph (blood) and "non-essential" tissues while the DBM also continues to feed and develop. It is not until the DBM larva has puapated that it has almost entirely been consumed by the wasp larva which then pupates to emerge as an adult wasp. Symptoms of parasitisation by *D. semiclausum* include inhibition of host growth, host castration, changes in metabolism and a reduction in host haemocytes (blood cells) (5,7,8). *Ds*IV has been observed assembling in the nuclei of calyx (part of the ovary) cells of female wasps and then budding into the lumen of the ovaries of *D. semiclausum* (6). However, little molecular characterisation of the effects of PDV or venom has been performed for *D. semiclausum* although venom proteins and those produced by PDVs have been described from other parasitoid wasp species.

Venoms from parasitoid wasps are produced in a specialised venom gland that is associated with the reproductive system of female wasps. Venom from ectoparasitoid wasps (those developing outside their host), and endoparasitoid wasps without a PDV, have been associated with paralysis, antimicrobial and proteolytic activities while the physiological effects of venom from endoparasitoids that produce a PDV appear more subtle, particularly in ichneumonids (9) such as *Diadegma*. Similarities between venom proteins and proteins produced by PDVs have been noted, as have independent and synergistic effects between venom and PDVs (9). The PDV of *Cotesia rubecula* requires venom for successful expression of viral proteins (10) and the venom of *C. melanoscela* has been demonstrated to facilitate uncoating of the PDV particle *in vitro* and to be involved with virus persistence *in vivo* (11). It has also been proposed that venom is present to protect the wasp egg from the host immune system in the period before expression of the PDV genes and some venom proteins have been shown to affect immune functions of the host. *C. rubecula* venom has been found to contain an inactive serine proteinase homolog, and a small protein structurally similar to kunitz-type proteinase inhibitors and w-atracotoxin-HV1A from the funnel web spider, that inhibits melanisation. A serpin from the venom of *Leptopilina boulardi* has also been shown to target the phenoloxidase cascade of its *Drosophila* host (12). A venom calrecticulin has also been identified from *C. rubecula* that is associated with the PDV particle and has been demonstrated to prevent haemocyte spreading and encapsulation (13).

The venoms of only a few ichneumonid wasps have been investigated in detail to date. Venom of *Pimpla turionellae* was reported to display paralytic, cytoxic and cytolytic effects and was found to contain bioacitves such as melittin-like protein, apamin and noradrenalin along with several proteins including phospholipases (14,15). *Pimpla hypochondriaca* does not have a PDV and relies solely on venom which has been shown to down-regulate the host immune system, and was demonstrated to

reduce the occurrence and extent of encapsulation (16), which the immune system performs against foreign objects. This venom was also found to have an effect on the respiratory pattern of the host pupae (16) and to contain some antimicrobial properties (17). Sequencing of cDNA libraries generated from the venom gland have identified genes for putative secreted venom proteins by the presence of a signal peptide at the N-terminus. N-terminal sequencing has also confirmed the presence of serine protease, trehalase and laccase homologs as well as other proteins such as pimplin that have not shown close sequence identity to other protein sequences in the GenBank database (18-20). The venom of *Tranosema Rostrale* has also been investigated but no effects on melanisation or host developments were observed (21,22). The venom of *Campoletis sonorensis* shares epitopes with expression products from its polydnavirus (23). However, *C. sonorensis* was able to successfully parasitise hosts when venom apparatus had been surgically removed (24).

Characterisation of parasitoid venom proteins and polydnavirus expression products will aid our understanding of the parasitoid-host interaction. Relatively little is known of the biochemical pathways and protein interactions involved with the manipulation of host/pest physiology and suppression of host/pest immune systems. Higher understanding of these processes may allow their exploitation and lead to the discovery of novel molecules for biotechnology applications, particularly useful for agriculture. Parasitoid venom and polydnavirus proteins will have developed a high affinity and selectivity for their biological targets and can be chemically synthesised or recombinantly produced making them attractive leads as potential novel insecticides. More ambitiously, transgenic expression of appropriate proteins could provide new strategies for protecting crops from insect pests. Venom and polydnavirus proteins provide a pool of compounds that could specifically control pest species while being gentler to beneficial insects and benign to the environment. They are also likely to use new modes of action to control pests increasing the weaponry available to combat pests and insecticide resistance. Furthermore, tolerance to *Bacillus thuringiensis* toxin, a commonly used biopesticide against DBM, has recently been correlated with an elevated bollworm immune response (25) suggesting that immune-suppressants could also increase the effectiveness and lifespan of current control strategies, or act synergistically with them.

Against this background the concept for this current project was formed. We aimed to isolate proteins from the venom of *D. semiclausum*, and/or its PDV (*Ds*IV), and assess their potential for further development as controls for DBM or other pests. In this report we describe the effects of total *D. semiclausum* venom on blood cells of two Brassica pests, DBM and the Cabbage white butterfly (*Pieris rapae*: Pieridae) and identify 9 putative wasp venom proteins. Twenty three *Ds*IV genes expressed in DBM have also been identified, 5 of which did not belong to any of the known protein families and represent new *Ds*IV genes. We also performed experiments to understand how a previously isolated virus protein (CrV2) acts in suppressing immunity of pest caterpillars. In addition, we used next generation sequencing to examine the genes expressed by DBM larvae, particularly those immune genes that are altered when DBM is parasitised by *D. semiclausum*. This knowledge provides important fundamental information required for assessment of the compounds for development as bioinsecticides. Several of the compounds may have promise for commercial use, however, a further 12-24 months research is required to further characterise their function and mode-of-action.

CHAPTER 1: Materials & Methods

As the materials and methods for this kind of molecular project are necessarily technical in nature in order to allow for reproducibility by other scientists, we have provided all methods in a separate chapter in order to remove complexity and clarify the following chapters which deal with results and discussion related to different aspects of the research, and their relation to industry goals.

Rationale for production of wasp venom gland cDNA (gene) library

To characterise the constituents of *D. semiclausum* venom a cDNA library was generated from RNA extracted from the venom gland. The library would tell us what genes were being expressed in the venom gland and what proteins may be present in the venom. This library was then screened for potential venom protein candidates by sequencing clones and identifying open reading frames that encoded proteins with an N-terminal signal peptide for secretion. This lead to a number of candidate venom proteins being identified. The sequences of these proteins were analysed by various bioinformatic methods to provide clues as to how these proteins may function to mediate successful parasitism. Since obtaining venom from wasps is time consuming and yields only small amounts, it was necessary to produce larger quantities of the candidate proteins and peptides for further characterisation. This was done by synthesis of peptides (<50 amino acids) where possible and recombinant protein production. Since many of the candidate proteins did not have significant similarities with any proteins of known function we designed assays to test for effects on various aspects of the immune functions of haemocytes. The main defence against parasitism is an encapsulation response by the host. This involves recognizing foreign material as non-self, activation of the phenoloxidase cascade, proliferation and differentiation of haemocytes and changes to their adhesive properties and the production of cytotoxic molecules. Much of the encapsulation response is mediated by haemocytes and our candidate proteins were tested for effects on haemocytes such as uptake of peptides, viability and morphology. Inhibition of melanisation was also tested as well as apoptosis, calcium flux and endocytosis. Working with small DBM larvae was often difficult and since effects of venom were observed using *Pieris rape* haemocytes, other model haemocytes or cell lines such as *Sf*9 insect cells were also used. The technical details of the individual methods used are described below:

General materials

All chemicals and reagents were of analytical grade and purchased from Sigma-Aldrich unless otherwise stated. Primers were purchased from Geneworks. All buffers were prepared in milli-Q water.

Insect cultures

DBM and *D. semiclausum* (collected from Gumeracha, South Australia) cultures were maintained in laboratory conditions at 22˚C with a photoperiod cycle of 14h light and 10 dark. Young cabbages were introduced to moths for egg lay and then transferred into clean cages (30cm x 30cm). Shortly after leaf mining was observed mature female and male wasps were introduced into the cages with a smear of honey on the roof. Larger (fitter) females were preferentially chosen to continue the culture. The presence of up to 10 female and male wasps was maintained throughout the development of DBM larvae and fresh cabbage plants supplied as required. Each complete cycle took approximately 1 month and when the opportunity arose the culture was supplemented with a few new individuals.
DBM and *P. rapae* were reared on cabbage plants under the same conditions *as D. semiclausum*. Adults were supplied with honey solution.

Venom collection

Mature female wasps (probably mated) were collected and stored frozen at -80°C until required. Wasps were sterilised in 80% ethanol and dissected in PBS or water. The venom apparatus attached to the ovipositor was located and sacs were then isolated. Once the required number of sacs had been dissected, tubes were vigorously vortexed and centrifuged for 5 min to release venom into solution and remove remaining tissue and cellular debris. For experiments with cells, venom was used fresh. For PAGE, venom was used fresh or stored at -80°C.

Determination of protein concentration

The amount of protein extracted from a set number of venom sacs was determined using a Micro BCA™ Protein Assay kit (Pierce) according to the manufacturer's instructions. Absorbance measurements were taken on a Metertech AccuReader at 550nm.

Polyacrylamide gel electrophoresis (PAGE)

For SDS-PAGE, samples were mixed 4:1 with sample loading buffer (50mM Tris-HCl, pH 6.8, 2% SDS, 10% glycerol, 1% β-mercaptoethanol, 12.5mM EDTA 0.02% bromophenol blue) and heated for 5 min at 90°C. SDS-PAGE was carried out using Bio-Rad mini protean apparatus. Polyacrylamide gels were prepared with a 15% resolving gel and a 4% stacking gel (Protogel 30% acrylamide 0.8% Bis-acrylamide; National Diagnostics) or alternatively, pre-cast TGX gels (Bio-rad) were used. Once samples were loaded, gels were electrophoresed at 200V in running buffer (3g/L Trizma, 1g/L SDS, 14.5g Glycine) until the dye front reached the bottom of the gel. Proteins were then detected using a silver staining method. The gel was soaked in fixative (50% methanol, 10% acetic acid) for at least 30 min and then in 5% methanol and 7% acetic acid for 30 min. The gel was then washed in several changes of milliQ water over at least 2 hours-overnight. The gel was then sensitised in 5ug/ml dithiothreitol for 30 min and stained using 0.1% silver nitrate for 30 min. The gel was then developed by rinsing rapidly with milliQ water and then soaking in developer (3% sodium carbonate, 0.05% formaldehyde) until the desired level of staining was obtained. Development was ceased by soaking the gel in 5% acetic acid and then storing in milliQ water. Alternatively, Coomassie blue staining was used to visualise proteins as described for Tris-tricine PAGE.

Tris-tricine PAGE was performed using a 16.5% pre-cast Tris-tricine ready gel (Bio-rad). Venom was diluted 1:1 with Tris-tricine sample buffer (200mM Trizma; pH 6.8, 2% SDS, 25% glycerol, 0.01% bromophenol blue, 0.02% 2-mercaptoethanol (added fresh)) and denatured at 95°C for 5 min before loading on to the gel. Electrophoresis was carried out in cathode buffer (0.1M Trizma, 0.1M tricine, 0.1% SDS) and anode buffer (0.1M Trizma, pH 8.9) at 200V until the dye front reached the bottom of the gel. The gel was washed and then stained with Coomassie blue (0.1% Coomassie blue R-250, 40% methanol, 10% acetic acid) for 30 min and destained in 40% methanol and 10% acetic acid until background staining had been removed. Gels were then washed in water and images obtained.

Acid Urea PAGE was performed according to Wiese *et al*. (26) using 15% acrylamide (37.5:1 Bis) mini gels containing 6M urea with a 7.5% stacking gel. Tanks were filled with running buffer (5% acetic acid) and gels were pre-run at 200V until the current stabilised. Samples were mixed 1:1 with sample buffer (6M urea, 250mM acetic acid, 100mM potassium acetate, 15% sucrose and 0.001% methyl green) and loaded onto gels. Since the acidic conditions renders most proteins positively charged the gels were electrophoresed in the reverse direction in fresh running buffer at 200V until the dye front reached the bottom of the gel. Gels were then stained with Coomassie blue as previously described for Tris-tricine gels.

Venom antibody production

Antibodies against venom proteins were produced in rabbit using the services of the University of Adelaide Laboratory Animal Services. A pre-exposure bleed was collected and the first injection followed a week later. 40 venom sacs were dissected from *D. semiclausum* into phosphate buffered saline. The solution was centrifuged for 5-10 min to remove venom from the sacs and to pellet cellular debris. The supernatant was then removed and an equal volume of complete adjuvant was then added. Test bleeds were performed the following week and booster injections the week following test bleeds. Booster injections contained venom from 30-50 sacs that had been centrifuged and the supernatant added to an equal volume of incomplete adjuvant. 4 booster injections were performed before the final bleed. Collected blood was centrifuged to remove cells and the serum was decanted, glycerol added to 50% and sodium azide to 0.2%. The antibody preparation was then stored at -20˚C.

Western blots

Western blots were performed using mini protean and mini Trans-Blot apparatus from Bio-Rad. Following SDS-PAGE, proteins were transferred to nitrocellulose membranes (Hybond C; GE LifeSciences) in transfer buffer (25mM Tris, 190mM glycine, 20% methanol, pH 8.5) at 100V for 1 hour. Membranes were washed in TBS (3g/L Trizma, 8.8g/L NaCl, 0.2g/L KCl) and blocked in blocking solution (2-5% skim milk powder in TBS) for at least 1 hour. Primary antibody was then added (1:4000 venom antiserum or 1:5000 anti-polyhistidine) and incubated for at least 2 hours. Membranes were then washed with TBST (TBS with 500uL/L Tween-20 detergent) and alkaline phosphatase conjugated secondary antibody (1:5000) added if required for over an hour. Following washing with TBST the membranes were developed in development buffer (100mM Tris, 100mM NaCl, 50mM $MgCl_2$, pH 9.5) using nitroblue tetrazolium chloride (NBT) and 5-bromo-4-chloro-3'indoyphosphate p-toluidine salt (BCIP) according to the manufacturers direction until the desired level of staining was achieved.

cDNA (gene) library construction

The venom apparatus was dissected from 30 female wasps that had been frozen at -80˚C. The mRNA was then purified using a GenElute™ Direct mRNA miniprep kit (Sigma) according to manufacturer's directions. The cDNA library was constructed using a Creator™ SMART cDNA Library kit (Clontech) according to the manufacturer's protocol. Ligation reactions were transformed into 5-alpha competent cells (New England Biolabs) by heat shock transformation and the library grown on Luria broth agar (1.5% w/v) plates with 30µg chloramphenicol at 37˚C overnight. The unamplified library contained 4680 colony forming units/ml. Single colonies were analysed by PCR using M13 primers and recombinant colonies were chosen for sequencing performed by the Australian Genome Research Facility (AGRF) following plasmid purification.

Bioinformatics of venom gland cDNA (gene) library

To identify potential venom cDNAs, open reading frames were located using NCBI's ORF finder (http://www.ncbi.nlm.nih.gov/projects/gorf/). The presence of N-terminal signal peptides was predicted using SignalP 3.0 (27,28) at (http://www.cbs.dtu.dk/services/SignalP/). SecretomeP was also used to detect secreted protein without a classical signal peptide (29) (http://www.cbs.dtu.dk/services/SecretomeP/) Theoretical isoelectric points (pI) and molecular weights were calculated using the protparam tool on ExPASy, (http://au.expasy.org/tools/protparam.html)(30). NeuroPred (31) was used to predict cleavage sites.

To identify similarities with other proteins, searches for conserved motifs were performed using ScanProsite (http://au.expasy.org/tools/scanprosite/?PS00495) and the Simple Modular Architecture Research Tool (SMART) (32,33). Searching for homologous proteins was conducted by BLASTp

search of the NCBI database (http://blast.ncbi.nlm.nih.gov/Blast.cgi). Structural homologs were searched for using I-tasser (34,35) (http://zhanglab.ccmb.med.umich.edu/I-TASSER/). Models generated by I-tasser are given a C-score that ranges from -5 to 2 and is based on the quality of the threading alignments and convergence of the structural assembly refinement simulations with higher scores reflecting a model of better quality. During testing, when the C-score was greater than -1.5, 90% of the predictions were correct (35). FUGUE was also used to search for structural homologs from sequence data which is scanned against a database of structural profiles (36) (http://tardis.nibio.go.jp/fugue/prfsearch.html). Phyre was the final program used to search for structural similarities (37) (http://www.sbg.bio.ic.ac.uk/~phyre/index.cgi). Alignments were made using ClustalW (http://www.ebi.ac.uk/Tools/msa/clustalw2/). WolfPsort was used to predict the cellular location of proteins (38)(http://wolfpsort.org/). Significant post-translational modifications were further investigated using myristoylator (http://au.expasy.org/tools/myristoylator/) and disulfind (http://disulfind.dsi.unifi.it/) (39). Rapid Automatic Detection and Alignment of Repeats (Radar; http://www.ebi.ac.uk/Tools/Radar/) was used to show the repeating nature of DsVn4. Repetitia (http://protein.bio.unipd.it/repetita/) (40) was used to confirm the solenoid nature of DsVn4.

Peptide synthesis

Where possible, predicted cleavage products (of whole venom proteins) were synthesised by Mimotopes, which amount to 9 separate synthesised peptides (peptides 1-9). These peptides are summarised in Table 1. 1-4 mg at a purity of at least 70% was obtained. Peptides that couldn't be synthesised generally contained "difficult" residues such as methionine, cysteine, arginine and tryptophan. Where cleavage prediction resulted in a C-terminal amidation signal, peptides were altered to include an amidated C-terminus. A biotin tag was also conjugated to the N-terminus to allow peptide localisation to be monitored using neutravidin. A previous study suggested that background staining of endogenous biotin in haemocytes should not pose a significant problem (41). Upon arrival, peptides were diluted to 1mM in sterile milliQ water, aliquotted and stored at -80°C until required.

Generation of *E. coli* expression constructs and production of recombinant protein in *E. coli*.

Primers were designed for each construct that contained appropriate restriction enzyme sites (usually *Bam*H1 and *Hind*III) for cloning into pQE30 and which would result in the absence of the signal peptide. Genes were amplified from cDNA library isolates by PCR using a high fidelity polymerase. PCR products were sub-cloned into pCR-blunt and then digested from purified plasmid. Digested fragments were ligated into pQE30 and transformed into M15[pREP4] *E. coli*. Recombinant *E. coli* were selected using ampicillin and kanamycin. Colonies were checked by PCR for the presence of recombinant pQE30 and sequencing ensured the construct was correct.

Recombinant M15[pREP4] *E. coli* was cultured until the OD_{600nm} reached ~0.5. Unless otherwise stated, cultures were induced by the addition of 1mM IPTG to produce recombinant protein. Incubation continued for 3 hours and then the cultures were harvested by centrifugation and the cell pellet frozen for further analysis.

Peptide	Molecular Weight (kDa)	% Purity	cDNA venom clone origin	Synthesised Peptide Sequence
Peptide 1	1462.52	93	DsVn4	BIOTIN-SPLNPKLLGSLV-NH2
Peptide 2	2593.85	83	DsVn2	BIOTIN-SPATKAGIIAKIQEMIKARQGR-OH
Peptide 3	1326.28	77	DsVn4	BIOTIN-SPISTAALASLA-NH2
Peptide 4	1976.07	92	DsVn6	BIOTIN-NADPLNAAALIAALKKR-OH
Peptide 5	1354.21	88	DsVn1	BIOTIN-DADGKFYASR-NH2
Peptide 6	5668.5	79	DsVn3	BIOTIN-SADPGKIMDKLVQMIKSRLGRKAERSADPDPDPGMLDLMKNIPFIGKFL-OH
Peptide 7	4327.63	89	DsVn4	BIOTIN-SPLSAGALASLAGNATSKLPNCEHADHHCIRNFGFPGCHV-OH
Peptide 8	3772.31	97	DsVn6	BIOTIN-EEAEAETMVRREAAAAGLQEMHAESKR-OH
Peptide 9	2033.08	70	DsVn7	BIOTIN-EISPDELLVVKSHLDL-OH

Table 1: Summary of putative active peptides synthesised based on sequence derived from *D. semiclausum* venom library

Construction of recombinant baculoviruses for protein expression in insect cells

In general, constructs were made so that signal peptides were left intact. ORFs of cDNAs were amplified using primers that incorporated appropriate restriction enzyme sites at either end. Often these PCR products were subcloned into pCR-blunt. Recombinant baculovirus was generated using the Bac-to-Bac system (Invitrogen) according to the manufacturer's directions. Briefly, products were ligated in to pFastBac1 and recombinant pFastBac1 was used to heat shock transform competent DH10Bac *E. coli*. Recombinant bacmid was purified from successful clones and used to transform *Sf*9 insect cells to produce budded virus. Successive rounds of amplification increased the viral titre for protein production.

Collection of haemocytes and staining of cells for fluorescent microscopy

Hemolymph was collected from larvae by removing a proleg and allowing the larvae to bleed into Sf900II medium (Invitrogen) saturated with phenylureathiosulphate (PTU). DBM larvae were generally bled directly into the well of a printed glass slide whereas *P. rapae* larvae were bled into microfuge tube and haemocytes aliquotted onto the slide. Cells were fixed in 4% paraformaldehyde for 15 min, washed with PBS and then permeabilised with 0.1% TritonX-100 for 4 min. Slides were then washed using TBST. If required, primary antibody (1:200-500) in TBST was added and incubated for 2 hours. Once cells had been washed with TBST they were then stained with 0.01 mg/ml FITC-phalloidin for 40-60 min. Staining with TRITC-secondary antibody (1:200) or TRITC-neutravidin (1:125) could also be conducted simultaneously with FITC-phalloidin staining and the incubation time extended to 1-2 hours. If cell nuclei required staining, DAPI was applied at 0.2ug/ml in PBS for 5 min. Slides were then washed with TBST and examined under a Leica DM IL inverted fluorescent microscope.

*Sf*9 insect cell culture and viability tests

*Sf*9 insect cells were maintained using serum free Sf900II SFM medium (GibcoBRL). Cells were kept in suspension using Schott bottles with lids loosened for adequate oxygenation at 27°C with gentle shaking. When the cell density reached >2 x10^6 cells per ml, as determined by cell counting on a haemocytometer, cells were passaged to between 0.5-1 x10^6 cells/ml.

The effect of proteins on *Sf*9 insect cell viability was tested using *Sf*9 insect cells in log phase of growth. Cells were incubated with the indicated concentrations of venom or peptides in triplicate. For controls, an equivalent volume of water (peptide) or PBS (venom) was added. After the desired incubation periods at 27°C with shaking, samples were taken, mixed 1:1 with trypan blue (0.4%) and loaded onto a haemocytometer for counting. Cells that excluded the trypan blue were considered viable and cells that stained blue were unviable.

Melanisation assay

Pieris rapae larvae were bled onto 10µL *E. coli* lysate. 15µL of activated hemolymph was then added to 10µL of 1mM peptide. L-DOPA was dissolved in PBS to 1.4mg/mL and 200µL distributed into the appropriate wells of a 96-well plate. 5µL of treated hemolymph was then added to wells and absorbance measured at 490nm using a Metertech AccuReader.

Phagocytosis assay

Piers rapae were bled into medium saturated with PTU and allowed to spread in the wells of a printed glass slide. Old medium was then removed and replaced by 200µM peptide in fresh medium. Cells were treated for 2 hours at room temperature and then 5µL of pHrodo *E. coli* BioParticle conjugates (Invitrogen) resuspended in PBS to 1mg/mL were added. Following a further 2 hours incubation cells were washed with PBS and viewed using an inverted fluorescent microscope with TRITC filters to view phagocytosed *E. coli* particles and brightfield to see the whole cell population.

Calcium flux assay

Piers rapae were bled into medium saturated with PTU and allowed to spread in the wells of a printed glass slide. 5mM stock of Fluo4-AM in DMSO was diluted to 5µM in PBS and applied to cells for 1 hour. Cells were washed using medium and incubated a further 30 min to allow complete de-esterification of intracellular AM. Cells were then treated with peptide in PBS and fluorescence monitored under a fluorescent microscope using FITC filters.

Apoptosis assay

Pieris rapae larvae were bled into medium saturated with PTU and allowed to spread in the wells of a printed glass slide. Cells were treated with venom and then FITC-annexinV (Invitrogen; 1:20) and propidium iodide (0.001mg/ml) applied to the slides in annexin-binding buffer (10mM HEPES, 140mM NaCl, 2.5mM $CaCl_2$, pH 7.4). After 15 min incubation, cells were washed with annexin-binding buffer and viewed under a fluorescent microscope using FITC filters to observe annexin binding and TRITC filters to observe propidium iodide staining.

Minimum inhibitory concentration (MIC) assay

A range of bacterial species was subjected to MIC assay (Table 2). Bacteria were cultured in Muller Hinton broth (MHB) (Bacto Laboratories, Cat. No 211443) at 37°C overnight. A sample of each culture was then diluted 50-fold in fresh MHB broth and incubated at 37°C for 2-3 hrs. The compounds (peptides 1-9) were serially diluted two-fold across the wells of 96-well non-binding surface plates (NBS, Corning). The concentration of the compounds in the assay wells ranged from 64 µg/ml to 0.03 µg/ml. The resultant mid-log phase bacterial cultures were diluted to a final concentration of 5X10^5 CFU/mL, and added to the assay plates. All plates were covered and incubated at 37°C for 24 hrs. MICs were the lowest concentration of the compounds in the assay wells that showed no visible bacterial growth.

Minimum bacterial concentration (MBC) assay

A range of bacterial species was subjected to MBC assay (Table 2). For the determination of the minimal bactericidal concentration (MBC), 30µL of Resazurin (0.01% w/v) was added to each well of the 96-well non-binding surface plates (NBS, Corning) after MIC values were recorded. The plates were then incubated at 37°C for a further 18 to 24 hrs. Wells with blue coloration indicated dead microorganisms, whereas wells with pink coloration indicated living microorganisms. MBCs were the lowest concentration of the compounds in the wells with blue coloration.

Data analysis of assays on total venom, peptides and cDNA clones

Data was analysed using Prism™4.0 (GraphPad Software Inc. San Diego CA, USA). Data is presented as mean ±SEM where n≥3. Fluorescent images were manipulated using ImageJ 1.42q (http://rsbweb.nih.gov/ij/). Protein structures were manipulated using UCSF Chimera (42). MICs were determined visually after 24 hr incubation and the MIC was defined as the lowest concentration in which no bacterial growth was visible after incubation. Both MIC and MBC were determined by visual inspection only.

ID	***Organism***	***Strain***	***Type***
GP_001	*Staphylococcus aureus*	ATCC 25923 (MSSA)	Gram +ve
GP_013	*Streptococcus pneumoniae*	ATCC 33400	Gram +ve
GP_018	*Bacillus subtilis*	ATCC 6633	Gram +ve
GP_027	*Enterococcus faecalis*	ATCC 29212	Gram +ve
GN_001	*Escherichia coli*	ATCC 25922	Gram -ve
GN_003	*Klebsiella pneumoniae*	ATCC 700603 Multi-resistant strain	Gram -ve
GN_022	*Pseudomonas aeruginosa*	ATCC 10145	Gram -ve

Table 2: Bacterial species utilised for peptide antibacterial assays (MIC and MBC assays)

Insect culture, parasitisation and sample preparation for deep sequencing analysis

DBM and *D. semiclausum* were raised on cabbage plants and host larvae, respectively, at 25°C. Twenty five 3rd and 4th instar DBM larvae each were exposed to the parasitoid wasp until parasitisation was observed. Individual larvae that had been attacked by the parasitoid were collected and fed on fresh cabbage leaves. Larval samples were taken in four different time intervals after parasitisation (6, 12, 24 and 48 hrs post-parasitisation) and the samples were kept at -80°C until RNA isolation. The same numbers of mixed larval instars (3rd and 4th) of non-parasitised larvae were collected as control. It is worth mentioning that DBM larvae parasitised at 3rd instar continue to develop to 4th instar.

Total RNA was extracted from all larval samples using Tri-Reagent™ (Molecular Research Center Inc.). RNA extracted from the time points post-parasitisation were pooled and therefore temporal expression data was lost. This was also applied to non-parasitised samples. The pooled RNA sample concentrations were measured using a spectrophotometer and integrity was ensured through analysis on a 1% (w/v) agarose gel. The samples with total concentration of 3.9 and 4.1 µg/µl for parasitised and non-parasitised larvae, respectively, were used for cDNA library production.

The cDNA library was prepared by using 5 µg of starting material into the Illumina mRNA Sequencing Sample preparation procedure (kit RS-930-1001). This involved purification and fragmentation of mRNA, first strand cDNA synthesis, second strand cDNA synthesis, repairing ends, addition of "A" bases to 3' ends, ligation of adapters, purification of ligated products, PCR amplification to enrich cDNA templates. The library was validated and quantified in preparation for deep sequencing.

Deep sequencing and *de novo* transcriptome assembly

The validated and quantified cDNA library was subjected to deep sequencing using a Genome Analyzer IIx Next generation sequencer on a 66 cycle single-end sequencing run, following the supplier's instructions (Geneworks, Adelaide). The GAII analyzer data was output as sequence tags of 65 bases. Sequence.txt files (in FASTQ format) were generated using Illumina Pipeline version 1.5.1. The CLC Genome Workbench (version 4.0.2) (43) algorthim for *de novo* sequence assembly was used to assemble contigs from a pooling of all the short-read data using default parameters (similarity=0.8, length fraction=0.5, insertion/deletion cost=3, mismatch cost=3).

Deep sequencing RNA analysis

The contigs arising from the *de novo* assembly were then used as a reference set of transcripts for RNAseq analysis. Short-read sequence data from parasitised and non-parasitised larvae were separately mapped against the reference set of assembled transcripts using the CLC Genome Workbench RNAseq function (min. length fraction=0.9, maximum mismatches=2). The relative transcript levels were output as RPKM (Reads Per Kilobase of exon model per Million mapped reads) values, which takes into account the relative size of the transcripts and only uses the mapped-read datasets (i.e. excludes the non-mapped reads) to determine relative transcript abundance. In this way, the output for each dataset can be directly compared as the number of mapped reads per dataset and transcript size has already been taken into account.

Reads from the parasitised and non-paratisised larvae were cleaned and combined, before *de novo* transcriptome assembly was carried out using Oases 0.1.18 (44). The individual sets of reads were then mapped back to the transcripts using BWA 0.5.8a (45). The average read depth for each transcript was then calculated using SAMtools 0.1.8 (46). The transcripts that had a greater than two-fold average read depth difference between the parasitised and non-parasitised sets were selected for annotation. We used both CLC and Oases to compare assembly of contigs. In general, Oases produced similar contigs to CLC, although contig lengths produced by Oases were in some instances longer.

Deep sequencing BLAST homology search and annotation

BLASTX algorithm (47) with an E-value cut off of 10^{-6} at National Center for Biotechnology Information (NCBI) non-redundant protein sequence database, was used to determine the homology of sequences with known genes. In the absence of DBM and *D. semiclausum* genome sequences, we discarded annotations that showed similarity to hymenopteran genes and tried to use annotations that showed the highest similarity to lepidopteran genes. Gene ontology and annotation were performed on all assembled contigs greater than 200 bp length by BLAST2GO software (www.blast2go.org) (48). For gene ontology mapping, Blast2GO which performs four different mapping strategies was used, and the program defaults were applied for all annotation steps (48). BLAST2GO allows the selection

of a significance level for the False Discovery Rate (FDR) which was used as a cut-off at the 0.05% probability level. The data from InterPro terms (49), enzyme classification codes (EC), and metabolic pathways (KEGG, Kyoto Encyclopedia of Genes and Genomes) were merged with GO terms for a wide functional range cover in annotation. For some of the identified *D. semiclausum* ichnovirus (*Ds*IV) genes, ORFs were predicted and identified by using ORF finder at NCBI (http://www.ncbi.nlm.nih.gov/gorf/gorf.html). Predicted ORFs with highest BLASTp E-values in internal comparisons involving other IV genes were accepted for further analyses.

Quantitative RT-PCR (qRT-PCR) validation of deep sequencing data

Quantitative RT-PCR technique was used on the same RNA samples which were used for transcriptome profile study to verify deep sequencing results. In addition, to observe gene expression levels at different time points after parasitisation for a selected group of genes another experiment was performed by parasitizing 2nd instar DBM larvae. The RNA samples were extracted from parasitised larvae at 16, 24 and 48 hrs after parasitisation.

First strand cDNA was synthesised from 1μg of RNA using M-MuLV reverse transcriptase (New England BioLabs). The qPCR reaction consisted of 2 μL of diluted cDNA (10 ng), 5 μL of Platinum SYBR Green SuperMix-UDG with ROX (Invitrogen), and 1 μM of each primer set (Table 3) in 10 μL total volume. Reactions were performed in triplicates in a Rotor-Gene thermal cycler (QIAGEN) under the following conditions: 50°C for 2 min; 95°C for 2 min; and 40 cycles of 95°C for 10 s, 60°C for 15 s, and 72°C for 20 s, followed by the melting curve (68°C to 95°C). Melting curves for each sample were analyzed after each run to check the specificity of amplification. Gene copy numbers were calculated using the Rotor-Gene software and an endogenous reference actin gene was used for normalisation.

Gene	Forward primer (5'-3')	Reverse Primer (5'-3')
Storage protein 1	CAAGACACGCTACGACGC	GTCGGCATGACGAAGTAC
Insulin receptor	GTACCCCTCGATCTCGCG	CCCACGTCAAGGGAACCC
JH epoxide hydrolase	AGGATCTACGCGGAGGGC	TGGTACACCACTTCGTAC
Ecdysteroid regulated protein	AACCCGAAGAGCCGAAGC	CTCTGTAGTCGCTGCTAC
Cuticle protein	CAGGATGACGAGTCTGGC	GTCTGCCTCGTATTCTAC
Toll receptor	CCTCCGGCAACGCCCTAG	CGCACAGAAATTCAGAGG
Hemolin	AGCTCCAGAGACTACGCC	GTGTTGTAGGAACCATTG
Gloverin	AGCTAGCCCGGCATCCGC	GACGGTAGCCCGCCTTAC
pxSerpin 3	GAATAGCTTCTACTACGC	TGATAGCGAATTCGGTAC
Actin	ATGGAGAAGATCTGGCAC	GGAGCCTCCGTGAGCAGC

Table 3: A list of primers used for qRT-PCR analyses to validate deep sequencing data

Confirmation of CrV2:Gα interaction by Far Western blot analysis

Purified *CrV2 and Drosophila* $G\alpha_o$ proteins were produced as per previously established methods described in Cooper *et al*. 2011 (50). *Drosophila* $G\alpha_o$ and bovine serum albumin were subjected to SDS-PAGE on an "any kD" TGX gel (Bio-Rad) using a non-reducing sample buffer. Proteins were transferred onto a Hybond-C nitrocellulose membrane (GE healthcare life sciences) at 100 V for 1 hr. Membranes were blocked with 5% skim milk powder in TBS buffer (8.8 g/L NaCl, 0.2g/L KCl, 3 g/L Trizma) for > 2 hr. Membranes were then probed with CrV2 in Sf900II medium or conditioned medium overnight. Membranes were then washed with TBST buffer (see above) and probed with rabbit anti-CrV2 (1:10 000) in blocking solution for 2 hr. Following washing with TBST, membranes were probed with alkaline phosphatase-conjugated goat anti-rabbit IgG (1:20 000) in blocking

solution for 2 hr. Membranes were washed with TBST and developed using 5-bromo-4-chloro-3'-indoyphosphate p-toluidine salt, and nitro-blue tetrazolium chloride, to detect any CrV2 bound to $G\alpha_o$.

Antibody labelling of CrV2 in haemocytes *in vitro*

Larval Cabbage white butterfly (*Pieris rapae*) were surface sterilised in ice-cold 70% ethanol for a few minutes and then kept on ice until they were bled from a severed proleg directly into an ice-chilled 1.5 ml microcentrifuge tube containing ~200 µL of Sf900II medium (Invitrogen) saturated with phenylthiourea (PTU, which inhibits melanisation reactions). Haemocytes were aliquoted into wells of a printed glass slide and incubated at room temperature until cells attached and spreading was observed. Obviously spread cells were considered to be a plasmatocyte morphotype and attached cells that retained a rounded, apparently unspread, conformation were considered as a granulocyte morphotype. Insect cell-culture medium containing secreted, baculovirus-expressed CrV2 was applied to the haemocyte-containing slides and incubated for the desired time. Medium was then removed and cells fixed in 4% paraformaldehyde for 15 min, permeabilised with 0.1% TritonX-100 for 4 min and washed in TBST (8.8 g/L NaCl, 0.2 g/L KCl, 3 g/L Trizma, 500 µL/L Tween-20 detergent). Anti-CrV2 polyclonal rabbit antibodies (see (51)) in TBST (1:500) were added to the glass slide and incubated for 1.5-2 h at room temperature. Cells were washed with TBST and flurophore-conjugated anti-rabbit antibody (1:200-250) with 1:50 dilution of FITC-Phalloidin (0.1 mg/ml) in TBST, were applied to slides for 1 h at RT in darkness. Cells were then washed with TBST and stained with 1:10 000 dilution (1 µg/ml) of DAPI for 5 min. Cells were then washed with TBST and PBS, a coverslip was applied, and the coverslip sealed with nail varnish.

.

CHAPTER 2: Analysis of Total Venom of *Diadegma semiclausum* (results and discussion)

The first step in characterising venom of *Diadegma semiclausum* was to investigate the effect of total extracted venom on the haemocytes (blood cells) of two key Brassica pest caterpillars, which are the key immune cells in these pests. This was performed to confirm that there are direct effects and to gain an idea as to how the effects are manifested. Experiments were also performed to gain an understanding of the complexity of the venom (i.e. how many different individual proteins are present in the total venom) to facilitate isolation and analysis of individual compounds that could be developed as bioinsecticides. Results of these experiments are presented and discussed below.

Diadegma semiclausum culture

D. semiclausum were successfully reared under laboratory conditions. In general, parasitism of DBM hosts was >90% and on average 40% of the population was female. This laboratory culture provided the venom gland tissue for RNA extraction and whole venom from the venom sac (Figure 1) and has also been a source of *Diadegma* to initiate cultures at other sites. The quality of the venom apparatus varied with age. Venom sacs appeared fuller when wasps were allowed to mature for at least 5 days before collection whereas glands often appeared developed even in the absence of venom accumulated in the sac. Wasps were harvested by freezing and storing at -80°C until required.

Figure 1: Example of a venom sac and gland being dissected from *D. semiclausum*

Effect of parasitisation on host haemocytes

A comparison of non-parasitised DBM larvae with *D. semiclausum* parasitised DBM larvae showed that haemocytes were less spread when parasitised and the spindle shaped cells present from control larvae were absent in parasitised larvae (Figure 2). These effects were observed late in parasitism and it is possible that these effects are a result of polydnavirus expression rather than a direct effect of venom components. Polydnavirus proteins expressed in the host were identified using deep sequencing of parasitised and non-parasitised DBM larvae and are discussed later (see Chapter 4).

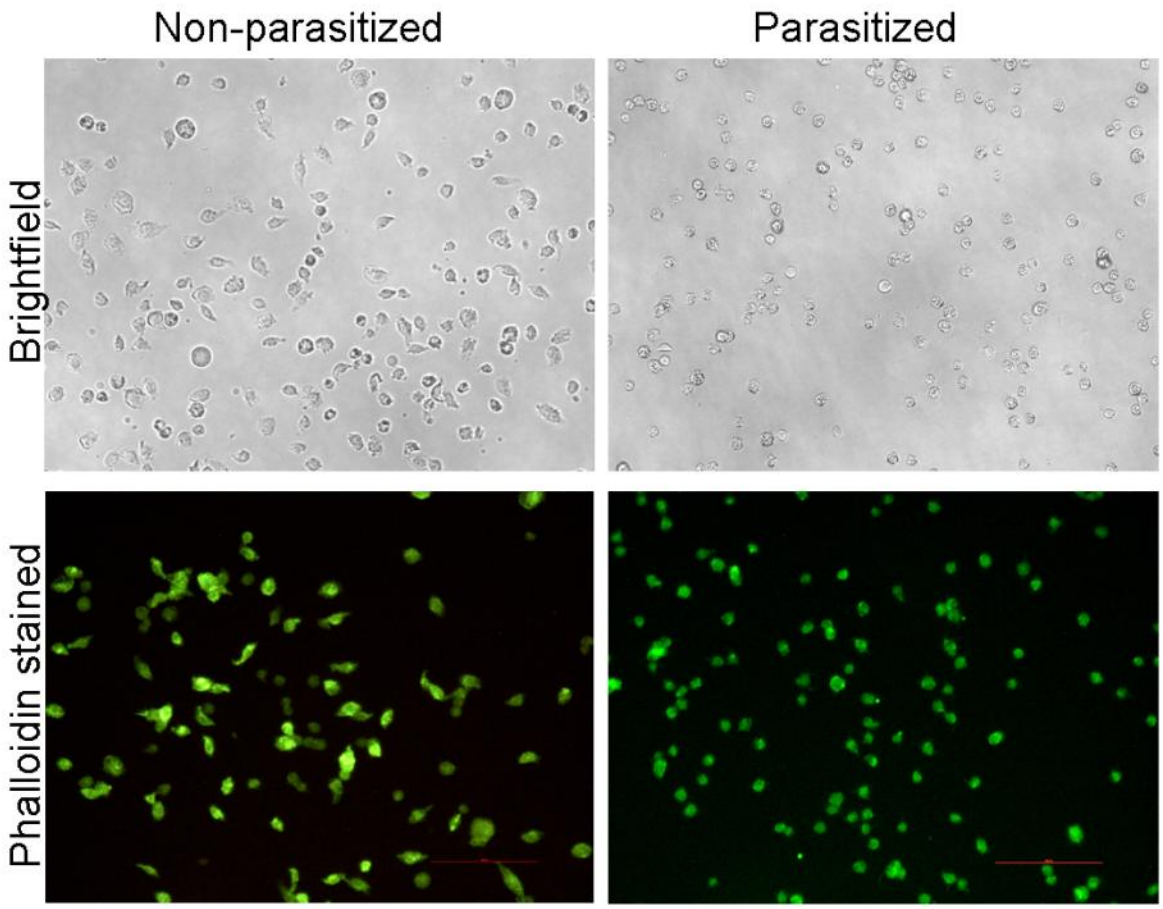

Figure 2: Haemocytes from parasitised larvae appear less spread and more rounded. Left: Images of haemocytes from DBM larvae that had not been parasitised compared to Right: haemocytes from DBM larvae parasitised by *D. semiclausum*. Top are bright field images, bottom are images showing cells stained with FITC-phalloidin to show the cell cytoskeleton. Images were obtained using a 20x objective lens, scale bar =100µm.

Proteomic analysis of *D. semiclausum* venom

The concentration of protein in venom was determined using the bicinchoninic (BCA) assay (Pierce). It was calculated that on average, each sac contained 1-1.4µg protein. This is within the range of other venom sacs where an average of 0.04µg and 180µg protein per venom sac have been reported for *Pimpla turionellae* (52) and *P. hypochondriaca* respectively. BCA assay is reported to be less sensitive to amino acids sequences of protein than Bradford assay, however, catecholamines are among the possible interfering substances and at this stage, their presence in *D. semiclausum* venom cannot be ruled out since they have been found in the venom of *P. turinionellae* (52). When Bradford assay was conducted the change in absorbance was not proportional to the amount of venom added in the linear range.

Analysis of *D. semiclausum* venom by SDS-PAGE revealed relatively few high abundance larger molecular weight proteins (Figure 3A). There were at least 3 distinct mid-range molecular weight proteins and a high abundance of low molecular weight material. In an attempt to provide further resolution of the venom proteins, venom was also separated by Tris-tricine PAGE and by acid-urea PAGE. Tris-tricine PAGE is optimal for the separation of low molecular weight proteins and indeed emphasised the abundance low molecular weight proteins which further resolved into 2 groups

(Figure 3B). Since distinct, larger protein bands are present, it seems unlikely that this material is merely a result of protein degradation. Acid-urea page uses both molecular size and charge for separation (Figure 3C). This makes it possible to resolve proteins of similar size but different charge. Using this technique also made it clear that the small positively charged venom proteins were not stable in the gel and could easily be resolubilised and washed from the gel. It is possible that these methods are not sensitive enough to detect proteins that are present in low abundance when high abundance proteins are also present. Running the gels in a second dimension may also reveal further complexity of the venom by separating proteins of similar sizes by another property such as isoelectric point.

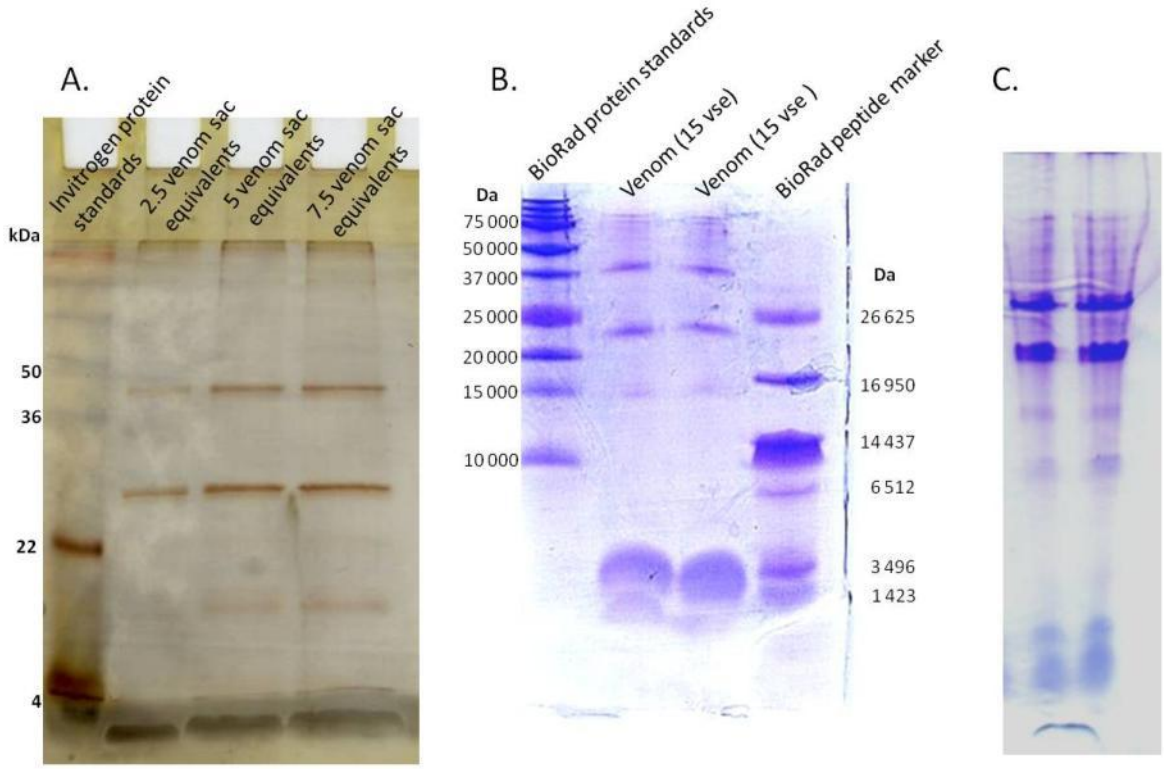

Figure 3: *D. semiclausum* venom obtained from dissected venom sacs was separated by different PAGE methods. A: Silver stained SDS-PAGE using a 15% polyacrylamide gel. B: 15 venom sac equivalents (vse) separated by tris-tricine PAGE. C: 45 (left lane) or 90 vs (right lane) separated by acid-urea PAGE.

A rabbit was immunised with *D. semiclausum* venom to produce antibodies that could be used to detect venom proteins. When the final bleed antiserum was used in a western blot procedure to detect protein in the venom, only a single band developed (Figure 4). Different concentrations of antibody were tested and different blocking methods trialled but no other venom bands became apparent. It is likely the low molecular weight material may not have been large enough to illicit an immune response although it is surprising no response to the ~40kDa band was seen.

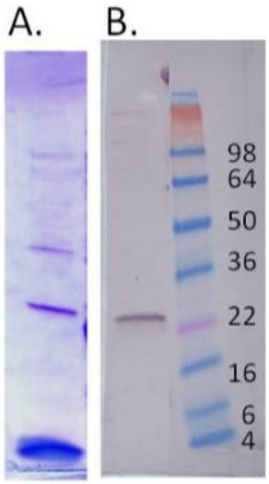

Figure 4: Venom antisera detects one venom protein. A: Coomassie stained SDS-PAGE of *D. semiclausum* venom (16vse) on a TGX 'any kD' precast gel. B: Venom antiserum western blot of proteins shown in A. Proteins were transferred to nitrocellulose membrane that was incubated with venom antiserum and then anti-rabbit secondary antibody conjugated to alkaline phosphatase. Membranes were developed using NBT and BCIP. One venom protein was detected at ~24kDa.

Mass spectroscopy analysis of venom proteins

Mass spec analysis is being carried out collaboratively with Dr. Tim Chataway, Flinders proteomics facility. Bands from SDS-PAGE gel separations were supplied for analysis (Figure 5). Preliminary analysis of band 4 by PEAKS detected a high level of homology with venom allergen 5 from *Vespa Crabro* (23kDa). Venom allergen 5 is most commonly found in venoms of social Hymenoptera and is part of a group of proteins expressed by salivary and venom glands of variety of animal species (53). Venom allergen 5 is a cysteine rich secretory protein (CRISP) and its biological function is currently unknown. Venom allergen 5-like proteins have also been discovered in the venom of braconid wasps *Chelonus inanitus* (53) and *Microtonus hyperodae* (54). Interestingly, the band harbouring this peptide corresponds to the protein detected by our anti-venom serum. A degenerate primer was constructed to isolate venom allergen 5 from the venom gland cDNA library using RACE. However, this was unsuccessful. Numerous other potential homologs were found within the band analysed as is expected from a one-dimensional gel and more precise matches could be obtained by further separation of proteins in a second dimension prior to MS analysis.

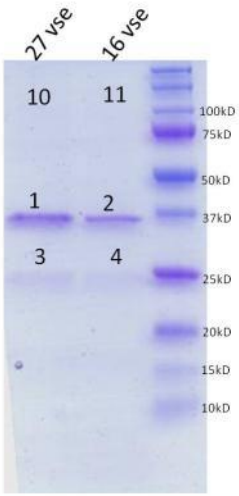

Figure 5: SDS-PAGE of venom displaying bands sent for mass spec analysis.

Effects of whole venom on haemocytes

The effects of whole venom on haemocytes were investigated to give an indication of what function individual venom proteins may have and show that bioactives were present in the venom. When *D. semiclausum* venom was applied to DBM haemocytes that had spread over a glass slide, there were fewer spread cells (plasmatocytes). The same phenomenon was apparent when venom was applied to *Pieris rapae* haemocytes (Figure 6). Although *P. rapae* is not a host for *D. semiclausum*, the haemocytes have a much more distinct morphology than DBM haemocytes and bleeding the larvae without contaminating the hemolymph with fat body is much more readily achievable at much higher yields since larvae are significantly bigger. For these reasons *P. rapae* hemolymph was often used as a model for the effects of *D. semiclausum* venom components. The action of venom on *P. rapae* haemocytes suggests that the mechanism of venom action may be more generic and not host specific. Therefore, candidate proteins could have broad spectrum effects or may be specific or optimal for the control of DBM.

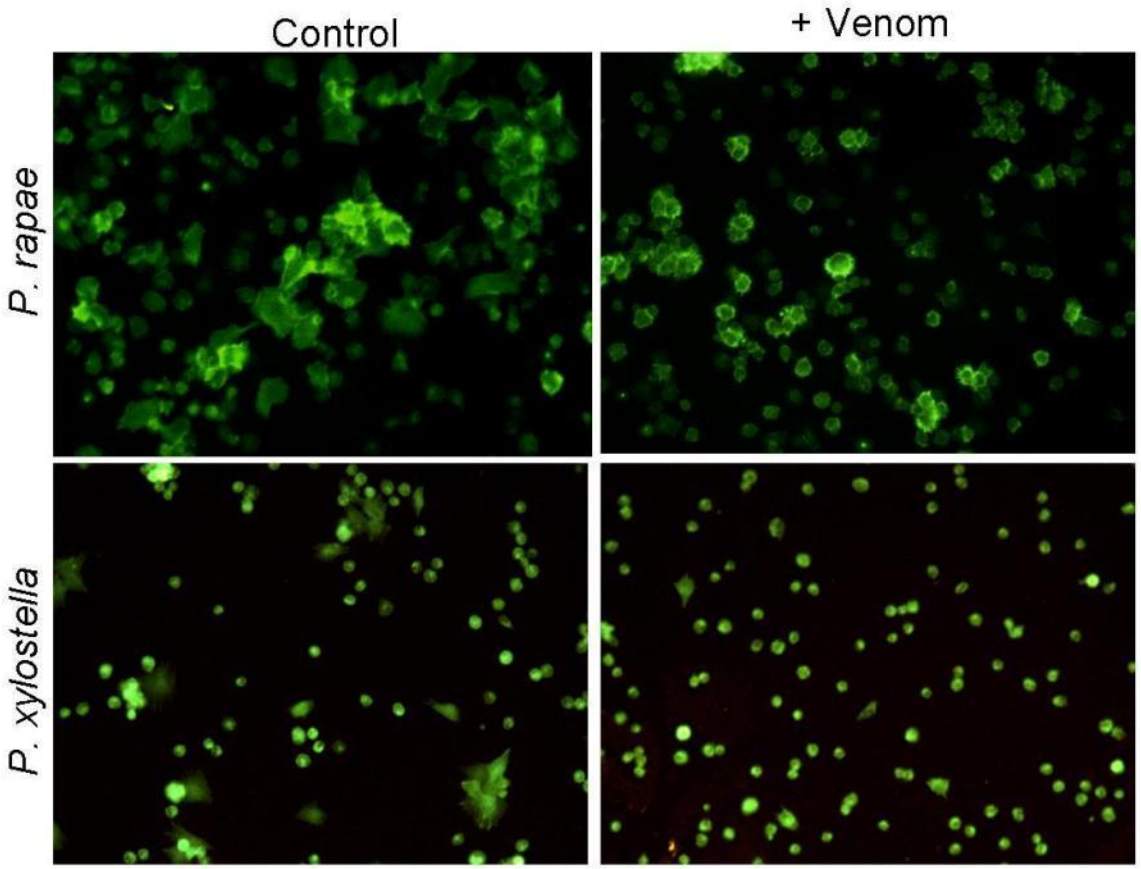

Figure 6: Effect of *D. semiclausum* venom of *P. rapae* and *P. xylostella* haemocytes. *P. rapae* and *P. xylostella* were bled into Sf900II medium saturated with PTU. *P. rapae* hemolymph was aliquotted into wells of a printed slide and haemocytes were allowed to attach and spread for 2 hours at room temperature. Medium was then removed and replaced by PBS on control cells or PBS containing 4.7 vse and incubated for a further 2 hours. *P. xylostella* were bled directly into the wells of a printed slide and 0.7vse applied shortly after and incubated for 1.5 hours. Haemocytes were then fixed and stained with FITC conjugated phalloidin. The presence of venom appears to have reduced the spreading of plasmatocytes.

Venom anti serum was used to detect whether venom proteins were interacting with haemocytes. After venom treatment, cells were fixed and permeabilised. The venom antiserum was applied and bound antibody detected using a secondary anti-rabbit antibody conjugated to TRITC. The stronger red signal from venom treated cells indicated that the antibody was detecting venom proteins associated with the haemocytes and therefore probably acted to change some function of these immune cells. Presumably the same venom protein as detected by western blot (Figure 4) is being detected associated with the cells unless some aspect of the western blotting procedure was preventing the detection of more venom proteins. Using the current method it is difficult to determine whether the antibody is detecting proteins bound to the outside of the hemoctyes or whether protein has been taken into the cell.

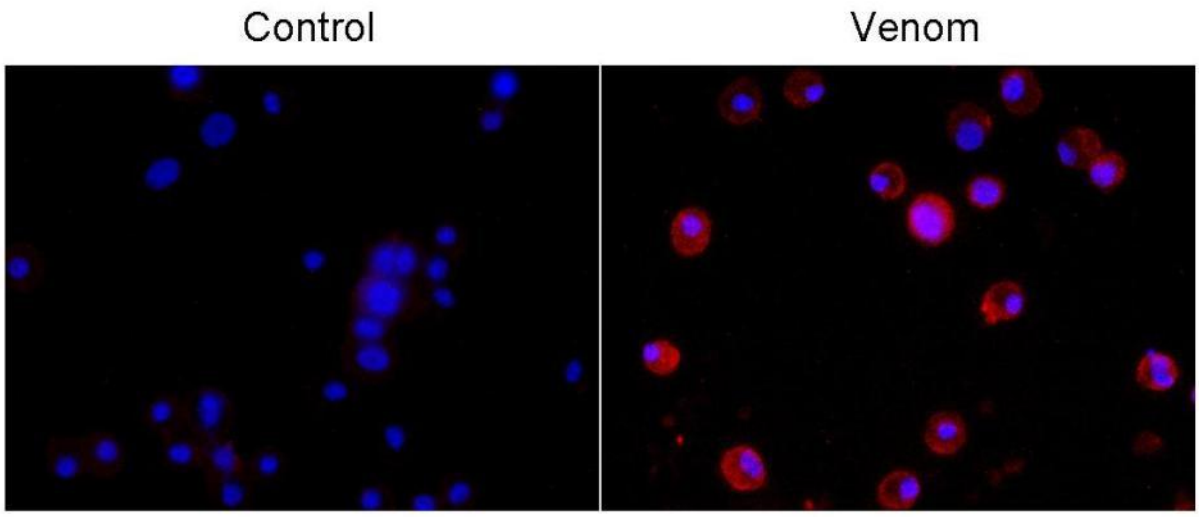

Figure 7: Uptake of venom by DBM haemocytes. Haemocytes were bled into Sf900II medium saturated with PTU and venom from 0.7 venom sac equivalents or an equivalent amount of PBS (control) added. Cells were then incubated at room temperature for 1.5 hours. Cells were then fixed, permeabilised and a 1:200 dilution of primary venom antibody added for 1 hour. After washing, a 1:200 dilution of TRITC conjugated secondary antibody was then added and incubated for a further 1.5 hours. Cells were then viewed on an inverted fluorescent microscope using a 60x objective lens.

Similarly to DBM, a higher red signal was also obtained from venom treated *P. rapae* cells compared to control cells (Figure 8). Furthermore, when the nuclei of haemocytes from *Pieris* were exposed to venom and stained with DAPI, there was a significant absence of the larger nuclei normally associated with spread plasmatocytes (Figure 8 and Figure 9). It is difficult to distinguish whether this is a feature of the cells becoming more rounded in general or if nuclear shrinkage or pyknosis is occurring. Nuclear shrinkage or condensation is usually associated with the approach of cell death and calcium flux has also been associated with this response (55,56). Venom from other parasitoid wasps has also been reported to induce intracellular calcium release (57,58) and it is possible that proteins in *D. semiclausum* venom may induce calcium flux or cell death. To date *D. semiclausum* venom has not been observed to cause further symptoms of apoptosis such as nuclear fragmentation or membrane blebbing. However, venom did decrease the viability of *Sf*9 insect cells by a small but significant amount after 30 min (Figure 10).

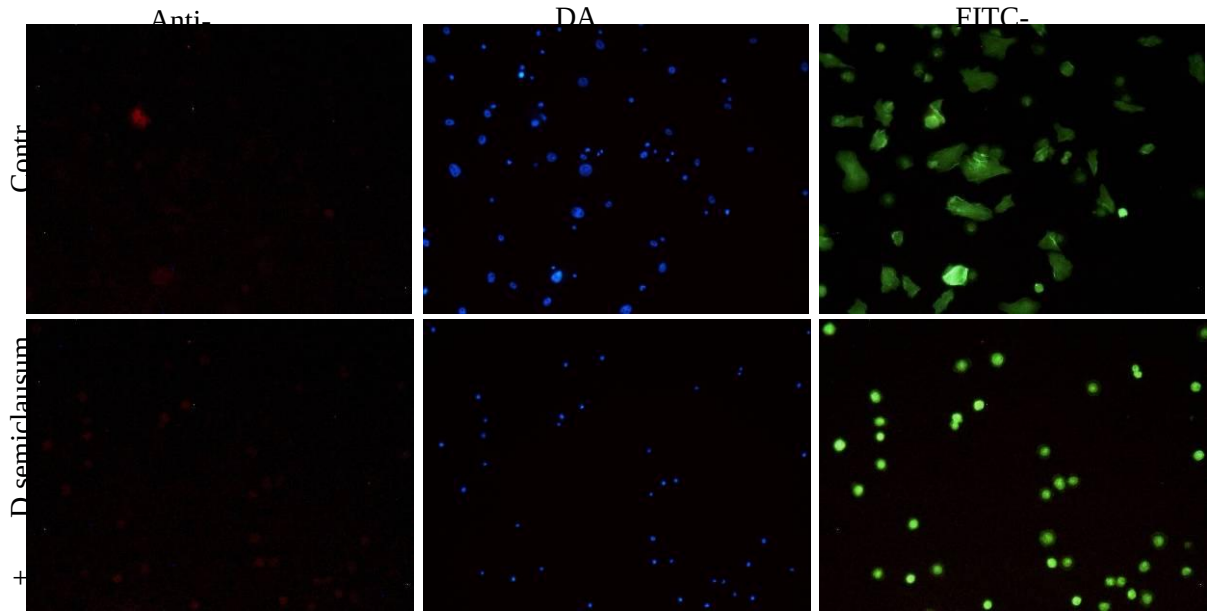

Figure 8: Venom from *D. semiclausum* unspreads *P.rapae* haemocytes and reduces nucleus size. *P. rapae* haemocytes were allowed to spread on a printed glass slide. Medium was removed and replaced with PBS containing *D. semiclausum* venom (10 vse) and incubated for 2.5 hours. Cells were then fixed, permeabilised and incubated with rabbit anti-venom (1:200) for 1.5 hours. Following washing, cells were incubated with TRITC anti-rabbit secondary antibody (1:250) and FITC phalloidin for 1 hour. DAPI was then applied to cells for 5 min followed by washing. FITC-phalloidin staining of venom treated cells showed that they were unspread compared to control cells and DAPI staining showed that the nuclei appeared uniformly small in size where as in control cells nucleus size was more varied.

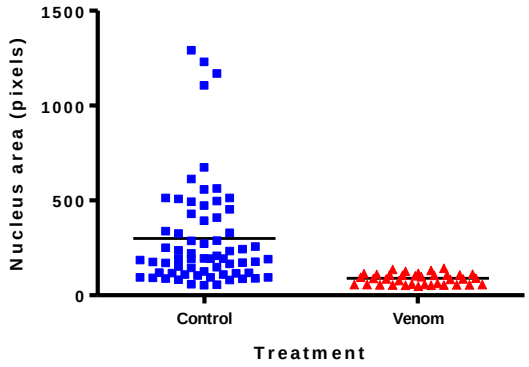

Figure 9: Venom treated cells have a significantly smaller average nucleus size. Images from Figure 8 were analysed using ImageJ to calculate the area of thresholded DAPI stained nuclei. Mean nucleus areas were compared by unpaired t-test (p-value <0.05).

The cytoxicity of venom was tested against *Sf*9 insect cells and found to produce a small but significant decrease in viability (Figure 10). It is yet to be determined what causes the cell death and whether haemocytes are more susceptible to the effects of venom than *Sf*9 insect cells.

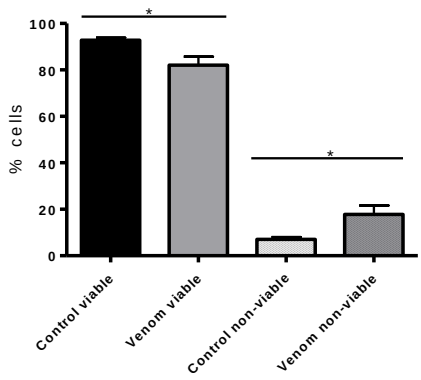

Figure 10: Venom decreases *Sf*9 insect cell viability. Incubation of venom (8vse) with *Sf*9 insect cells decreased cell viability in 30 min, detected by trypan blue staining.

Analysis of total venom: Laypersons' summary

Total venom was extracted from the venom sac of the wasp, *Diadegma semiclausum*. Analysis of proteins in the venom showed that there were at least 3 distinct mid-sized proteins and a high abundance of smaller proteins. We estimate that total venom is composed of between 10-20 different proteins. When the total venom was applied to blood cells of DBM and Cabbage white butterfly or to Sf9 insect cells, in each case, deleterious effects were observed. The most obvious effects were that:

- some venom components entered the DBM and cabbage white butterfly cells
- caterpillar blood cells were not able to "spread" on foreign surfaces (which indicates immune-suppression)
- nucleus size was reduced in treated blood cells
- venom reduced viability of cultured *Sf*9 insect cells

These experiments have shown that the venom is complex and causes pathology in caterpillar blood cells and cultured insect cells, including effects that are clearly immune-suppressive. Therefore, the venom is likely to contain a range of compounds that could be used to target the two key caterpillar pests of Brassica crops, DBM and Cabbage white butterfly.

CHAPTER 3: Analysis of *Diadegma semiclausum* Venom Gland cDNA (gene) Library and Synthesised Peptides (results and discussion)

A cDNA (gene) library was constructed using RNA extracted from the venom gland of *D. semiclausum.* Library clones were sequenced by the AGRF. NCBI's ORF finder was used to detect open reading frames and SignalP 3.0 was used to determine if an N-terminal signal peptide was present as venom proteins will most likely require a signal peptide for secretion from the venom gland. Other transcripts that do not contain a signal peptide are likely to be housekeeping proteins. 9 putative venom protein sequences have been obtained from sequencing approximately 30 clones from the cDNA library (Table 4).

As described in Table 4, all of the discovered open reading frames encode what appear to be relatively small proteins, less than or equal to ~20kDa. The process by which the library is constructed should only produce full length cDNA transcripts but the process does favour smaller transcripts that amplify and ligate more efficiently. This may make it difficult to find clones with larger cDNA inserts. The theoretical isoelectric points (PI) calculated without the signal peptide ranged from acidic to basic. The high abundance of these low molecular weight proteins or peptides is in contrast with an early study comparing the venom profiles from various Hymenoptera (59). In this study it was shown that the presence of low molecular weight proteins and peptides was more typical of bees, ants and social wasps whereas two ichneumonid egg parasitoids (*Chelonus* sp.) included in the study lacked these as did the other braconid parasitoid wasps, *Microplitis* sp. and *Cotesia congregata*, and 2 other unknown species of ichneumonid wasps. Furthermore, the venom of a *Chelonus sp*. was found to be primarily acidic by isoelectric focussing whereas the putative venom proteins discussed here are predicted to range between acidic to basic.

The range of proteins identified from sequencing just a fraction of the clones from the cDNA library suggests that the venom is more complex than it appears when analysed by gel electrophoresis methods. Tris-tricine PAGE did not show an abundance of proteins in the range of 5-15kDa as many of the putative venom cDNAs appear to be. There was however a very large amount of peptide ~3kDa and it appears possible that some of the putative venom cDNAs could be processed into smaller peptide products that could account for this material.

Many secreted proteins such as antimicrobials, neuropeptides, hormones and growth factors are synthesised as inactive precursors (pre-proproteins) (60). Once the signal peptide has been removed to reveal the proprotein, further post-translational processing can occur including cleavage by proprotein convertases (PCs) to release bioactive peptides. Pro-regions are thought to be involved with folding the active proteins correctly or their transport and localisation. These regions can also consist of recognition signals for proteases to covert the proproteins into mature products. Cleavage often occurs at motifs that contain multiple basic residues and can produce diverse molecules from a single multifunctional precursor. Neuropred can be used to predict such cleavages and was developed using insect, mammal and mollusk cleavage data and sites were common in many of the putative venom cDNAs (31). Further processing of the cDNAs could account for the large amount of low molecular weight material observed by PAGE. Unfortunately pro-regions cannot be distinguished from the active peptides by sequence alone. Where possible, the predicted cleavage products were commercially synthesised for further study.

Venom Protein	Amino Acid Sequence	Theoretical PI	Theoretical MW (kDa)
DsVn1	**MKLHFGIIFFVLALVFAVGQATA**EEAGAEADTM VRRDADGKFYASRGKRSPDPSILDVITDLVNKAM DATG	4.57	5.14
DsVn2	**MNVRFGIIFLVVASVFAISHVNC**EEANAETMVRR EAAAAGLEEIHEQSKRSPATKAGIIAKIQEMIKARQ GRSAEAMNMDRARRNPDPSILDVITDLVNKAMDA TG	5.84	9.04
DsVn3	**MNVRFGIIFLIVAMVFAIGQVSS**EEAEAETMVRR EASPTYAAAVNKAYTPGKRSADPLDAKKFLAELK KRLGRSADPGKIMDKLVQMIKSRLGRKAERSADP DPDPGMLDLMKNIPFIGKFL	9.6	10.96
DsVn4	**MSGFLVLVCMVAVSVAVES**AELRARRSPLNPKLL GSLVGKRDAESAENRARRSPISTAALASLAGKRDV QAAELRARRSPLNPKLLGSLVGKREAESADNRAR RSPLSAGALASLAGKRDVQAAELRARRSPLNPKLL GSLVGKRDAESADNRARRSPLSAGALASLAGKRD VQAAELRARRSPLNPKLLGSLVGKRDV	11.76	19.06
DsVn5	**MTKVLMTLFLVLMIASFVVC**GTGECALKGKKCG HNTPCCLPLMCNFYVRRCMK	9.13	3.66
DsVn6	**MNVRFGIIFLLVAMVFAIGQVSS**EEAEAETMVRR EAAAAGLQEMHAESKRNADPLNAAALIAALKKRL GRSADPGKVSVHDFLAAMQGRKGRKAERSPSADP DPGMLDFMKDLPFIGGFMG	7.04	10.48
DsVn7	MMEVYFGIIFFVLAVAWCGGEISPDELLVVKSHLD L	4.31	1.807
DsVnADAMTS	MTPAAQLSRHGFRWSKCSKRYFDRYFKSSASQCL DDKPLWMTIRGENLPGRWLTLDGQCRNSGMERG CEVPNLPFCFVKGCKAENSDECVVDQWQTLPGTK CGDQKICDAKRACVKV	8.86	13.32
DsVnWD	**MLPAAMAAAGIRLSSG**INAECKYTIQEEGHSDWV SCVRFSPNHANPIIVSAGWDRVVKVWNLTNCRLKI NHNGHGGYLNTVTVSPDGSLCASGGKDCKAMLW DLNDGKHLHTLEHNDIITALCFSPNRYWLCAAFGP WIKIWDLESKEMVDELKPDVIVPMNNKAEPPQCLS LAWSTDGQTLFAGYSDNTIRVWQVSVSSCH	5.86	20.83

Table 4: Amino acid sequences of translated ORFs from cDNA clones that contained a predicted signal peptide for secretion shown in bold. Theoretical isoelectric points (pI) and molecular weights were calculated using the ExPASy Protparam tool and predictions did not include the signal sequences.

Further investigations into each of the identified *D. semiclausum* venom cDNA sequences (DsVns) will now be described individually.

DsVn1

The DsVn1 sequence was the most abundant within the clones sequenced from the cDNA library. BLASTP analysis of DsVn1 against the NCBI database did not return any significant matches. While no proteins in the NCBI database appeared similar to DsVn1, when DsVn1, 2, 3 and 6 were aligned using ClustalW similarities between the proteins could be seen particularly in the N-terminal and C-terminal regions (Figure 11). DsVn1 and 2 share a similar C-terminus and likewise DsVn3 and 6. DsVn3 and 6 also have a more similar middle region although comparisons with DsVn2 can still be drawn. It would appear that these proteins are variations upon each other with DsVn1 being the most simplified version.

```
                 ....|....| ....|....| ....|....| ....|....| ....|....|
                         10         20         30         40         50
DsVn1            MKLHFGIIFF VLALVFAVGQ ATAEEAGAEA DTMVRRDAD- --GK------
DsVn2            MNVRFGIIFL VVASVFAISH VNCEEA--NA ETMVRREAA- --AAGLEEIH
DsVn3            MNVRFGIIFL IVAMVFAIGQ VSSEEA--EA ETMVRREASP TYAAAVNKAY
DsVn6            MNVRFGIIFL LVAMVFAIGQ VSSEEA--EA ETMVRREAA- --AAGLQEMH
Consensus        *:::*****: ::* ***:.: ...***  :* :*****:*     .

                 ....|....| ....|....| ....|....| ....|....| ....|....|
                         60         70         80         90        100
DsVn1            ---------- ---------- ---------- ---------- -FYASR----
DsVn2            EQSKRSPATK AGIIAKIQEM IKARQGRSAE ---------- AMNMDR----
DsVn3            TPGKRSADPL D--AKKFLAE LKKRLGRSAD PGKI-MDKLV QMIKSRLGRK
DsVn6            AESKRNADPL N--AAALIAA LKKRLGRSAD PGKVSVHDFL AAMQGRKGRK
Consensus                                                     .*

                 ....|....| ....|....| ....|....| .
                        110        120        130
DsVn1            GKRS----PD PSILDVITDL --VNKAMDAT G
DsVn2            ARRN----PD PSILDVITDL --VNKAMDAT G
DsVn3            AERSADPDPD PGMLDLMKNI PFIGKFL--- -
DsVn6            AERSPSADPD PGMLDFMKDL PFIGGFMG-- -
Consensus        ..*.    ** *.:**.:.::   :.  :
```

Figure 11: ClustalW alignment of putative venom proteins DsVn1, 2, 3 and 6. Signal sequences are underlined

DsVn1 contains a number of dibasic amino acid sites and analysis by NeuroPred suggested 2 likely cleavage sites (Figure 12). The peptide DADGKFYASRGKR was of interest as this peptide revealed a C-terminal amidation site (GKR) which is a common post-translational modification of biologically active peptides. Biotin-DADGKFYASR-NH2 (Peptide 5) was synthesised by Mimotopes however to date, no functional effects have been observed. The C-terminal peptide (SPDPSILDVITDLVNKAMDATG) also appears interesting since it is common to DsVn1 and DsVn2 with only the substitution of asparagine for serine (both uncharged polar amino acids) at the N-terminus. Furthermore, modeling of the peptide structure by I-tasser suggested that this peptide formed an amphipathic helix in which hydrophobic residues align on one side of the helix (Figure 13). Although many amphipathic structures interact with membranes, the net negative charge of this peptide could indicate an interaction with the membrane is unlikely this case. Unfortunately this peptide could not be synthesised.

```
Sequence   EEAGAEADTM VRRDADGKFY ASRGKRSPDP SILDVITDLV NKAMDATG
Mollusc    .......... .r........ ..r.rC.... .......... ........
Mammal     .......... .rC....... ..r.rC.... .......... ........
Insect     .......... .rC....... ..r.rC.... .......... ........
Consensus  .......... .rC....... ..r.rC.... .......... ........
```

Figure 12: Cleavage of DsVn1 predicted by Neuropred. Cleavage sites are indicated by 'C'. Peptide 5 was synthesised by Mimotopes and is highlighted in yellow.

Figure 13: I-tasser model of the C-terminal peptide of DsVn1 (SPDPSILDVITDLVNKAMDATG) shows an amphipathic helix where hydrophobic residues (green) are aligned on one side of the helix. Uncharged polar residues are shown in cyan, negatively charged residues in red, positively charged residues in blue and proline in yellow.

Full length DsVn1 is being investigated by producing recombinant protein in both *E. coli* and *Sf*9 insect cells. However, technical trouble has been encountered with expression in *E. coli* where DsVn1 was expressed with a larger fusion protein that requires cleaving to release DsVn1. DsVn1 was expressed in *Sf*9 insect cells using baculovirus infection (Figure 14). However, while the protein did appear to be expressed it did not seem to be highly secreted from the cells making it unclear whether the pre-proprotein had been processed into a mature form.

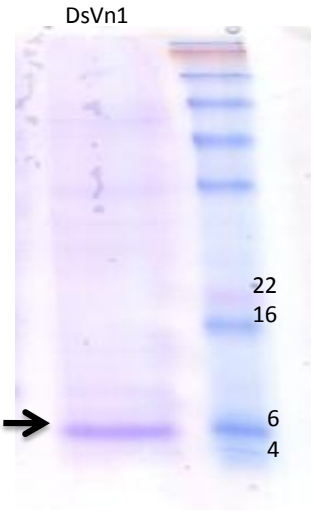

Figure 14: His-tagged (C-terminus) DsVn1 was expressed in *Sf*9 insect cells using recombinant baculovirus . Left lane: Partially purified His-tagged DsVn1 (arrow) from infected *Sf*9 insect cell lysate captured with Ni-resin (Bio-rad). Right lane: Invitrogen protein standards with sizes (kDa) indicated. Predicted MW of His-tagged DsVn1 with signal sequence is 8.4kDa.

DsVn2

As discussed for DsVn1, DsVn2 shares similarities with DsVn1, DsVn3 and DsVn6. Again, BlastP of the NCBI database did not return any significant matches. Amplification of DsVn2 from genomic wasp DNA generated a fragment 697bp long, approximately double the length of the cDNA. Sequencing of this cloned fragment revealed the presence of 3 introns between the 4 exons encoding DsVn2 (Figure 15).

```
atgaacgttcgttttggaataatatttttggtcgtggcgtcggtgttcgccatcagccat
 M  N  V  R  F  G  I  I  F  L  V  V  A  S  V  F  A  I  S  H
gtcaactgcgaggaagccaatgccgaaaccatggtccgccgggaagctgctgccgcaggg
 V  N  C  E  E  A  N  A  E  T  M  V  R  R  E  A  A  A  A  G
ttggaagaaatacatgaacaaagcaaacggtaacgaagtcattcaaaatcgctcaacaaa
 L  E  E  I  H  E  Q  S  K  R  -  -  -  -  -  -  -  -  -  -
ttactcatttttcggacaatcttcgtaattaccttcttgataatcaattaaaaaaaaat
 -  -  -  -  -  -  -  -  -  -  -  -  -  -  -  -  -  -  -  -
agaaaaaaaaattgacatttcacgatgttctcccatgaaaacgaaatttttctatttctt
 -  -  -  -  -  -  -  -  -  -  -  -  -  -  -  -  -  -  -  -
aatatttgaaaactggaaatttgcagaagtcccgcaacaaaagcagggatcattgcaaaa
 -  -  -  -  -  -  -  -  -  -  S  P  A  T  K  A  G  I  I  A  K
attcaagaaatgataaagtaagtcacgaaataattgtttgccgtttgaatatttatgtaa
 I  Q  E  M  I  K  -  -  -  -  -  -  -  -  -  -  -  -  -  -
acgtaagttattgatatgattatttttatttttttattttcaaggGCAAGGCAAGGAAGG
 -  -  -  -  -  -  -  -  -  -  -  -  -  -  -  -  A  R  Q  G  R
agcgctgaagcaatgaacatggaccgtgctcgtcggtaagaaaattcataacgacgatgc
 S  A  E  A  M  N  M  D  R  A  R  R  -  -  -  -  -  -  -  -  -
aatagagaattcgagccattaagaaaccataaaataagaatttcatgaatcgttttattc
 -  -  -  -  -  -  -  -  -  -  -  -  -  -  -  -  -  -  -  -  -
ttcctcatgccacgtcaatccgcagtaatcctgatccaagtattttggacgttatcactg
 -  -  -  -  -  -  -  -  -     N  P  D  P  S  I  L  D  V  I  T
acctcgtcaacaaagccatggacgctactgg
D  L  V  N  K  A  M  D  A  T  G
```

Figure 15: Genomic DNA sequence of DsVn2 showing the presence of 3 introns. Exons are highlighted in bold.

DsVn2 was also predicted to contain 3 potential peptide cleavage sites to yield a possible 4 peptides (Figure 16). Of the 4 predicted peptides only 1 could be synthesised.

```
Sequence  EEANAETMVR REAAAAGLEE IHEQSKRSPA TKAGIIAKIQ EMIKARQGRS
Insect    .........r .......... .....rC... .......... .....r..C.
Consensus .........r .......... .....rC... .......... .....r..C.
Sequence  AEAMNMDRAR RNPDPSILDV ITDLVNKAMD ATG
Insect    .......r.r C......... .......... ...
Consensus .......r.r C......... .......... ...
```

Figure 16: Cleavage prediction for DsVn2 by Neuropred. Cleavage sites are indicated by 'C'. Peptide 2 is shown highlighted in yellow.

The following peptide of DsVn2 (SPATKAGIIAKIQEMIKARQGR) has a molecular weight of 2.368kDa and pI of 11.1. Biotin-SPATKAGIIAKIQEMIKARQGR-OH was synthesised by Mimotopes as Peptide 2. When Peptide 2 was incubated with *Pieris* haemocytes, staining with TRITC-neutravidin was significantly more intense suggesting peptide 2 was interacting with the haemocytes (Figure 17) and there was a number of particularly bright cells which were small, round and clearly absent in control experiments (Figure 18). In some cases it appeared the peptide was concentrated within the nucleus (Figure 19). Furthermore, where the peptide was concentrated in the

nucleus, FITC-Phalloidin staining was weak suggesting the absence of F-actin. The small, round, intensely stained TRITC-neutravidin cells could be dead, however, Peptide 2 (60µM) did not appear to have any effect on *Sf*9 cell viability under the conditions tested (Figure 27).

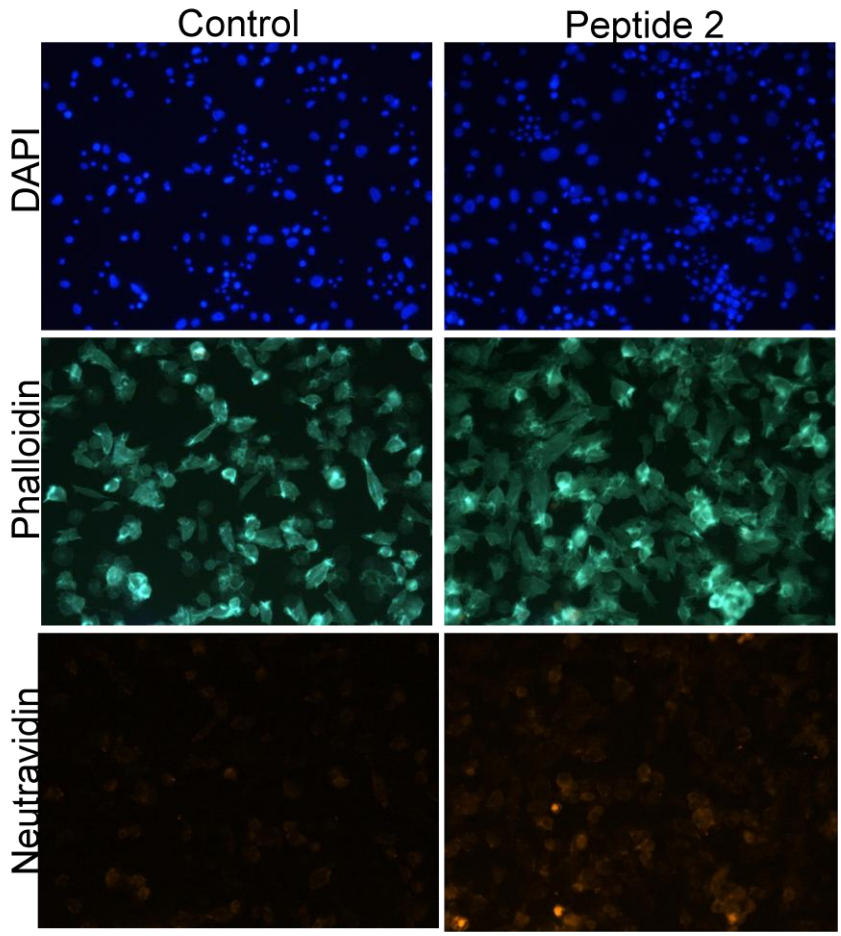

Figure 17: Peptide 2 from DsVn2 accumulates in haemocytes. Peptide 2 (143µM) was incubated with *Pieris* haemocytes spread on a printed glass slide for 2 hours. The cells were then fixed and made permeable. Biotin-tagged peptide 2 was detected using TRITC-neutravidin (coloured orange), FITC-phalloidin was used to show F-actin (green) and DAPI to stain the nucleus (blue). Images were taken using a 20x objective lens.

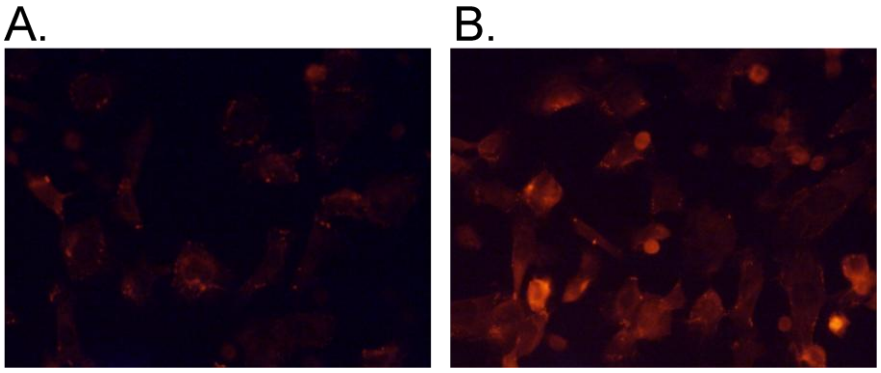

Figure 18: Staining with TRITC-Neutravidin is brighter in cells treated with peptide 2. Peptide 2 (143µM) was incubated with *Pieris* haemocytes spread on a printed glass slide for 2 hours, shown in (B). Control cells were similarly treated in the absence of peptide, shown in (A). The cells were then fixed and made permeable. Biotin-tagged peptide 2 was detected using TRITC-neutravidin (coloured orange), FITC-phalloidin was used to show F-actin (green) and DAPI to stain the nucleus (blue). Images were taken using a 40x objective lens.

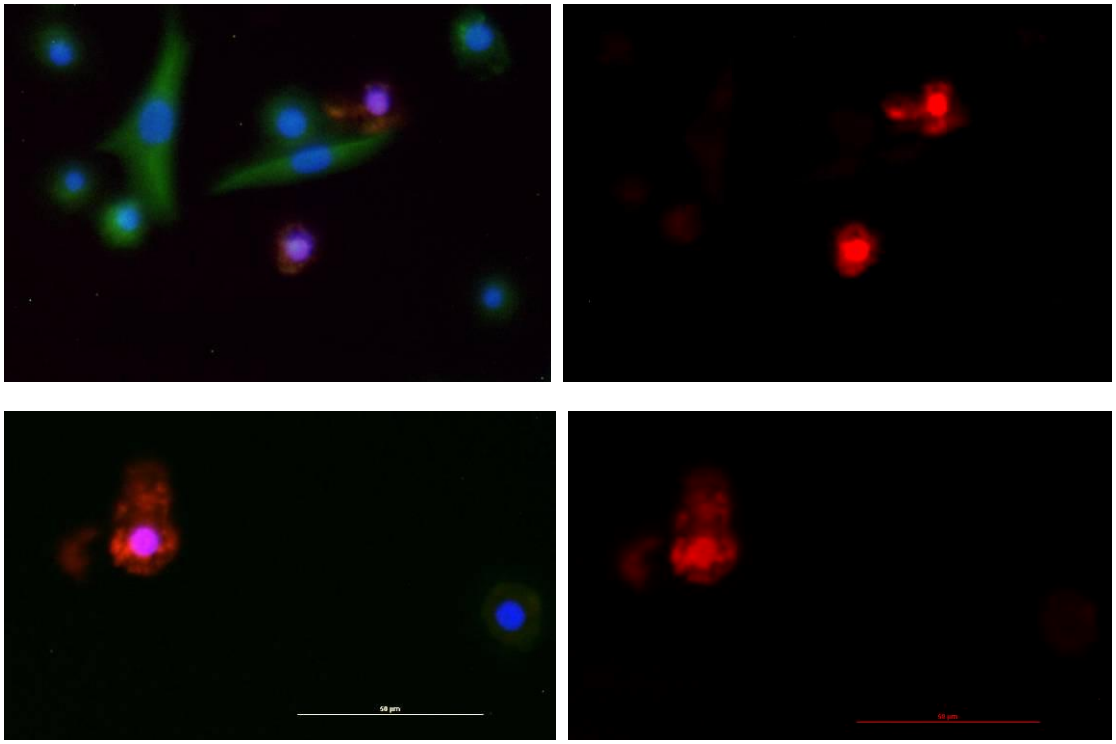

Figure 19: Examples of Peptide 2 from DsVn2 accumulates in haemocyte nucleus. Peptide 2 (111µM) was incubated with *Pieris* haemocytes spread on a printed glass slide for 2 hours. The cells were then fixed and permeabilised. Biotin-tagged peptide 2 was detected using TRITC-neutravidin (red), FITC-phalloidin was used to show F-actin (green) and DAPI to stain the nucleus (blue). Peptide 2 appeared to accumulate in the nucleus of some haemocytes in which F-actin staining was also weak. Scale bar shows 50µm.

The antimicrobial peptide database found peptide 2 to be similar to PGLa, a 21aa peptide from the South African clawed frog, *Xenopus laevis* (Figure 20). PGLa is active against gram negative and positive bacteria. However, no antimicrobial activity of peptide 2 (or any other peptide) was detected against various species of bacteria (gram positive or negative; see Antimicrobial assays below).

```
                 ....|....| ....|....| ...
                          10         20
PGLa             GMASKAGAIA GKIAKVALKA L--
Peptide 2        SPATKAGIIA -KIQEMIKAR QGR
Clustal Co       . *:*** **  ** ::
```

Figure 20: Alignment of peptide with antimicrobial peptide PGLa

Full length constructs for expression of DsVn2 have been made for *E. coli* and *Sf*9 insect cell expression. DsVn2 has been expressed as a fusion protein in *E.coli* and attempts are now being made to separate DsVn2 from the fusion protein.

DsVn3

Like DsVn1, and DsVn2, no proteins in the NCBI database were identified using BlastP that shared a significantly similar amount of sequence with DsVn3. NeuroPred predicted a number of potential cleavage sites within DsVn3 (Figure 21). Cleavage at these sites exposes a C-terminal amidation site on the first peptide (EEAEAETMVRREASPTYAAAVNKAYTP-NH2) which suggests this could be an active peptide. However, we were unable to have this peptide synthesised.

```
Sequence EEAEAETMVR REASPTYAAA VNKAYTPGKR SADPLDAKKF LAELKKRLGR
Insect   .........r .......... ........rC .......rC. ....r.C..C
Sequence SADPGKIMDK LVQMIKSRLG RKAERSADPD PDPGMLDLMK NIPFIGKFL
Insect   .......... .......r.. .......... .......... .........
```

Figure 21: Prediction of cleavage sites in DsVn3 by NeuroPred. Cleavage sites are indictated by 'C'. Synthesised peptide 6 is highlighted in yellow.

The C-terminal peptide from DsVn3 was synthesised by Mimotopes (Biotin-SADPGKIMDKLVQMIKSRLGRKAERSADPDPDPGMLDLMKNIPFIGKFL-OH) as peptide 6. Peptide 6 has similarities with the C-terminal peptide of DsVn6 and contains a low complexity region in the middle.

Application of peptide 6 to *Pieris* haemocytes produced significantly brighter red signals in some cells which were particularly small and round and absent from control cells (Figure 22). It is also possible that the green phalloidin signal is also less intense than in control cells. On closer examination it is even more evident that TRITC-neutravidin staining is more intense in small round cells and also appears more evenly distributed through the plasmatocytes compared to control cells (Figure 23). Examination of the small, round, intensely neutravidin stained cells shows this staining to be in the cytoplasm surrounding the nucleus suggesting that peptide 6 exerts its activity here (Figure 24).

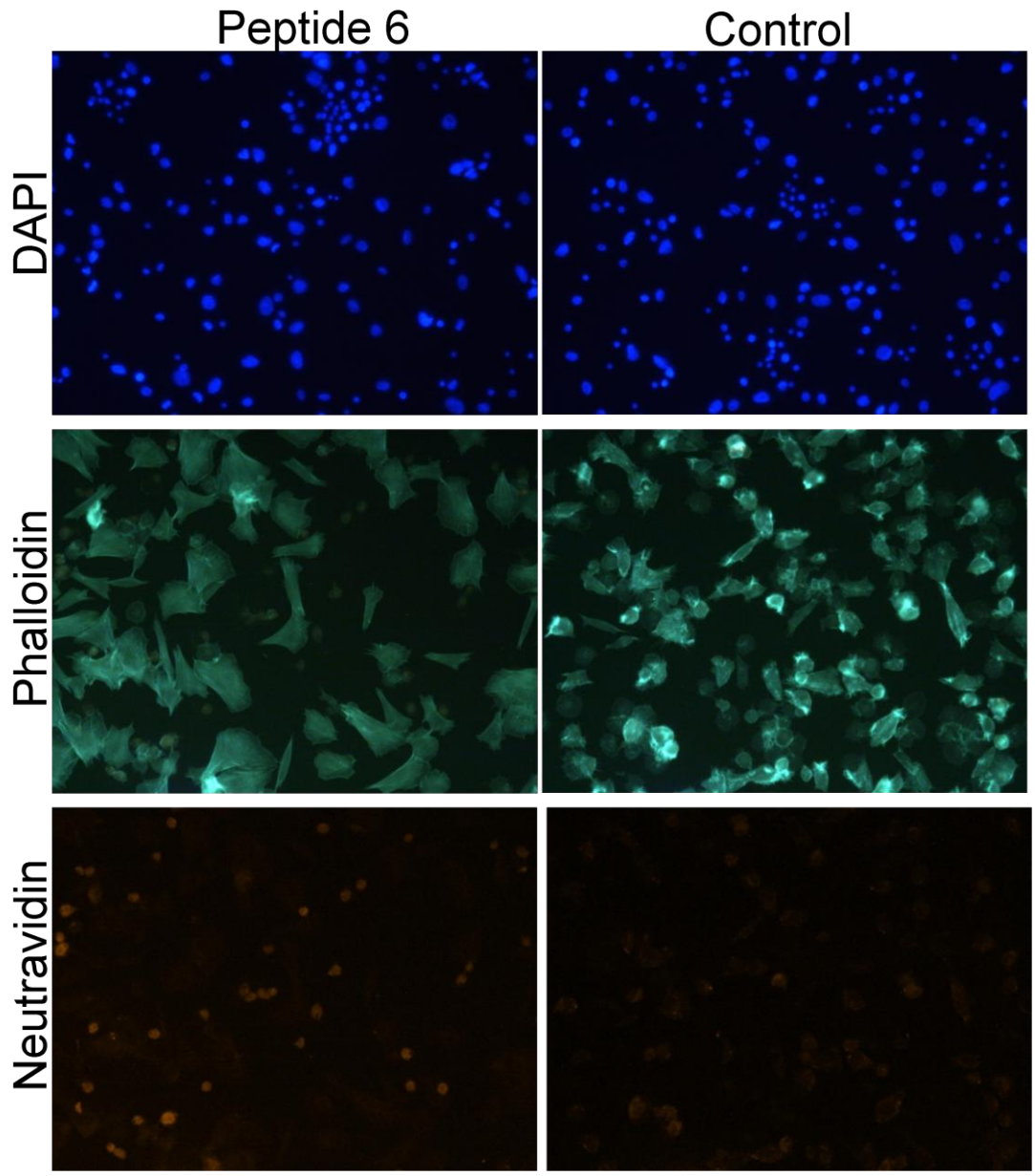

Figure 22: Peptide 6 from DsVn3 accumulates in some haemocytes. Peptide 6 (77µM) was incubated with *Pieris* haemocytes spread on a printed glass slide for 2 hours. The cells were then fixed and made permeable. Biotin-tagged peptide 2 was detected using TRITC-neutravidin (coloured orange), FITC-phalloidin was used to show F-actin (green) and DAPI to stain the nucleus (blue). Images were taken using a 20x objective lens.

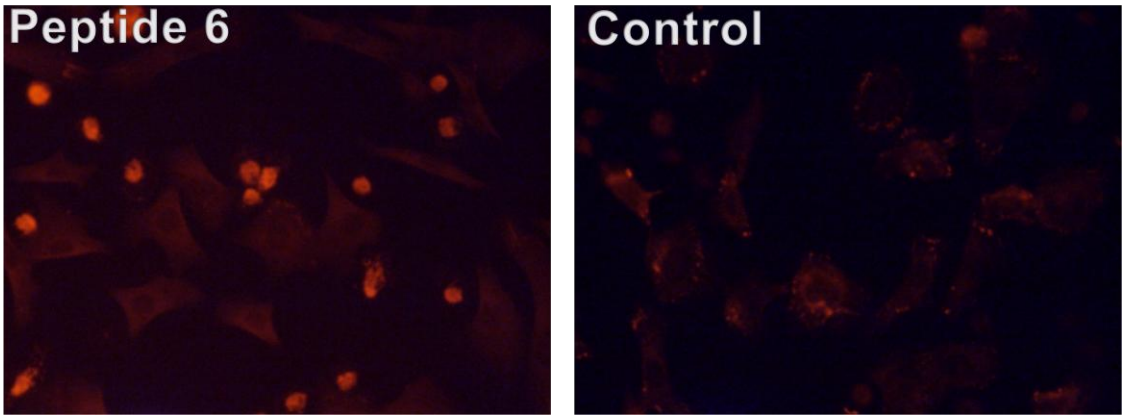

Figure 23 Staining with TRITC-Neutravidin is brighter in cells treated with peptide 6. *Pieris* haemocytes spread on a printed glass slide were treated with or without Peptide 6 (77µM) and incubated for 2 hours. The cells were then fixed and made permeable. Biotin-tagged peptide 6 was detected using TRITC-neutravidin which appears as red.

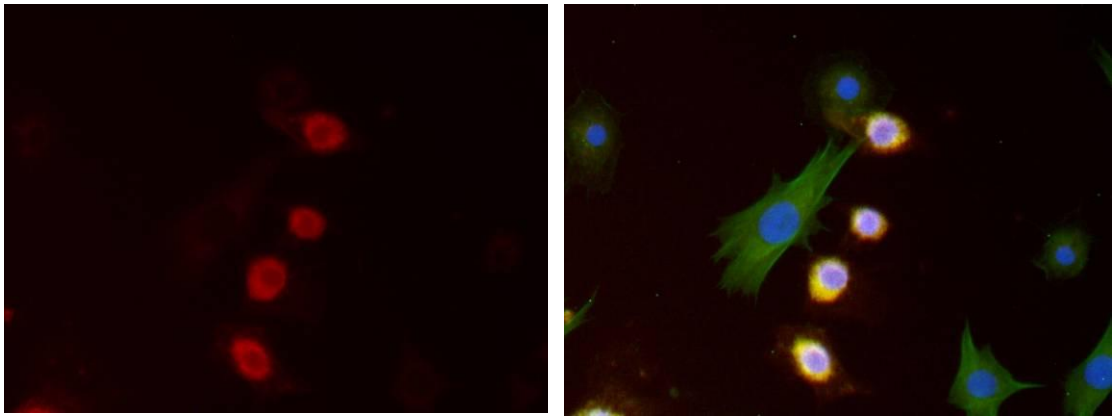

Figure 24: Peptide 6 accumulates within the cytoplasm of some haemocytes. *P. rapae* haemocytes were allowed to spread on a glass slide. Peptide 6 (75uM) was added and incubated 2 hours. Cells were then fixed and permeabilised. Biotin-tagged peptide was detected using TRITC-neutravidin (red) shown left. F-actin was detected using FITC-phalloidin (green) and the nucleus was stained with DAPI (blue) and the right image shows these features overlayed on the TRITC-neutravidin image.

Treatment of haemocytes with peptide 6 also reduced their viability as shown by propidium iodide staining (Figure 25). Quantitation of viable and non-viable cells showed that there was a significant difference between control and peptide 6 treatments (Figure 26). It is possible that the intensely stained cells from Figure 22 are dead.

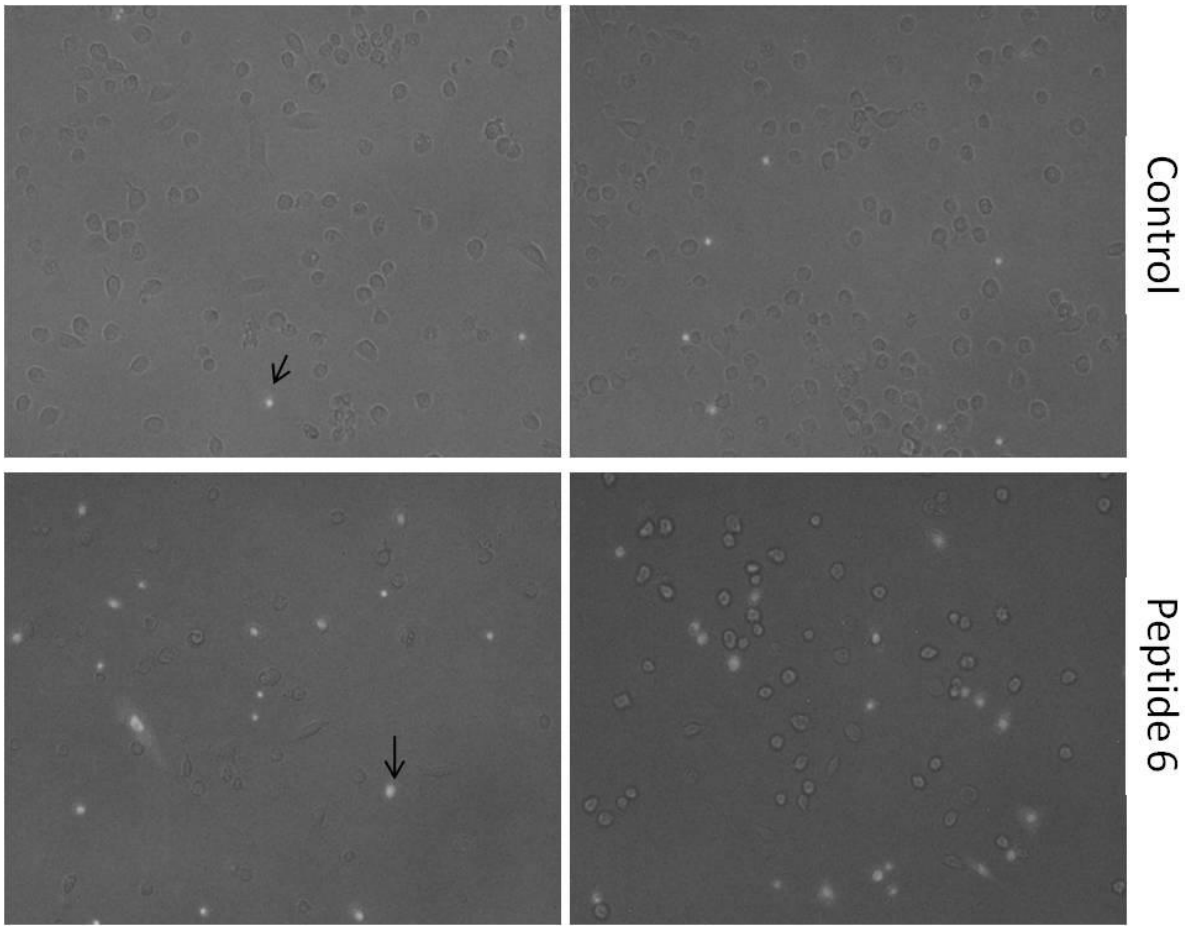

Figure 25: The presence of Peptide 6 caused significantly more cell death than in the absence of peptide 6 (control). *Pieris* hemoctyes were allowed to spread before the addition of peptide 6 in PBS or an equivalent amount of PBS with 0.01mg/ml propidium iodide. Images were taken 15 min later. Bright spots (examples indicated with arrows) show propidium iodide staining of non-viable (permeable) cells.

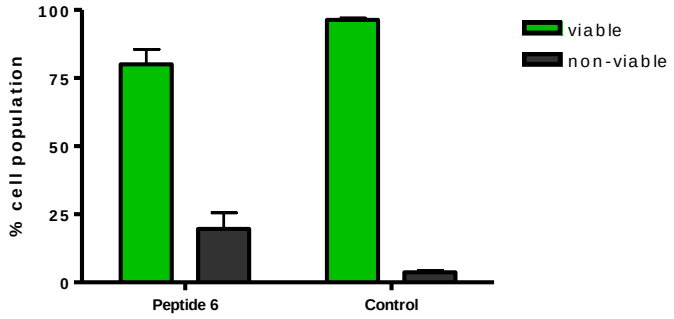

Figure 26: Significantly less haemocytes were viable once treated with peptide 6 compared to the haemocytes in the control treatment.

Peptide 6 was also observed to have a significant effect on the viability of *Sf*9 insect cells. After 4 hours incubation of cells with 30uM peptide 6, cell viability was almost 50% less than control cells (Figure 27A). A dose response curve to peptide 6 suggests an EC_{50} of 3.6uM (Figure 27C) and the effect appears to occur rapidly (Figure 27B). Again, it appears that not all *Sf*9 insect cells are

susceptible to the effect of peptide 6 as 50% of cells remained viable even at high concentrations of peptide 6 and longer incubation times.

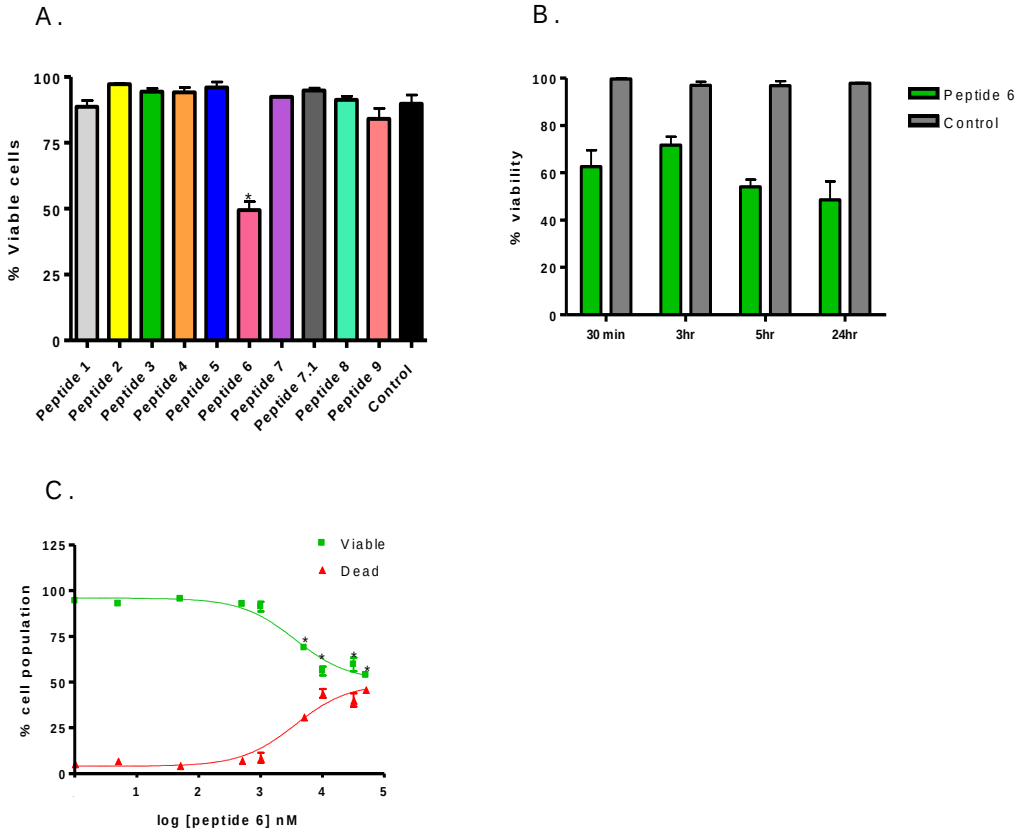

Figure 27: Peptide 6 reduces *Sf*9 insect cell viability. A. 30µM peptide 6 decreased cell viability by ~50% after 4 hours whereas other peptides had no effect and were similar to the control (equal volume of water). B. Viability of *Sf*9 insect cells incubated with peptide 6 and without (control) over time. C. Dose response curve of *Sf*9 insect cells to peptide 6 (0-50µM) indicated an EC_{50} of 3.6µM. Concentrations that resulted in significant differences from the absence of peptide 6 are indicated (*).

Although Peptide 6 appears to be able to penetrate insect cells, no antibacterial effects were observed.

DsVn4

DsVn4 is made up of repeating units as shown by results from RADAR (http://www.ebi.ac.uk/Tools/Radar) for de novo repeat detection (Figure 28). Repetitive domains in some proteins have been suggested to act as immunomodulators (61). Structural proteins were also predominant in the proteins found to contain long oligopeptide repeats including silk moth fibroins and *Drosophila* salivary glue proteins. It is also worthy of note that a venom protein from a parasitic wasp (*Chelonus* sp.) has been identified that contained a dozen tandem repeats of a 14-residue sequence thought to have occurred by internal duplication and it was proposed that venom proteins prone to mutation through internal duplications and deletions will enable the parasite to keep pace with a host under selection pressure to evade the action of that protein (62). Highly mutable venom proteins may also have provided mechanisms for evolution and the development of wasps with venom effective against various hosts. The repeats within DsVn4 and similarities between DsVn1,2,3 and 6 may be further evidence for the importance of this.

```
RADAR
--------------------------------------------------------------------------------
No. of Repeats|Total Score|Length  |Diagonal| BW-From|   BW-To|   Level
             7|     334.88|      22|      24|      79|     100|       1
--------------------------------------------------------------------------------
    1-   22 (49.89/16.95)  AELRARRSPLNPKLLGSLVGKR
   27-   48 (43.57/14.20)  AENRARRSPISTAALASLAGKR
   53-   74 (49.89/16.95)  AELRARRSPLNPKLLGSLVGKR
   79-  100 (45.88/15.21)  ADNRARRSPLSAGALASLAGKR
  105-  126 (49.89/16.95)  AELRARRSPLNPKLLGSLVGKR
  131-  152 (45.88/15.21)  ADNRARRSPLSAGALASLAGKR
  157-  178 (49.89/16.95)  AELRARRSPLNPKLLGSLVGKR
--------------------------------------------------------------------------------
```

Figure 28: RADAR results showing the presence of repeats within DsVn4

BlastP search of the NCBI database shows DsVn4 to be most similar to conserved hypothetical proteins produced by *Trypanosoma Brucei*. *Trypanosoma Brucei* is an obligate parasite with 2 hosts; an insect vector (Tsetse fly) and a mammalian host including humans in which it causes African sleeping sickness. Sequences with less significant similarity include egg protein SP1531 from the parasitic flatworm, *Schistosoma japonicum*, wghich alternates between a mammalian host in which eggs are laid and a snail host. DSC-1 from *Lymnaea stagnalis* (a snail) also showed a small amount of similarity and contained a cleavable signal peptide and repeating units. Finally a small amount of similarity was found with a variant of the kassinin precursor from *Kassina senegalensis* (frog). On closer inspection, it appears one of the peptides liberated by cleavage of DsVn4 is highly similar to a peptide predicted to be produced by the kassinin precursor (discussed further later).

I-tasser modelling of DsVn4 produced a model that was most similar to ankyrin (8/10 matches) although the model did not have a particularly high confidence score (Figure 29). Furthermore, FUGUE also found ankyrin repeat domains (that form solenoid structures) to share structure homology with DsVn4. Also in agreement with the predicted model by I-tasser, REPETITA repeat detection found DsVn4 to have a solenoid structure. The non-globular shape of solenoid proteins is thought to facilitate protein-protein interactions (63).

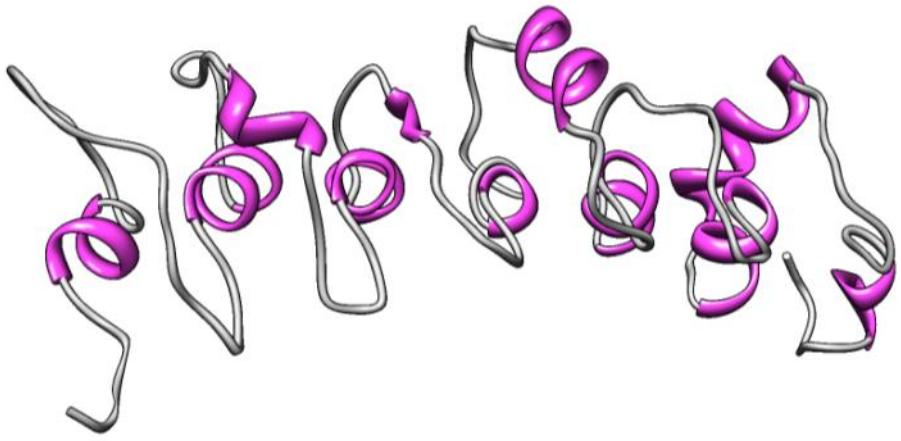

Figure 29: I-tasser model of DsVn4 (C-score -2.31)

The potential of DsVn4 to be a precursor protein was investigated by identifying potential cleavage sites of protein convertases and furins. NeuroPred predicts 14 cleavage points that highlight the repeating nature of DsVn4 as cleavage would yield a number of peptides multiple times (Figure 30). Six unique peptides would be produced from cleavage of DsVn4 and 3 of the predicted peptides from DsVn4 were able to be synthesised by Mimotopes. These are Peptide 1 (Biotin-SPLNPKLLGSLV-NH2), Peptide 3 (Biotin-SPISTAALASLA-NH2) and Peptide 7 (BIOTIN-SPLSAGALASLA-NH2).

```
Sequence  AELRARRSPL NPKLLGSLVG KRDAESAENR ARRSPISTAA LASLAGKRDV
Insect    ...r.rC... .......... rC.......r .rC....... ......rC..
Consensus ...r.rC... .......... rC.......r .rC....... ......rC..
Sequence  QAAELRARRS PLNPKLLGSL VGKREAESAD NRARRSPLSA GALASLAGKR
Insect    .....r.rC. .......... ..rC...... .r.rC..... ........rC
Consensus .....r.rC. .......... ..rC...... .r.rC..... ........rC
Sequence  DVQAAELRAR RSPLNPKLLG SLVGKRDAES ADNRARRSPL SAGALASLAG
Insect    .......r.r C......... ....rC.... ...r.rC... ..........
Consensus .......r.r C......... ....rC.... ...r.rC... ..........
Sequence  KRDVQAAELR ARRSPLNPKL LGSLVGKRDV
Insect    rC.......r .rC....... ......rC..
Consensus rC.......r .rC....... ......rC..
```

Figure 30: Neuropred cleavage prediction of DsVn4. Cleavage sites are indicated by 'C' and synthesised peptides are highlighted. Peptide 1 is shown in blue, peptide 3 in yellow and peptide 7 in green.

To date, application of synthesised Peptide 1 has had no observable effect on *Pieris* haemocytes, *Sf*9 insect cell viaibility and has not shown any antimicrobial properties.

The peptide SPISTAALASLAGKR is unique within DsVn4, being one of the few peptides not repeated identically. There is a site for C-terminal amidation (GKR) indicating hormone/neuropeptide structural similarities as well. This peptide was synthesised by mimotopes and is referred to as Peptide 3 (Biotin-SPISTAALASLA-NH2). A BLASTp search of the NCBI database identified sequence similarity with the precursor protein of Kassinin, a tachykinin found in the skin secretions of the amphibian *Kassina senegalensis*. Two kassinin precursors have been identified that contain a signal peptide followed by the kassinin domain, and further putative domains separated by typical propeptide convertase sites (64). Cleavage of the preprokassinin2 at these sites yields a peptide that contains a c-terminal amidation signal (APISDALLASLAGKR) and is very similar to Peptide 3 (85%). Likewise, cleavage of preprokassinin 1 also yields a similar product although Ala12 also present in Peptide 3 is substituted for Val. There are 3 other conserved sites between preprokassinin1 and 2 that are not conserved in Peptide 3 as shown by the alignment using ClustalW (Figure 31). The authors report that at the time, no structurally similar peptide could be located in the NCBI database and suggest that this could represent a novel bioactive peptide encoded by 2 skin peptide precursors. It is also noted that the presence of C-terminal amidation site is highly suggestive of a bioactive nature since this motif is a common feature of the majority of invertebrate regulatory proteins.

```
                                    ....|....| ....|
                                            10
Peptide from Preprokassinin1    APISDALLAS LVGKR
Peptide from Preprokassinin2    APISDALLAS LAGKR
Peptide 3 from DsVn4            SPISTAALAS LAGKR
Clustal Consensus               :*** * *** *.***
```

Figure 31: ClustalW alignment of putative peptides from preprokassinins and Peptide 3

```
....|....| ....|....| ....|....| ....|....| ....|....|
                   10         20         30         40         50
Prepro Kas    -MKTLILLTV LACGLLFMAS ST-AADTPKS DQFIG-LMGK RESPDLD---
DsVn4         MSGFLVLVCM VAVSVAVESA ELRARRSPLN PKLLGSLVGK RDAESAENRA
Clustal Co        *:*: : :* .: . :: .  *  :* .  :::* *:** *:: . :


              ....|....| ....|....| ....|....| ....|....| ....|....|
                        60         70         80         90        100
Prepro Kas    KRAPISDALL ASLAGKR--- ---------S VVDDLVN-LM GKREAPDVE-
DsVn4         RRSPISTAAL ASLAGKRDVQ AAELRARRSP LNPKLLGSLV GKREAESADN
Clustal Co    :*:*** * * *******             . :  .*:. *: ***** ..:


              ....|....| ....|....| ....|....| ....|....| ....|....|
                       110        120        130        140        150
Prepro Kas    ---------- ---------- ---------- ---------- ----------
DsVn4         RARRSPLSAG ALASLAGKRD VQAAELRARR SPLNPKLLGS LVGKRDAESA
Clustal Co


              ....|....| ....|....| ....|....| ....|....| ....|....
                       160        170        180        190
Prepro Kas    ---------- ---------- ---------- ---------- ---------
DsVn4         DNRARRSPLS AGALASLAGK RDVQAAELRA RRSPLNPKLL GSLVGKRDV
Clustal Co
```

Figure 32: Alignment of preprokassinin with DsVn4. Signal peptides are shown in red, cleavage signals are highlighted in blue and kassinin is underlined

To date, no effects of peptide 3 have been seen on *Pieris* haemocytes or *Sf*9 insect cells and no antimicrobial activity has been detected.

Peptide SPLSAGALASLAGKR appears twice within DsVn4 and was synthesised by Mimotopes as Peptide 7 (Biotin-SPLSAGALASLA-NH2). To date no biological effects from this peptide have been observed.

Expression of preproDsVn4 has been attempted using baculovirus in *Sf*9 insect cells. However, no expressed protein could be detected even though virus DNA was detected in cells and cells showed infection symptoms. Constructs for ProDsVn4 (no signal peptide) were then attempted for expression in *E. coli*. However, this was technically difficult due to the repeating nature of the protein and to date, a correct construct has not been obtainable.

DsVn5

Cleavage of the signal peptide from preDsVn5 is predicted to release mature DsVn5. Unlike DsVn1, DsVn2, DsVn3 and DsVn4, DsVn5 is unique in that 6 cysteine residues are present and no other cleavage sites are predicted. Cleavage of the signal peptide also reveals a N-myristoylation site, however Myristoylator (http://au.expasy.org/cgi-bin/myristoylator/myristoylator.pl) predicts this site to not be modified. All of the cysteine residues are predicted to be connected by disulfide bonds by Disulfind (http://disulfind.dsi.unifi.it/) and in the predicted configuration the disulphide bonds form an inhibitor cysteine knot (Knottin) (Figure 33). Knottins are small disulfide rich proteins containing an inhibitor cysteine knot that makes the protein very stable. Knotting has been found to have various biological actions including toxicity, inhibitory, anti microbial, insecticidal, cytotoxic or hormone activity. Common examples of knottins include conotoxins, spider toxins and cyclotides from plants. One knottin has reached the market for the treatment of chronic pain (Prialt).

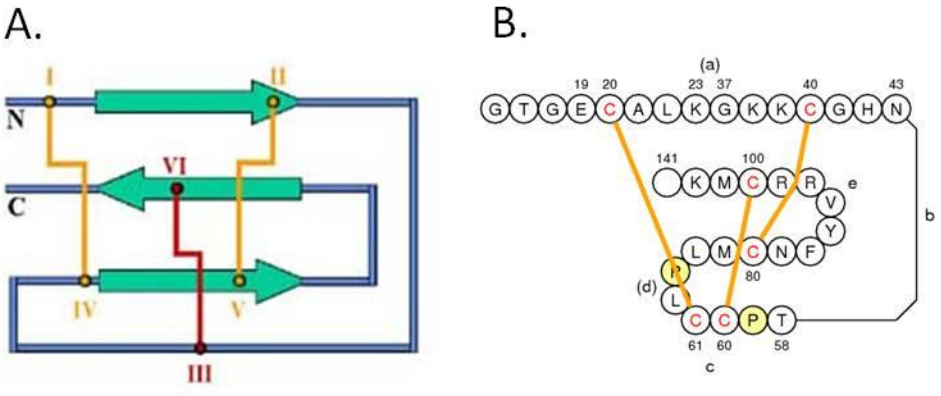

Figure 33: DsVn5 is a potential knottin. A: Diagram of disulphide bond configuration of a knottin. B: Diagram of the predicted arrangement of disulphide bonds of DsVn5.

Analysis by I-tasser generated a 3D model with a C-score of -0.19. The model shows 2 anti-parallel beta strands forming a small double stranded beta sheet near the C-terminus (Figure 34).

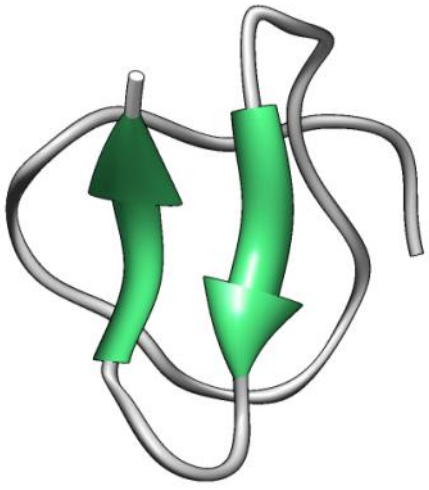

Figure 34: Model of DsVn5 construted by I-tasser (C-score -0.19) shows 2 anti-parallel beta strands forming a small double stranded beta sheet near the N-terminus.

When this structure was compared to structures in the PDB database to find structural analogs, the most significant match was to ADO1 a toxin from the saliva of the Assassin bug, *Agriosphodrus dohrni* (TM score 0.7) (65). Analysis by Phyre and FUGUE also found similarity to this protein. Assassin bugs feed on other insects and some species are blood sucking parasites of mammals. The saliva of assassin bugs contains a mixture of peptides used for immobilizing and digesting prey and as defense against competitors and predators (66). ADO1 has 35 amino acid residues, is cross-linked by 3 disulphide bridges and its 3D structure determined by NMR shows that the protein consists of a compact disulphide bonded core and a β-sheet region made from two antiparallel β-strands making it appear structurally similar to DsVn5 (65). The assassin bug toxins have previously been described as relatively homologous to ω-conotoxins which are neurotoxic peptides isolated from marine cone snails (66).

A comparison of amino acids sequence between DsVn, ADO1 and Iob1 (a toxin from another assassin bug species *I. obscurus*) showed conservation of the cysteine residues as well as a number of other residues thought to interact with the receptor (Figure 35). These assassin bug toxins have been shown to block calcium channel currents with ADO1 preferential blocking P/Q type calcium channel currents while another assassin bug toxin Ptu1 (shown aligned with DsVn 5 (Figure 35)) is more selective for N-type calcium channels. Compared to conotoxins, Ptu1 appears less toxic and its action on specific ion channels was reversible (66).

```
                ....|....| ....|....| ....|....| ....|.
                         10         20         30
DsVn5            -GTGECALKG KKC-GHNTPC CLPLMCNFYV RRCMK-
ADO1             -ADDDCLPRG SKCLGENKQC CKGTTCMFYA NRCVGV
Iob1             GADEDCLPRG SKCLGENKQC CEKTTCMFYA NRCVGI
Consensus         .  :*  :* .** *.*. * *    * **. .**:
```

Figure 35: Alignment of DsVn5 with most closely related proteins ADO1 and Iob1. Conserved cysteine residues are shown (C) and functionally important residues for ADO1 and Iob1 are highlighted (X). Other conserved residues are shown as (X).

```
 ....|....| ....|....| ....|....| ....|
                    10         20         30
DsVn5             GTGECALKGK KC-GHNTPCC LP-LMCNFYV RRCMK
Ptu1              AEKDCIAPGA PCFGTDKPCC NPRAWCSSYA NKCL-
Consensus          .  :*   *   * * :.***  *   *. *. .:*:
```

Figure 36: Alignment of DsVn5 with less closely related protein Ptu1. Conserved cysteine residues are shown (C) and functionally important residues are highlighted (X). Other conserved residues are shown as (X).

OCLP1 (omega-conotoxin like protein1) is a putative protein from the honey bee genome 74 amino acids long consisting of a signal peptide followed by a cysteine rich domain of about 30 amino acids (67). This protein is reported most closely related to the before mentioned assassin bug toxins where the 6 cysteine residues are conserved and some of the residues known to be functionally important (Figure 37). However, OCLP1 is not found in the venom but is expressed in the brain. When injected into fish, OCLP1 caused reversible reduction in locomotor activity. Although most homologs of OCLP1 are reported as voltage gated ion channel inhibitors, homologs from *Anopheles gambiae* and POI from *Musca domestica* have previously been suggested to function as inhibitors of melanisation by inhibiting phenoloxidase (68,69). Alignment of POI with DsVn displays some homology, mostly in the conserved cysteine residues but also near the C-terminus (Figure 38).

```
                 ....|....| ....|....| ....|....| ....|....| ....|....| ....|
                          10         20         30         40         50
DsVn5            GTGECALKGK KCGHNTPCCL PLMCNFYVRR CMK-------- --------- -----
OCLP1            AASKCGRHGD SCVSSSDCCP GTWCHTYANR CQVRITEEELM KQREKILGR KGKDY
Consensus        .:.:*. :*. .*  .: **     *: *..* *
```

Figure 37:Alignment of DsVn5 with less closely related protein OCLP1. Conserved cysteine residues are shown (C) and functionally important residues are highlighted (X). Other conserved residues are shown as (X).

```
                 ....|....| ....|....| ....|....| ....|....
                          10         20         30
DsVn5            -GTG-----E CALKGKKCGH NTPCCLPLMC NFYVRRCMK
POI              AVTDNEIVPQ CLANGSKCYS HDVCCT-KRC HNYAKKCVT
Consensus           *.      : *  :*.**   :  **    * : *.::*:.
```

Figure 38: Alignment of DsVn5 with less closely related protein POI. Conserved cysteine residues are shown (C) and other conserved residues are shown as (X).

Another family of toxins functionally homologous to ω-conotoxins are ω-atracotoxins, peptide neurotoxins from the Australian funnel-web spider that block insect but not vertebrate voltage-gated calcium channels (70). These toxins also contain six conserved cysteine residues that form 3 disulphide bridges in an inhibitory cysteine knot conformation. The 3D structure contains a disulphide rich globular core with a protruding β-hairpin structure common to ω-atracotoxins which differentiates them from ω-conotoxins (71). This structure was found to be indispensible for insecticidal activity of the toxin (71). DsVn5 amino acid sequence can be aligned to ω-atracotoxin HV1A from *Hadronych versuta* showing the conservation of the cysteine residues. However, other highly conserved residues within ω-atracotoxins are not conserved in DsVn5 and the protruding β-hairpin structure is absent (Figure 39). A peptide from *C. rubecula* termed Vn4.6 has previously been found to show similarity to ω-atracotoxins (25%) although not all of the conserved cysteine residues were present in Vn4.6 (72). Vn4.6 was found to inhibit prophenoloxidase (72).

```
                  ....|....| ....|....| ....|....| ....|....|
                           10         20         30         40
DsVn5             GTGECALKGK KCGHNTPCCL PLMCNFY--- ----VRRCMK
w-actx HV1        -SPTCIPSGQ PCPYNENCCS -QSCTFKENE NGNTVKRCD-
Consensus          :  *  .*:  * :*  **     *.*         *:**
```

Figure 39: Alignment of DsVn5 with w-atracotoxin-HV1A. Conserved cysteine residues are shown (C) and functionally important residues are highlighted (X). Other conserved residues are shown as (X) and residues that form the β-hairpin are underlined.

I-tasser incorporates a methodology for annotating biological function using the predicted protein structures and identifying similarities with proteins of known function to report consensus gene ontology terms. High confidence prediction terms for DsVn5 for molecular function were binding and ion channel inhibitor, biological process terms were cellular, pathogenesis and cellular metabolic process and cellular location was predicted as extracellular. ProLoc also predicts DsVn5 as extracellular, probably due to the higher content of disulphide bridges and cysteine residues which further corroborates evidence of DsVn5 being an inhibitor or toxin.

Other proteins found to have similar structures included insulin-like growth factor binding proteins that regulate the availability of insulin-like growth factor. A secreted insulin binding protein has been identified from *Spodoptera frugiperda* cells and insulin signalling pathways have been shown to be involved with development and control of cellular metabolism (73). Similarity was also found with porcine colipase and mamba intestinal toxin 1 from *Dendroaspis polylepis* venom (structurally similar to colipase which is involved with fatty acid digestion) which is suggested to aid digestion (74). These proteins have a different cysteine scaffold but suggest that DsVn5 could have functions that control development of the host or provide nutrition for the developing parasitoid.

Full DsVn5 constructs have been made for the expression of DsVn5 in insect cells using baculovirus infection or stable transfection. Unfortunately DsVn5 is too long to be chemically synthesised and DsVn5 has also proven to be difficult to recombinantly express, most likely due to its small size. Expression constructs in *E. coli* failed to express protein as did baculovirus expression in *Sf*9 insect cells. The small size and high pI of DsVn5 may also make it difficult to detect the protein by the traditional means of PAGE and western blot.

DsVn6

Amplification of DsVn6 from genomic DNA produced a product 873bp in length, over twice the size of DsVn6 cDNA. Sequencing revealed the presence of 3 introns between 4 exons (Figure 40).

The N-terminal peptide of DsVn6 was synthesised as peptide 8 (Biotin-EEAEAETMVRREAAAAGLQEMHAESKR-OH and is similar to the N-terminal peptides (after signal peptide cleavage) of DsVn 1, 2 and 3. To date, no effect on *Pieris* haemocytes or *Sf*9 insect cells has been observed.

Biotin-NADPLNAAALIAALKKR-OH was also synthesised by Mimotopes and named Peptide 4. This peptide consists mainly of a low compositional complexity region. The antimicrobial database found that peptide 4 was most similar to mastoparan (INLKAIAALAKKLL-NH2). Mastoparans are cationic, amphiphillic peptide toxins from social wasp venom that are structurally similar to G-protein interacting regions of GPCRs and can activate G-proteins. Mastoparan is cell permeable and can cause cell lysis. In mammalian cells mastoparans can also induce exocytosis of hormones. To date no effects of peptide 4 have been observed of *Pieris* haemocytes or *Sf*9 insect cells.

```
atgaacgttcgtttcggaataatttttttgctcgtggcgatggtcttcgccattggccaa
 M  N  V  R  F  G  I  I  F  L  L  V  A  M  V  F  A  I  G  Q
gtcagctccgaggaagctgaggccgaaacgatggtccgtcgagaagctgctgccgcaggg
 V  S  S  E  E  A  E  A  E  T  M  V  R  R  E  A  A  A  A  G
ttgcaagaaatgcatggagaaagcaaacggtaacggaacacattcacacgaagaaaagtt
 L  Q  E  M  H  G  E  S  K  R
atttctcattttgactaaaatttgaagaaaaaaaaattaatttttcaaatccacaatgaa

ccatttttgttcatttttcggtcgttaattctcggcctaattctaatgtttaaaaactta

aaatttgcagaaatgctgatccactgaatgccgcggcacttatagcagcactcaaaaaac
            N  A  D  P  L  N  A  A  A  L  I  A  A  L  K  K
gactgtgagtaatctcgtaattacaaaaattttcttgaatgatttacacaagcaatggga
 R  L
ctacgagaaatgaataaatcaataaaaatcatgacttgttcatctctgtctaaaatgtca

agcaagaaagcaaatccgtcgaaagtggggttctgcaaaatttcttttaaaaagaataaa

taaaatgacaccaacgatttttttgttgtttcaacagaggtcgctctgccgatccagga
                                        G  R  S  A  D  P  G
aaagtatccgtgcacgatttcctggcagcgatgcaaggccgtaaaggaagaaaagcgtaa
 K  V  S  V  H  D  F  L  A  A  M  Q  G  R  K  G  R  K  A
ttatacaaattcaactatcgcataaattttctaaatgacatgattaatcaacaaacattc

tgattaatccaacagtcagcggtggcatctgagtttctgaatattaatttttatgttttc

tgtttgacaagcgagaggagccctagtgctgatcctgatcctggaatgctcgattttatg
            E  R  S  P  S  A  D  P  D  P  G  M  L  D  F  M
aaagacttaccattcataggcggatttatggga
 K  D  L  P  F  I  G  G  F  M  G
```

Figure 40: Genomic DNA secquence of DsVn6 showing the presence of 3 introns.

Neuropred predicts DsVn6 could be cleaved at 3-4 peptides and some of these peptides were synthesised by Mimotopes (Figure 41).

```
Sequence EEAEAETMVR REAAAAGLQE MHAESKRNAD PLNAAALIAA LKKRLGRSAD
Insect   .........r .......... .....rC... .......... .r.C..C...

Sequence PGKVSVHDFL AAMQGRKGRK AERSPSADPD PGMLDFMKDL PFIGGFMG
Insect   .......... .....r.... .......... .......... ........
```

Figure 41: Cleavage sites within DsVn6 predicted by Neuropred are indicated by 'C'. Peptides synthesised by Mimotopes are highlighted in yellow (peptide 8) and blue (peptide 4).

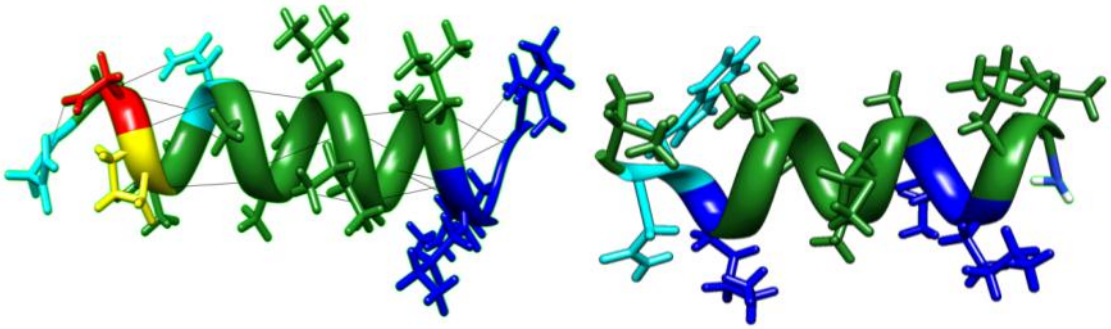

Figure 42: Comparison of Peptide 4 model with structure of MastoparanX (INWKGIAAMAKKLL-NH2).

It would be interesting to further investigate the C-terminal peptide of DsVn6 (SADPGKVSVHDFLAAMQGRKGRKAERSPSADPDPGMLDFMKDLPFIGGFMG) which is similar to peptide 6 from DsVn3 that shows cytotoxic properties. Unfortunately this peptide could not be synthesised.

A constructs for the expression of DsVn6 has been developed for *Sf*9 insect cells and the expressed protein (tagged with a hexaHistidine tag) was able to be purified from cells in which it was expressed (Figure 43). Efforts are now focussed on using the purified, recombinant DsVn6 for functional experiments, such as those conducted on total venom and synthesised DsVn-related peptides.

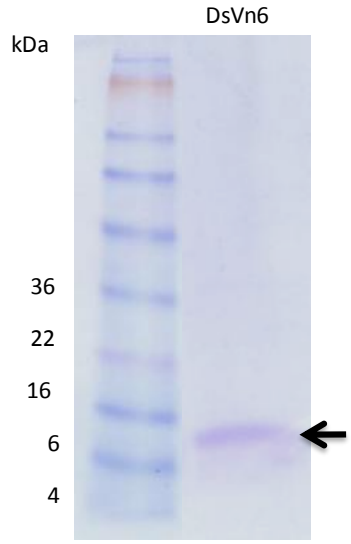

Figure 43: His-tagged (C-terminus) DsVn6 was expressed in *Sf*9 insect cells using recombinant baculovirus. Left lane: Invitrogen protein standards with sizes (kDa) indicated. Predicted MW of His-tagged DsVn6 with signal sequence is ~12 kDa. Right Lane: Partially purified His-tagged DsVn6 (arrow) from infected *Sf*9 insect cell lysate captured with Ni-resin (Bio-rad).

DsVn7

No homologous proteins were discovered in the NCBI database using BlastP. Mature DsVn7 was synthesised by Mimotopes (Biotin-EISPDELLVVKSHLDL-OH) as peptide 9. To date no biological effects have been observed.

DsVnADAMTS

BlastP located part of a conserved domain from the zinc binding metalloproteases in the N-terminus of DsVnADAMTS although the zinc binding active site is absent (Figure 44). DsVnADAMTS was also found to contain a Histidine acid phosphatase signature but no other conserved signature that is usually present in proteins belonging to the acid phosphatase family. Both metalloproteases and acid phosphatases have previously been reported in parasitoid venom (19,75).

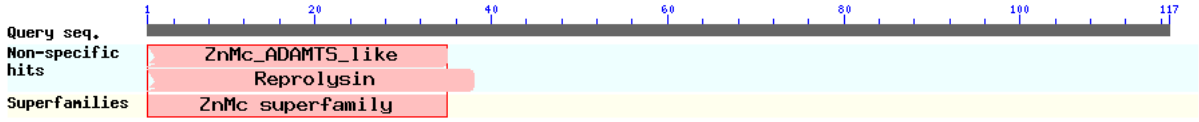

Figure 44: Putative conserved domains in DsVnADAMTS discovered by BlastP.

DsVnADAMTS was found to be most similar to a predicted protein from *Nasonia vitripennis*, A disintegrin and metalloproteinase with thrombospondin (ADAMTS) motifs-like. The Nasonia ADAMTS-like protein contains a signal peptide for secretion and homologs exist in ants, mosquitos, beetles, butterflies and lice. DsVnADAMTS is similar to the C-terminus of this protein but lacks a classical N-terminal signal peptide (Figure 42). 5' RACE was performed to generate full length cDNA, however, no further 5' sequence was obtained. ADAMTS members are secreted, extracellular matrix proteases with a wide range of activities and functions distinct from ADAM family members that are largely anchored on the cell surface. ADAMTS members have an ADAM-like protease domain, a disintegrin-like and cysteine rich domain. They also differ from ADAMs by containing thrombospondin type 1 repeats between the disintegrin-like and cysteine rich domain (10 cysteines) and repeats are also found at the C-terminus (76). Thromobospondin repeats are not present in DsVnADAMTS. This is similar to the ADAMTS-like protein reported from *Bombyx mori* (77), which was also the second most similar protein to DsVnADAMTS. The ADAMTS-like protein from *Bombyx mori* is proposed to cleave the extracellular matrix to degenerate and remodel tissues during the moulting periods.

PHYRE and I-tasser modelling (Figure 43) also found structural homologs of DsVnADAMTS to be various ADAMTS proteins as well as a number of snake venom metalloproteinases. Fugue returned 2 "Certain" structural homologs that were vascular apoptosis-inducing proteins, VAP1 (110kDa, pI 8.5, homodimeric) and 2 (monomeric, 55kDa, pI 4.5) from the hemorrhagic venom of the snake *Crotalus atrox*. These proteins have specific apoptotic activities against vascular endothelial cells. Both resemble metalloprotease/disintegrins and although VAP1 did not show protease activity against BSA it did degrade fibrinogen unless it had been pre incubated with EDTA or EGTA (78). In high salt conditions VAP2 detached cells from the substrate while under control conditions VAP2 caused changes in the shape of the cell edge. Likewise, under high salt conditions VAP2 cleaved gelatin better than under control conditions (79).

```
Nasonia          MLFLLFSSFVTLTVSSHGSKIHEQMTAEEVHSIFRTTHDEVPEYEVVPIAHAIHENSPKD 60
DsVnADAMTS       ------------------------------------------------------------

Nasonia          SIHRILQIKSFKRDMRLYLEPTEGILAASDLPMWTAEGDEDSPWGIKYTKISKGMKERMY 120
DsVnADAMTS       ------------------------------------------------------------

Nasonia          FYQDPYNLAAFTSTHDEHGEILFDGTIGDDFVVRPLPARLRKVFSKAKRSIHEEDFPQFN 180
DsVnADAMTS       ------------------------------------------------------------

Nasonia          RTVYHPNLKDTYHHVIYKKKEVSFDGIREKIGSYVLKNKTESESSRTKRSTKKTYNPKIV 240
DsVnADAMTS       ------------------------------------------------------------

Nasonia          YPQILVIVDYNEYLSLHNFAEVKRYIISFWNAVDLRYRVFVNPEVRLNIAGIIVATDPDG 300
DsVnADAMTS       ------------------------------------------------------------

Nasonia          TPYTQNHRTRPVDGPIIDADKALDNMAEYFFEELMNKDLDRFAIDRDYDMVMLMTQLNLC 360
DsVnADAMTS       ------------------------------------------------------------

Nasonia          NLEPNDHDFDCTTLGYAVRGGACTVNIRETKMEAVGLVEDNGGYVGIIPAAHEVGHLLGA 420
DsVnADAMTS       ------------------------------------------------------------

Nasonia          PHDGHEQEDKTTCPAYGGYIMTGMLMLTKNVFMWSSCSMEYFEDFFHSQRAQCLVDTPRK 480
DsVnADAMTS       --------------------MTPAAQLSRHGFRWSKCSKRYFDRYFKSSASQCLDDKPLW 40
                                     **    *::: * **.** .**: :*:*. :*** *.*

Nasonia          VRAMPRHLPGQILSVDEQCDRIKGTYACNK-DETACVHLDCFIPDSGGQCLPVAPAAEGS 539
DsVnADAMTS       MTIRGENLPGRWLTLDGQCRNSGMERGCEVPNLPFCFVKGCKAENSDECVVDQWQTLPGT 100
                 :    .:***: *::* ** .     .*:  : . *.  .*   :*.   :    :  *:

Nasonia          SCGKGRHCINGQCVSRNTSEVLLQFAPPPEEERPYSNNIGVDVGLNIPFNIERN 593
DsVnADAMTS       KCGDQKICDAKRACVKV---------------------------------- 117
                 .**. : *   :.  :
```

Figure 42: Alignment of DsVnADAMTS with the Nasonia ADAMTS-like protein by ClustalW.

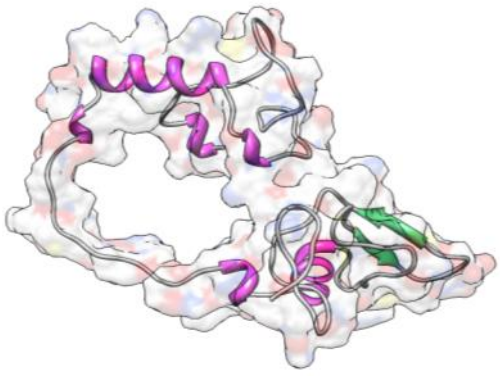

Figure 43: I-tasser model (C-score 0.97) of DsVnADAMTS

Although DsVnADAMTS does not contain a classical N-terminal signal peptide, SecretomeP 2.0 predicts that DsVNADAMTS could be a non-classically secreted protein (NN-score 0.749, 0.5 threshold). WoLF PSORT also predicts the protein to be extracellular. On this basis it was decided that further investigation into DsVnADAMTS might be worthwhile and constructs for the expression of recombinant protein in *E. coli* and *Sf*9 insect cells were developed. His tagged-DsVnADAMTS has

been successfully expressed in *E. coli* (Figure 44) and attempts are currently being made to purify the protein from the insoluble fraction of the *E. coli* for functional studies. So far, detergent extraction has been unsuccessful as have different induction conditions such as lower temperature, lower IPTG concentration and less time which have all left DsVnADAMTS remaining in the insoluable fraction (data not shown).

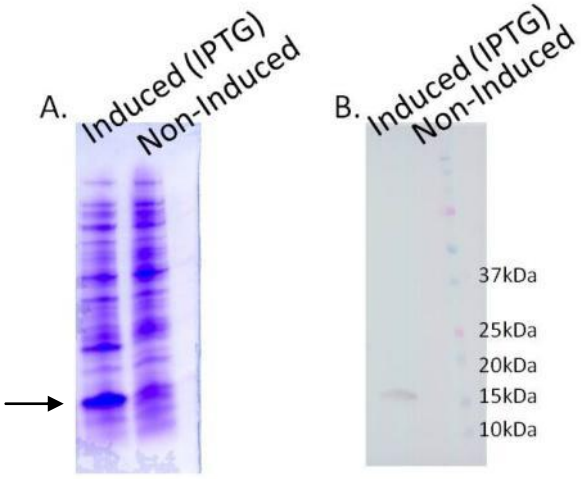

Figure 44: Expression of DsVnADAMTS in *E. coli*. A: Expression of DsVnADAM was induced in *E. coli* using IPTG. B: DsVnADMATS was detected by western blot in *E. coli* lysate that had been induced by IPTG using monoclonal anti-poly histidine conjugated to alkaline phosphatase.

DsVnWD

DsVnWD was found to contain 4 WD40 repeats that were located using SMART sequence analysis. WD-repeat proteins are thought to mediate diverse protein-protein interactions, no WD40 protein is currently known to possess catalytic activity (80). BLASTP search of the NCBI database showed DsVnWD to be most similar to a predicted *Nasonia vitripennis* protein similar to receptor for activated protein kinase C-like (Receptor for activated C-kinase; RACK proteins). RACK proteins share sequence similarity with G-beta proteins and both protein families contain WD-repeats. DsVnWD aligns closely with the 4th WD-repeat through to the 5th, 6th and 7th WD-repeats of the Nasonia RACK-like protein that are also highly similar to human RACK1 (Figure 45). DsVnWD is relatively unusual in having only 4 WD-repeats, RACKs and Gbeta subunits have 7 repeats as do most WD40 proteins. RACKS have been proposed to bind and stabilise activated PKC and shuttle it to different sites in the cell (81). RACK1 has been implicated in events at the cell membrane, ribosome and nucleus. RACK1 has been reported to be an important regulator of focal adhesion organisation, cell spreading and migration (82). The 6th WD-repeat contains a tryptophan(246) necessary for Src binding that is conserved in all 3 proteins and also has a PKC binding site and WD-repeats 5, 6 and 7 form an integrin binding domain (82,83). The sequence conservation in these areas suggests that integrin binding may be conserved in DsVnWD. A second PKC binding site is found in WD-repeat 3 that is absent in DsVnWD. The 4th WD repeat has been shown to be involved with forming homodimers although a serine residue that becomes phosphorylated to promote dimerisation is absent in the both the Nasonia protein and DsVnWD. The first 207aa of RACK1 have also been shown to bind Gbeta subunits at multiple sites (84).

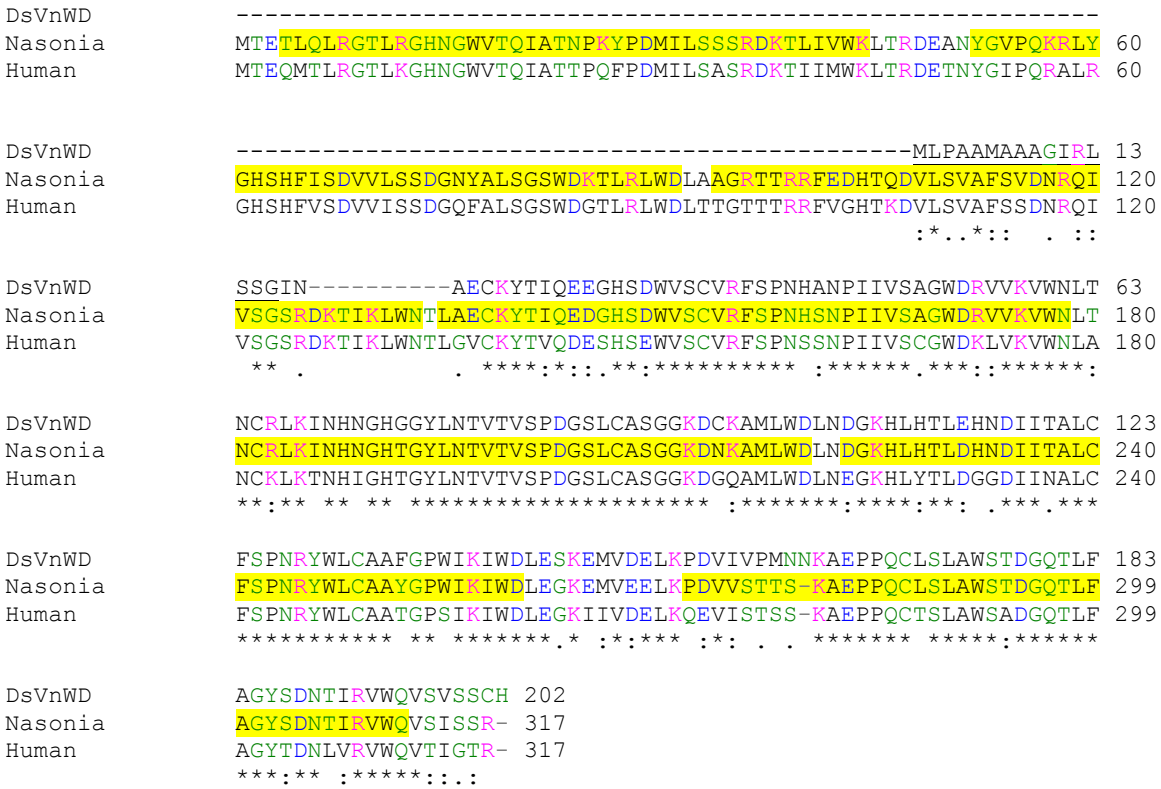

Figure 45: ClustalW alignment of DsVnWD with *Nasonia vitripennis* protein similar to receptor for activated protein kinase C-like (Receptor for activated C-kinase; RACK protein) and human RACK1. Signal sequence of DsVnWD is underlined. WD repeats of Nasonia RACK are highlighted in yellow.

Interestingly, a cDNA from a HeLa cell line cDNA library has been isolated that is 100% homologous with RACK1 from aa 30-143 making it a C-terminal truncation of RACK1 that contains 1 putative PKC binding site but lacks the sites reported to bind integrin β cytoplasmic tails and Src. The authors propose that truncated RACK1 proteins may act as a dominant negative through binding to active PKC but fails to interact with other binding partners (82). LACK (*Leishmania* homolog of receptors for activated C-kinase) is from a parasite that alternates between an invertebrate vector and mammalian host. LACK is essential for the establishment of the parasite and has also been found to be secreted from the parasite by a non-classical secretion pathway (85,86). These examples suggest it is possible that a truncated, extracellular RACK1 protein could exist and could aid parasitism.

Although the Neural Networks model of SignalP3.0 did not come to a consensus on whether DsVnWD contains a signal peptide the Hidden Markov Model predicts there to be a signal peptide (0.71) that is cleaved between amino acids 16 and 17. This proposed cleavage site would occur just prior to the predicted start of the first WD-repeat. Interestingly, this putative signal sequence also aligns poorly with the *Nasonia* RACK-like protein unlike the remainder of the sequence which shows a high degree of similarity. WolfPsort also predicts the protein to be extracellular providing further evidence that this protein is secreted and could be a venom protein.

Predicted structure analysis by I-tasser (Figure 46), Phyre and Fugue generally found most similarity with other WD-repeat proteins, often at their C-terminus.

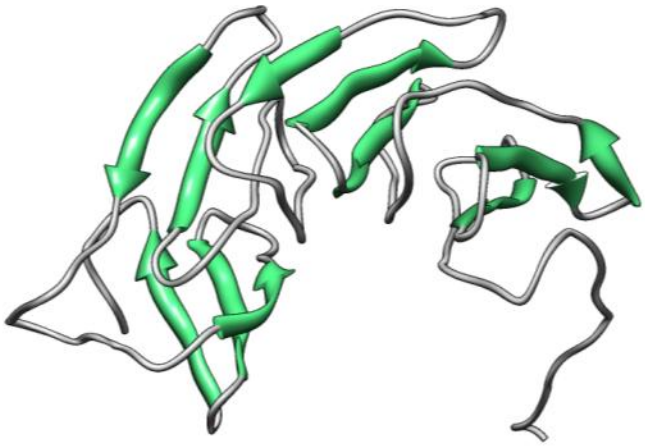

Figure 46: I-tasser model (C-score 0.01) of DsVnWD shows the presence of beta sheets formed by the WD40 repeats.

Recombinant DsVnWD was expressed in *E. coli* without the signal sequence (Figure 50). The protein was found to be located in the insoluble fraction most likely due to the high expression level. This made purification of the protein for further experiments difficult. Cholate extraction was used in an attempt to solubilise protein for purification but was unsuccessful with DsVnWD remaining in the insoluble fraction. Different induction conditions were also tested including lower temperature, less IPTG and less time but the amount soluble protein could not be increased.

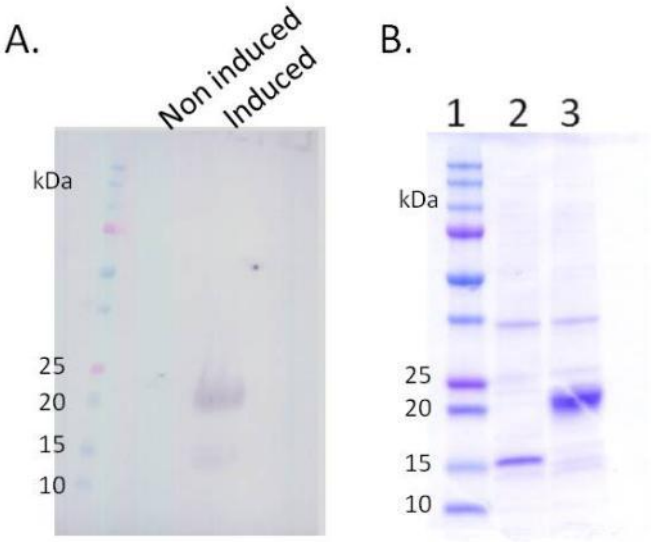

Figure 50: DsVnWD was expressed in *E. coli* but could not be solubilised for purification. A: Expression of DsVnWD by induced *E. coli* was detected by Western blot using an anti-polyhistidine antibody. DsVnWD protein was absent until induction by IPTG where a 20kDa his-tagged protein became detectable. Right: Following cholate extraction DsVnWD remained insoluble as did the majority of DsVnADAMTS. Insoluable fractions were separated by SDS-PAGE on a 4-20% TGX gradient gel and clearly shows the presence of DsVnADAMTS (lane 2) and DsVnWD (lane 3). Bio-Rad precision plus protein standards are shown in Lane 1.

Summary of expression constructs for production of *Diadegma* venom proteins

During the course of this project 9 putative venom cDNAs were isolated. Expression (cellular production) of the proteins was attempted in a number of vectors including pIZ for stable insect cell expression, pFastBac1 for insect cell expression via baculovirus infection and pQE30 or for bacterial expression (Table 5). Unfortunately expression was often not detectable in insect cell systems, and proteins were not soluble in bacteria. Had time allowed we would have pursued a fusion protein strategy to increase stability of the transcripts/protein in the insect cell expression systems and to improve solubility in bacteria.

Venom Protein	pIZ	pFastBac1	pQE30
DsVn1	-	Yes- 5his tag	-
DsVn2	Yes	Yes	-
DsVn3	-	Yes	-
DsVn4	Yes	Yes	-
DsVn5	Yes	Yes +/- signal sequence	Yes
DsVn6	-	Yes	-
DsVnADAM	-	Yes	Yes
DsVnWD	-	-	Yes

Table 5: Constructs created for expression (cellular production) of *Diadegma semiclausum* venom (DsVn) proteins. Constructs were cloned into pIZ vectpr for stable expression in *Sf*9 insect cells, pFastBac1 for expression in *Sf*9 insect cells using baculovirus, and pQE30 for expression in *E. coli*. Constructs for expression in *Sf*9 insect cells contained the signal peptide unless otherwise indicated and a hexaHistidine tag on the C-terminus. Constructs for expression in *E. coli* had an N-terminal His-tag and did not contain the signal peptide. Constructs highlighted in green successfully produced recombinant protein. Constructs highlighted in red did not produce any detectable recombinant protein. Constructs highlighted in yellow produced recombinant protein but purification was not possible. Un-highlighted cells with 'yes' are untested constructs.

Other immune and developmental Assays

Peptides and venom were also screened through a number of other assays. Many of these were preliminary experiments that could have been further optimised with regard to stoichiometry and signal:noise should time constraints have allowed. Also while these assays are commonly used, generally the conditions have been optimised for mammalian cells rather than insect or Lepidopteran cells.

Phagocytosis Phrodo-conjugated *E. coli* particles were used to test the phagocytosis capabilities of haemocytes. The presence of the peptides appeared to make no qualitative difference with granulocytes readily phagocytosing the *E. coli* particles, which then became fluorescent and could be observed under the microscope (Figure 51). Quantitative measurements could be taken using a fluorescent plate reader in the future. Although the phagocytosis immune response is aimed at pathogens smaller than a parasitoid, inhibition could have suggested changes to actin remodelling abilities or recognition of foreign bodies.

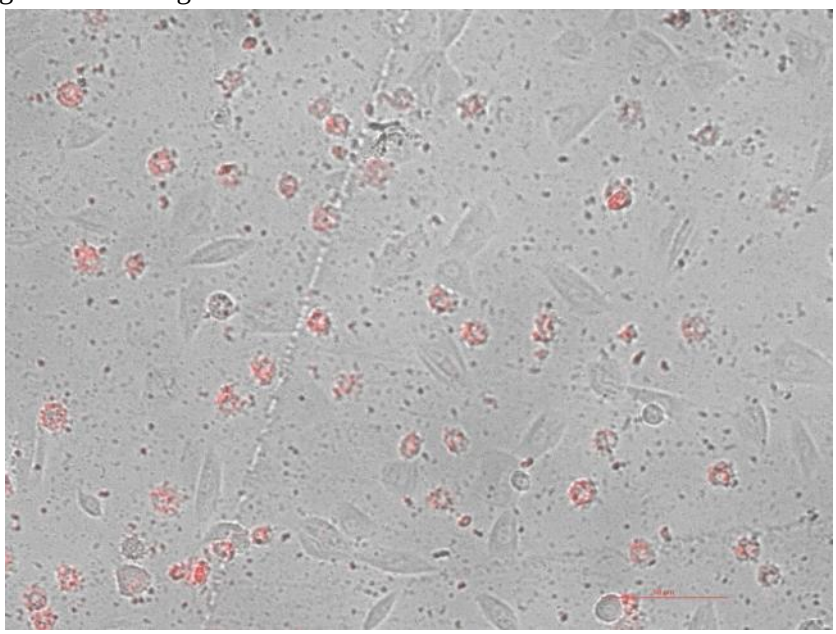

Figure 51: Granulocytes readily phagocytose pHrodo conjugated *E. coli*. The pH sensitive probe is essentially non-fluorescent at a neutral pH but dramatically increases in the acidic environment that follows endocytosis (red).

Prophenoloxidase assay *Pieris rapae* larvae were bled on to *E. coli* lysate to activate the prophenoloxidase cascade. This lysate was then added to L-DOPA (L-dihydroyphenylalanine; phenoloxidase substrate). Phenoloxidase activity was measured by recording formation of dopachrome from L-DOPA as an increase in absorbance at 490nm. The presence of the peptides following activation of the prophenoloxidase cascade had no significant effect after 15 min incubation (Figure 47A). At 15 min, peptides 2, 3, 6 and 7 had a small but significant reduction in absorbance compared to control (Figure 47B). This preliminary experiment suggests that the individual peptides do not significantly reduce phenoloxidase activity although it could be worth more thoroughly testing the effects of difference concentrations of peptides 2, 3, 6 and 7 on the reaction kinetics.

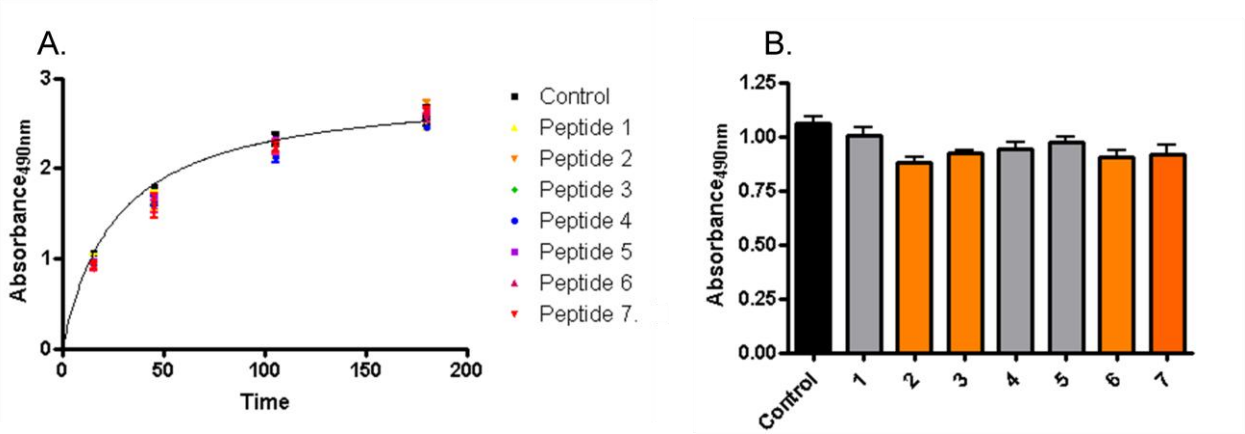

Figure 47: Effect of peptides on phenoloxidase activity. A: Timecourse of L-DOPA conversion to dopachrome which absorbs at 490nm in the presence of peptides (1-7) or absence (control). B: At 15 min treatment with peptides 2, 3, 6 and 7 showed a significantly reduced amount of absorbance compared to control (p-value <0.05). Final assay concentrations were 16.6µM (peptides 1, 2, 3, 4, 5, 7) and 8.3µM (peptide 6) and 1.4mg/ml L-DOPA.

Calcium flux Release of intracellular stores of calcium was measured using the fluorescent calcium indicator, Fluo4-AM. Fluo4-AM is cell permeable and exhibits a large fluorescence intensity increase on binding Ca^{2+} (K_d 345nM). The release of intracellular stores of calcium is stimulated by GPCR/G-protein signalling and has been associated with cell death induced by venom from the ectoparasitic wasp *Nasonia vitripennis* (58) and *P. hypochondriaca* (57). During preliminary testing, no observable qualitative differences were found between the presence and absence of venom or peptides suggesting that they do not activate calcium signalling. This experiment could be further expanded to test for inhibition of calcium signalling and extracellular calcium influx. Conditions could also be further optimised so that cells withstand the washing procedures involved better.

Apoptosis Induction of apoptosis (programmed cell death) was tested for using AnnexinV and propididium iodide. AnnexinV binds to phosphatidylserine which translocates from the cytolasmic side of the cell membrane to the cell surface soon after the induction of apoptosis. Propidium iodide is used to determine the difference between dead permeable cells (annexinV +ve, propidium iodide +ve) and cells undergoing apoptosis (AnnexinV +ve, propidium iodide –ve). Had time allowed, this assay could have been improved by optimising the AnnexinV binding conditions for insect cells that currently do not withstand the washing procedure well and quantitating the ratio of green to red fluorescence.

Developmental bioassay Due to their larger size and easier handling, *P. rapae* larvae (last instar) were injected with 1µL of 1mM peptide (peptide 2, 6, 7 or an equivalent volume of water) and their development monitored in a pilot experiment. At this small dose of peptide no developmental effects were observed. However, to be conclusive the experiment requires larger numbers of larvae at different instars and a higher dosage of peptide.

Antibacterial assays (MIC and MBC assays)

Many venom proteins are known to have antibacterial properties and so we screened the 9 peptides that were synthesised based on predicted active parts of the sequences found in the venom gland gene library (Table 1), for antibacterial properties:

Quality control of antibacterial assays

All experiments were performed in duplicates. A row with just bacteria and medium was prepared as a positive control, while another row containing just medium was prepared as a negative control to ensure the growth medium was not contaminated. Antibiotics Vancomycin and Colistin were incorporated into each of the 3 plates that were inoculated with Gram-positive and Gram-negative bacteria respectively to act as internal controls within assay plates. In addition the first plate contained additional known antibiotic. All control compounds show activity within the reported range (Table 6).

MIC and MBC assay results

The negative control (medium only) used in the assay had a contamination after the addition of resazurin and the 2nd 24h incubation, showing a pink colour. Both, the resazurin solution and the medium have subsequently been eliminated as possible source for contamination. Stock resazurin solution, aliquot of resazurin solution in the medium reservoir and growth medium alone were incubated for 24 in a sterile 96-well plate with additional 50 μL of growth medium. After 24 hours all solution showed no contamination (blue colour). In addition all control antibiotics shows expected values for their MIC. This indicates that the contamination has been introduced, after the reading of the MIC, during the addition of the resazurin solution. Thus, we are confident that the MIC values are not compromised (Table 7), but we rejected all the MBC values (therefore, not shown).

Compound ID	GP_001 *S. aureus* ATCC 25923		GP_013 *S. pneumoniae* ATCC 33400		GP_018 *B. subtilis* ATCC 6633		GP_027 *E. faecalis* ATCC 29212		GN_001 *E. coli* ATCC 25922		GN_003 *K. pneumoniae* ATCC 700603		GN_022 *P. aeruginosa* ATCC 25923	
	Lit MIC$_{(87)}$	**MIC**	**Lit MIC$_{(88)}$**	**MIC**	**Lit MIC$_{(89)}$**	**MIC**	**Lit MIC$_{(90\text{-}92)}$**	**MIC**	**Lit MIC$_{(93)}$**	**MIC**	**Lit MIC$_{(94,95)}$**	**MIC**	**Lit MIC$_{(96,97)}$**	**MIC**
Vancomycin MCC_000095_002	2	1	0.5	1	0.1-0.5	0.125	2	2/ 4	-	-	-	-	-	-
Penicillin G MCC_000188_001	0.125	≤ 0.03	0.006	≤ 0.03	1.562	0.06	16	2	-	-	-	-	-	-
Ciprofloxacin MCC_000166_001)	0.25	4	1	>64	Not obtained	0.25/ 0.5	1	>64	-	-	-	-	-	-
Oxacillin MCC_000236_001)	0.25	0.5	0.03	0.5/ 1	0.3	0.25	16	16	-	-	-	-	-	-
Colistin MCC_000094B_002	-	-	-	-	-	-	-	-	0.125-0.5	≤ 0.03	0.13-0.48	0.06	0.5-4	0.125 / 0.5
Penicillin G MCC_000188_001	-	-	-	-	-	-	-	-	16-64	32/ 64	>64	>64	16	>64
Ciprofloxacin MCC_000166_001	-	-	-	-	-	-	-	-	0.015	≤ 0.03	0.016-0.25	2/ 4	0.06-0.2	0.25/ 0.5
Ampicillin MCC_000238_002	-	-	-	-	-	-	-	-	2-8	64	>64	>64	0.48	>64

Table 6: Quality control data showing effectiveness of various antibiotics against target bacterial strains used for antibacterial asssays of synthetic peptides derived from sequences obtained from a Diadegma semiclausum venom gland cDNA (gene) library. All control compounds showed activity (MIC values) within ranges reported in literature (Lit Mic$_{(n)}$values, where n is the associated reference(s)). Dashes (-) represent that the test compounds were not relevant to the bacterial isolate tested.

Compound ID	**GP_001** ***S. aureus*** **ATCC 25923**	**GP_013** ***S. pneumoniae*** **ATCC 33400**	**GP_018** ***B. subtilis*** **ATCC 6633**	**GP_027** ***E. faecalis*** **ATCC 29212**	**GN_001** ***E. coli*** **ATCC 25922**	**GN_003** ***K. pneumoniae*** **ATCC 700603**	**GN_022** ***P. aeruginosa*** **ATCC 25923**
	MIC	MIC	MIC	MIC	MIC	MIC	MIC
Peptide 1	>64	>64	>64	>64	>64	>64	>64
Peptide 2	>64	>64	>64	>64	>64	>64	>64
Peptide 3	>64	>64	>64	>64	>64	>64	>64
Peptide 4	>64	>64	>64	>64	>64	>64	>64
Peptide 5	>64	>64	>64	>64	>64	>64	>64
Peptide 6	>64	>64	>64	>64	>64	>64	>64
Peptide 7	>64	>64	>64	>64	>64	>64	>64
Peptide 8	>64	>64	>64	>64	>64	>64	>64
Peptide 9	>64	>64	>64	>64	>64	>64	>64

Table 7: Activity of synthetic peptides (derived from sequences obtained from a *Diadegma semiclausum* venom gland cDNA library) against various strains of bacteria. None of the tested peptides showed significant antibacterial activity.

Diadegma venom proteins/peptides and their activities: Laypersons' summary

In order to characterise the individual proteins that comprise the *Diadegma* venom, a library of genes was produced from the wasp venom gland. This library was screened to obtain the DNA sequence for putative venom genes/proteins. This process led to the production of sequence data for 9 different *Diadegma semicalusum* venom proteins (DsVns) which are summarised in Table 4 (DsVn1-DsVn7, DsVnADAMTS and DsVnWD). Most of the venom sequences were unique, showing little similarity to characterised proteins making prediction of function difficult. DsVn1 and DsVn6 were able to be manufactured and purified for further experiments. DsVn5 also clearly shows toxin features (based on sequence and structural similarities) and once recombinant DsVn5 protein can be produced, the effect on ion channels could be investigated.

Based on the sequences obtained for these venom proteins, active peptides (protein fragments) were synthetically synthesised and subsequently were screened through a number of preliminary immune and developmental assays. Peptides 2 and 6, from Dsvn2 and DsVn3 respectively, were able to penetrate haemocytes. In particular peptide 6 showed toxicity against caterpillar blood cells and cultured *Sf*9 insect cells. None of the peptides appeared to have antibacterial activity which is a common property of venoms.

Much is left for further investigation. More venom transcripts could be identified using next generation sequencing providing a thorough database to identify 'hits' with venom peptides identified by mass spectrometry. More time is also required to optimise recombinant protein expression. The putative venom proteins identified to date have proved more challenging to produce recombinantly than envisioned due to their small size and insolubility when expressed in *E. coli*. Nevertheless, we have produced useful fundamental knowledge of the sequences, production systems and molecular function of the venom proteins, some of which appear promising in terms of further R&D as biopesticides. Further investigations would probably use a fusion protein strategy to increase solubility and stability of the venom proteins produced. Given time, functional assays could be more thoroughly investigated with regard to stoichiometry and the conditions optimised. The array of functional assays could also be expanded to investigate other potential functions such as effects on virus and caterpillar gene expression, amongst others.

CHAPTER 4: Deep Sequencing Comparison of Gene Expression in Parasitised and Healthy DBM Larvae (results and discussion)

Rationale for deep sequencing

Deep sequencing is a relatively recent technological development which allows researchers to generate huge amounts of DNA sequence data, relatively quickly. Recently, the newly developed deep sequencing approaches have significantly changed how the functional complexity of an organism can be investigated (98-100).

The term "deep sequencing" refers to the ability to generate sequences for even "rare" pieces of DNA, allowing the full repertoire of DNA sequences in complex samples to be obtained. For this project, deep sequencing had the advantage of allowing us to obtain the "transcriptome" of DBM larvae that were parasitised by *Diadegma semiclausum* and of healthy DBM larvae. A transcriptome is the complete set of expressed RNA transcripts (genes) in one or more cells. By applying this approach to parasitised and healthy DBM larvae, we are able to analyse both:

1. the DBM genes that are affected by parasitisation (to answer what DBM immune genes are involved)
2. the genes expressed by the *Diadegma semiclausum* ichnovirus (*Ds*IV) which facilitate parasitisation through immune suppression of DBM (to identify key immune suppressive genes)

Transcriptome profiling of organisms under stress, or in this case parasitisation challenge, helps us to obtain a better understanding of subsequent related cellular activities in organisms including growth, development, and immune defence.

The data arising from these experiments formed the basis for a scientific manuscript which is currently in press with *BMC Genomics.*

DBM transcriptome profile

To analyse the transcriptome of DBM host larvae following parasitisation by *D. semiclausum*, RNA samples isolated from host larvae at various time points after parasitisation were pooled together prior to sequencing. This may lead to bias in the results (e.g. a gene may first be upregulated and downregulated subsequently); however, we aimed at obtaining an overview of what occurs during parasitism and generate a transcriptome of DBM which has not previously been available and to isolate as many *Ds*IV virus genes as possible.

The deep sequencing analysis produced approximately 26.6 and 27.1 million single-end reads from RNA extracted from the whole body of non-parasitised (control) and parasitised larvae of DBM, respectively. *De novo* assembly of raw sequence data produced 172,660 contigs with a minimum contig size of 100 bp. Of these, 66% were between 100-199 bp and only 59,255 (34%) of the contigs were above 200 bp (Table 8). Only contigs above 200 bp were selected for further analysis and 6% of these had nucleotide lengths above 1000 bp (Figure 53).

We found 4992 contigs that shared their greatest homology with *Tribolium castaneum* (Red flour beetle) genes with a minimum E-value of 1e-06 (Figure 54). *Bombyx mori* (Silkworm moth) was another species with which a range of DBM genes showed high levels of homology (Figure 52). One reason for the higher number of hits is that 3 times more Red flour beetle genes than Silkworm moth genes, are reported in databases.

Parameters	Number
Total *de novo* assembled contigs with CLC software	172,660
Contigs used for BLAST (cut-off: above 200 bp length)	59,255
Best BLAST matches (cut-off: E-value >E-6)	26119
No Hits (contigs without any BLAST match)	33136
Not mapped with any Gene Ontology (GO) database	6087
Annotated sequences (cut off: GO weight 5E value >E-6)	20704

Table 8: Summery of contig statistics resulting from Illumina deep sequencing of parasitised and non-parasitised DBM larvae.

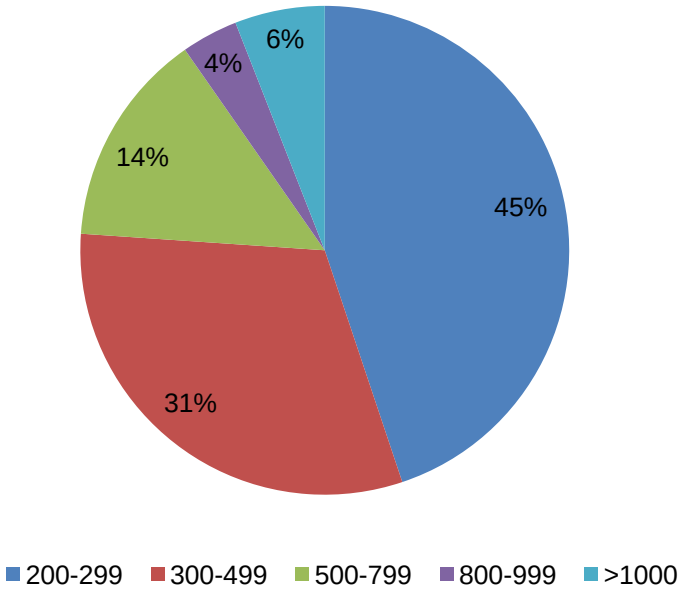

Figure 53: Distribution of contig size in assembled DBM transcriptome sequence data with CLC genomic workbench.

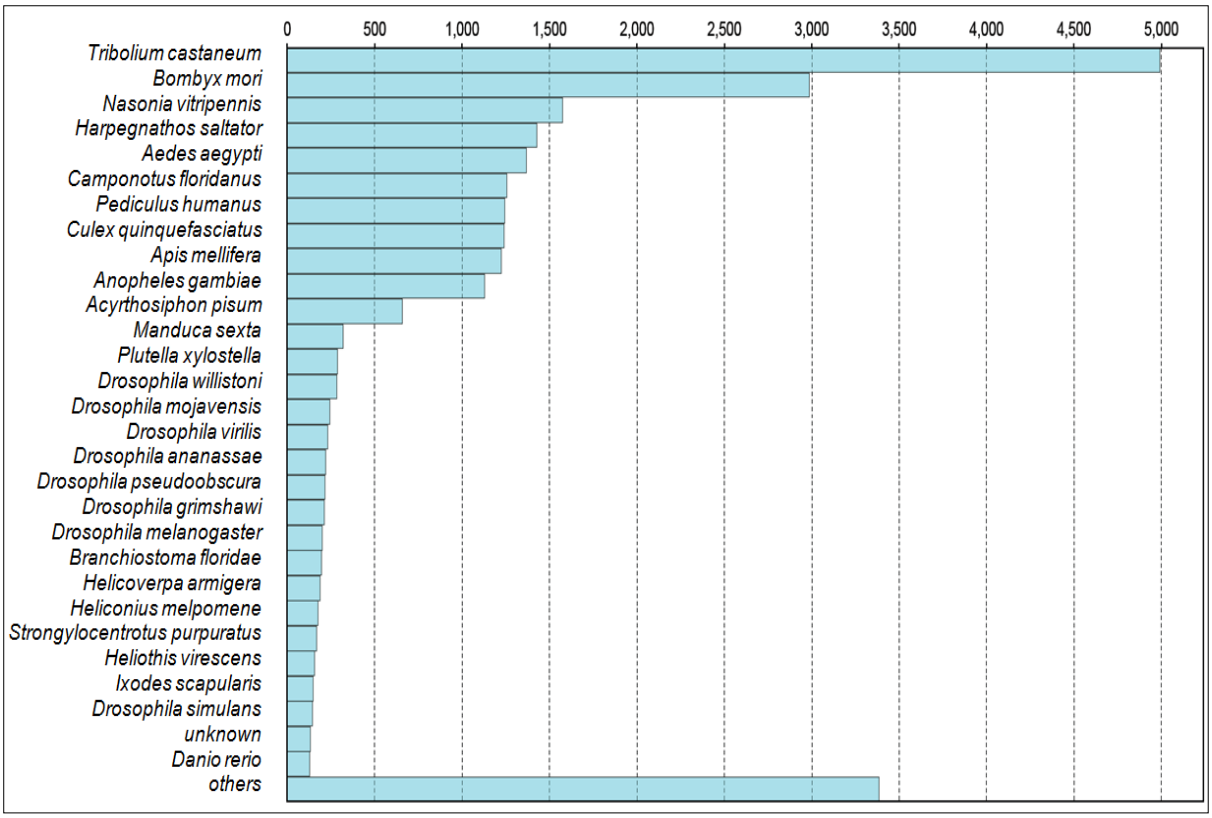

Figure 54: Species distribution of closest-match BLAST results of sequences obtained via deep sequencing.

Using a series of filtering and critical cut-off values for BLAST E-value and gene ontology (GO) weighting, 20704 sequences were annotated by B2GO software (www.blast2go.org) through Uniprot KB/TrEMBL and other available databases. GO-annotated consensus sequences were assigned to biological process clusters such as cellular component and molecular function, and distributed among various sub-categories such as metabolism, growth, development, apoptosis, immune defense, molecular processing, signal transduction, transcription regulator activity, catalytic activity etc. (Figure 55). Comparison of the transcriptome pattern of DBM for eight different GO terms (molecular function - Level 2) with those of silkworm (www.silkdb.org) showed high similarity in the distribution of genes across GO categories indicating that the transcriptome analysed was not biased towards particular categories (Figure 56).

Overall, from the assembled contigs of over 200 bp in length, 44% showed similarity with genes or proteins in the NCBI database. The rest may represent unknown genes, non-coding RNA or misassembled contigs that are expected due to the presence of large repetitive or duplicated regions. David et al. (2010) suggested that a significant proportion of transcript signatures detected outside predicted genes represent regulatory non-coding RNAs, because these large numbers of non-coding RNA can be antisense, intergenic or overlapping with protein-coding genes (98).

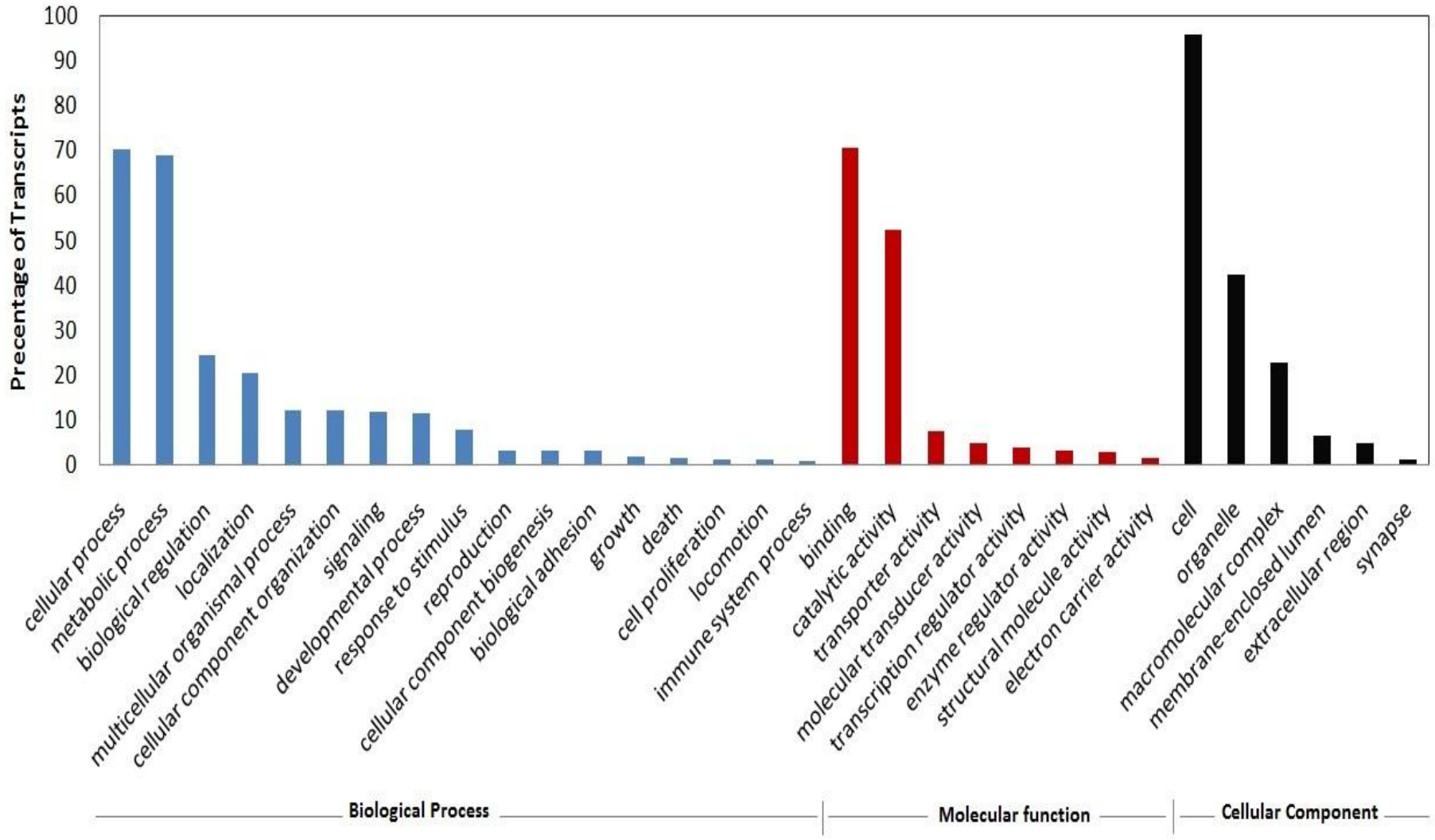

Figure 55: GO annotation of consensus sequences (Level 2). Blast2Go software categorised 14075 contigs in biological process, 18127 contigs in molecular function and 10048 contigs in cellular components.

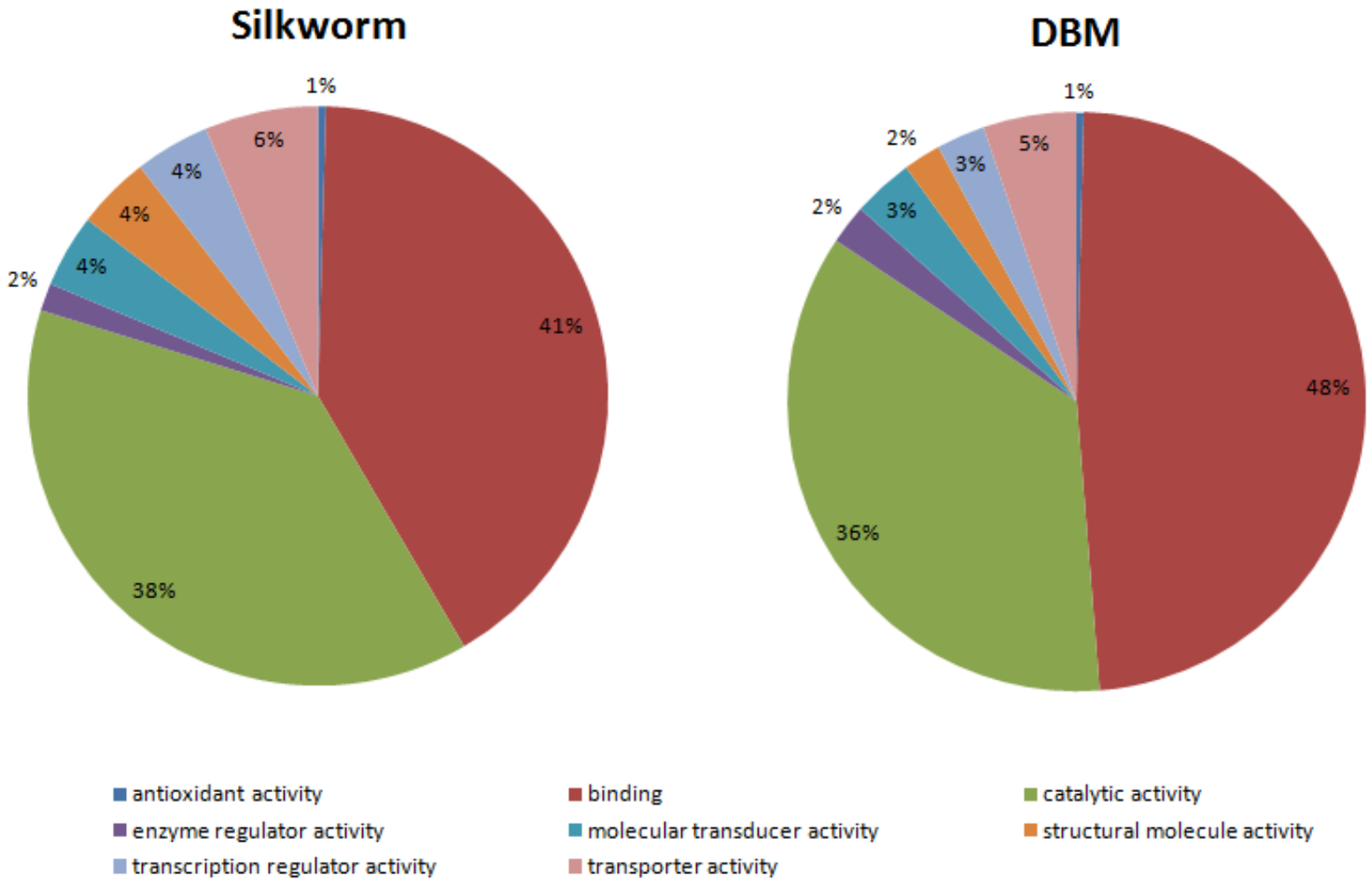

Figure 56: Comparison of DBM transcriptome pattern with that of *B. mori* (Silkworm moth), based on 8 different molecular function Gene Ontology (GO) terms (Level 2).

Effects of parasitism on the transcription of host immune related genes

Our sequencing data analyses indicate that parasitism has a significant impact on the transcriptome profile of DBM larvae, as expected. The 'Oases' package was used to assemble data for differential expression analysis. After filtering our dataset using criteria such as number of reads, contig length, E-value (for nearest homolog identity) with greater than 2-fold change, 928 contigs were short-listed. Figure 57 shows that most of the differentially expressed gene transcripts for these selected GO terms (Level 2), molecular function and biological process, were up-regulated. Among these contigs, only those related to immunity and development, which were differentially transcribed after *D. semiclausum* parasitisation, are displayed in Tables 9 and 10, respectively, since these are the genes most relevant to parasitism and development of biopesticides.

In instances where differential expression of DBM genes following *D. semiclausum* parasitisation may not be consistent with proteomic observations in other host-parasitoid systems previously reported (e.g. (101)), it is possible that post-transcriptional inhibitory effects of parasitoids' maternal factors (e.g. viruses or venom) contribute to these differences. It has been reported that virus genes are able to interrupt translation of caterpillar genes with their host translation inhibitory factors (HTIFs), which were initially characterised from *Campoletis sonorensis* virus (*Cs*IV) (102). Accordingly, in *Heliothis virescens* it was shown that lysozyme activity declined after parasitisation with *C. sonorensis* or injection of *Cs*IV; however, the transcript levels of the gene increased after parasitisation. This suggested that *Cs*IV may regulate host cell gene expression at the translation level. We also found that lysozyme transcript levels increased following parasitisation (Table 9). Another study also showed that lysozyme concentration and activity in DBM larvae parasitised by *Cotesia plutellae* was decreased (101); however, transcript levels were not measured in that study. Recently, Barandoc and Kim (103) showed that the translation of storage protein in DBM was inhibited by two virus genes (CpBV15α and CpBV15β). In another study, it was shown that expression of antimicrobial peptides (diptericin, cecropin A and drosomycin) were either unchanged or minimally induced in parasitised *Drosophila melanogaster* larvae by the wasp, *Leptopilina boulardi* (104). The authors of that study concluded that antimicrobial genes are regulated differently independent of those mediating cellular encapsulation.

Here, in this study, we found that antimicrobial peptides such as gloverin, moricin, lysozyme II and cecropin were up-regulated after parasitisation compared to transcription levels in control (non-parasitised) larvae. Among these, lysozyme II and gloverin had the highest transcription levels in parasitised DBM larvae relative to other antimicrobial peptides (Figure 58; Table 9). Transcription levels for cecropin 1 and pxCecropin E increased by more than 3-fold after *D. semiclausum* attack (Table 9). It has been reported that immune-related genes were also up-regulated in DBM larvae in response to microbial challenge (e.g. pxCecropin 5.94 fold, hemolin 3.18 fold and cecropin E 4.99 fold) (105). Barandoc *et al*. measured pxCecropin expression levels by qRT-PCR in parasitised DBM larvae and showed that pxCecropin was suppressed by *Cotesia plutellae* virus (106). Some antimicrobial peptides, such as moricin and gloverin, were previously found not to be induced by bacterial challenge of lepidopteran larvae, while lysozyme and cecropins are well-known inducible antimicrobial peptides (106,107). Recently, it has been reported that gloverin expression was changed after bacterial infection in DBM (108). Our data shows that immune responses after parasitoid attack appear to be different from microbial challenge responses, because gloverin and moricin-like peptide were up-regulated about 7 and 11 folds, respectively, after *D. semiclausum* attack.

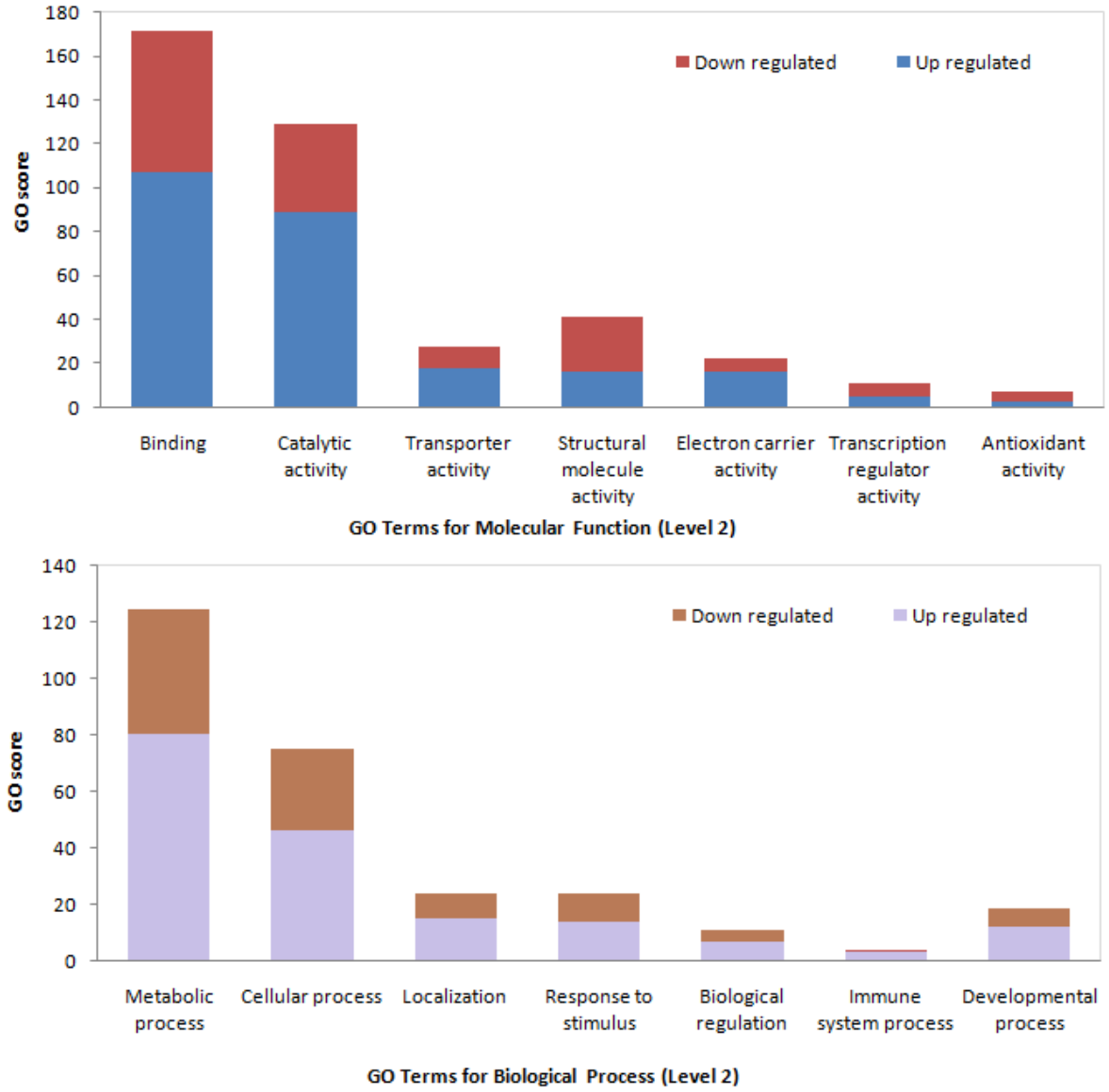

Figure 57: The gene ontology score for some selected GO terms (level 2) in up and down-regulated transcriptomes. (A) Molecular function (B) Biological process.

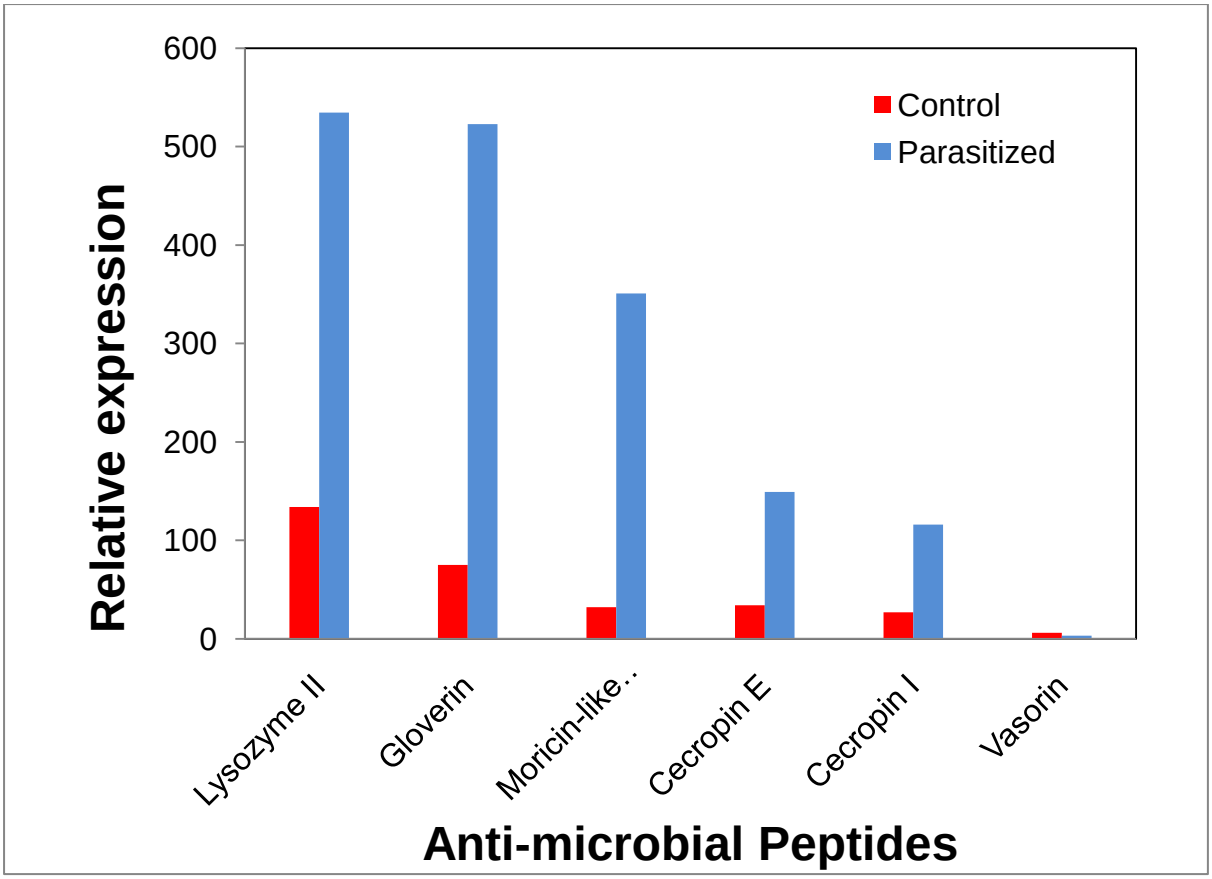

Figure 58: Relative gene expression values based on average read depth for selected antimicrobial peptide classes in non-parasitised (control) and parasitised DBM larvae.

Other related genes which were up-regulated in parasitised larvae included serine protease and serine protease inhibitor (pxSerpin 2) (Table 9). Serine proteases are major immune regulatory proteins, which are found in a wide range of species from insects to mammals. In contrast, a proteomics analysis showed that pxSerpin 2 was suppressed in DBM larval plasma during parasitism by *C. plutellae* (109). Additionally, Beck *et al***.** demonstrated that the ovarian calyx fluid of the ichneumonid endoparasitoid wasp, *Venturia canescens*, has the potential to suppress the host immune system due to the presence of a putative serpin activity (110). In this study, we found that serine protease inhibitors (serpin 7 and 13) were over-expressed two to seven-fold, respectively, after parasitism in DBM. Thus, the induction of serine protease inhibitors upon immune challenge in parasitised larvae could be a part of endoparasitoid immune suppressive strategy.

Many insect protease inhibitors are known to inactivate enzymes isolated from entomopathogenic fungi, and their involvement in insect-pathogen interactions has been widely postulated (111). Aguilar *et al.* reported that five serine proteases involved in a single metabolic cascade were up-regulated in the Malaria mosquito, *Anopheles gambiae*, upon microbial challenge, but they suggested a role for the proteases in protecting the mosquito from detrimental effects of an uncontrolled spread of immune reaction (112).

Serine proteases also play a significant role in the activation of the prophenoloxidase (proPO) cascade. In insects, proPO is activated upon injury or invasion, which results in localised melanisation of the wound area and/or melanotic capsules capturing invading microorganisms and parasites (72).

In the current study, proPO activating protease (PAP) transcription was up-regulated in parasitised larvae of DBM. In a genome-wide microarray study of *D. melanogaster*, several genes encoding enzymes of the melanisation cascade were found to be up-regulated by *Leptopilina boulardi* parasitisation (113), consistent with this study. Asgari *et al*. (2003) reported that venom protein (Vn50) from *Cotesia rubecula* is homologous to serine protease homologs (72). It is likely that the injection of this protein (or putative homologs thereof) by parasitoid wasps into the host body, may interfere with the proteolytic cascade that leads to the activation of proPO. cDNA microarray analysis of *S. frugiperda* haemocytes and fat body 24 hours after injection of *Hyposoter didymator* virus (*Hd*IV) revealed differential expression of several host genes (114). Among those, eight immune related genes showed differential expression in haemocytes with proPO-1 and proPO-2 showing up-regulation but PAP transcript levels declined. Other immune related genes that were differentially expressed in the haemocytes were galectin, which showed up-regulation, whereas scavenger R, immulectin-2, lysozyme and calreticulin showed down-regulation (114). A recent study confirmed up-regulation of proPOs in *S. frugiperda* larvae injected with *Hd*IV; however, in the same host injected with *Md*BV, proPO transcript levels declined (115) which suggested differential responses of the host to different PDVs.

Transcripts of most proteins which are involved in the Toll pathway such as Relish, Dorsal, Pelle, Cactus and Toll receptor (which are known insect immune-related genes) were found in our deep sequencing analysis, but only transcription levels of proteins that showed similarity to the Toll receptor were up-regulated 2.5 fold (Table 9)**.** In *D. melanogaster* larvae parasitised by *Asobara tabida* or *L. boulardi*, components of the Toll/Imd (Immune deficiency) pathways were up-regulated and antimicrobial peptide expression was increased (113,116). In addition, in *Drosophila*, Toll and Imd pathways are required for activation and stimulation of NF-κBs signal transduction and also responsible for innate immune response in parasitised *Drosophila* (117). NF-κB proteins are a family of proteins in eukaryotes that are involved in the control of a large number of cellular and organismal processes, such as immune responses, developmental processes, cellular growth, and apoptosis. Furthermore, NF-κB signalling is important in immune inducibility of pathogen-associated-molecular-patterns, and it is widely assumed that it plays a conserved role in invertebrate immune regulation (118,119).

It has been suggested that virus-expressed vankyrin proteins may interfere with NF-κB-mediated signaling during immune response and development in parasitised larvae (120,121). Fath-Goodin *et al.* (2009) reported that *Cs*IV vankyrin genes also encode proteins with sequence homology to the inhibitory domains of NF-κB transcription factor inhibitors (122). The results of our transcriptome analysis also indicated that genes known to be involved in insecticide resistance/detoxification are up-regulated following parasitism (Table 9). For example, it has previously been reported that cytochrome P450 (CYP) and glutathione-S-transferase (GST) activities increased in parasitised DBM larvae (123). Takeda *et al.* (2006) suggested that parasitoid larvae contributed to CYP activity enhancement since the parasitoid hatched two days after oviposition and the CYP activity was significantly increased three days after parasitisation (123)**.**

Our analyses also detected a considerable number of other immune related genes with variations in their transcription levels after parasitisation by *D. semiclausum*. However, only a small group of them were found to be biologically relevant (i.e. greater than two-fold change) affected by parasitoid attack. It is these genes which would likely be the target of immune-suppression by the *Diadegma* wasp. This information is useful in terms of detailed understanding how DBM larvae respond to parasitisation and in the context of this project, may aid in designing or screening novel immune suppressive biopesticides.

Transcription levels of host development related genes

Generally, larval endoparasitoids lay their eggs into the host hemocoel, and their progenies develop by consuming host haemolymph (blood) and tissues. As a consequence, the parasitoid's larval growth also fully depends on the host development (9,124,125). In DBM larvae parasitised by *D. semiclausum*, development is arrested at the prepupal stage (126). Developmental arrest before pupation is one of the most common effects of viruses and/or other maternal factors injected by many endoparasitoids into their hosts, such as venoms (127-130). In these interactions, the parasitoid larvae and viruses they are injected with, are responsible for increasing the juvenile hormone (JH) titer in host larvae (and inhibiting ecdysteroid levels from rising (131-135).

Based on our transcriptome data, parasitism by *D. semiclausum* leads to down-regulation of genes associated with ecdysteroid activities; for example, the ecdysteroid regulated protein transcription level was found down-regulated by more than 26 times in parasitised larvae (Table 10). Considering that ecdysteroids are required to trigger expression of the ecdysteroid regulated protein (136) and that parasitism in general leads to reductions in ecdysteroid titres (127,137-140), down-regulation of the ecdysteroid regulated protein was expected.

Juvenile hormone binding protein (JHBP) may protect JH from non-specific degradation and adsorption by preventing exposure of JH to epoxide hydration by JH epoxide hydrolase (JHEH), which generates the hormonally inactive JH diol (141). In agreement, JHBP transcript levels were upregulated more than 2 times and interestingly, transcription levels of JHEH were down-regulated more than 2 times (Table 10). In all the reported host-parasitoid systems, it seems that JH is maintained at high levels during parasitoid larval development (132,140,142). Therefore, an increase in JHBP and decrease in JHEH transcription levels after parasitism seems logical to maintain higher JH levels during parasitism. As indicated above, previous studies have shown that viruses may inhibit translation of specific storage or growth-associated proteins despite up-regulation or steady-state of transcript levels of the encoding genes following parasitism or injection of PDVs (143-145). In this study, we found that arylphorin and methionine-rich storage proteins were over-transcribed in parasitised larvae, relative to their healthy counterparts (Table 10); however, translation of such proteins may be affected similarly to reports indicated above, which still needs to be experimentally proven.

Quantitative RT-PCR validation of transcriptome analysis

To validate our deep sequencing data, 9 differentially regulated DBM genes were selected from immune and development related genes shown in Tables 9 and 10, for quantitative reverse transcription PCR (qRT-PCR) analysis using the same RNA samples used for deep sequencing. These were cuticle protein, the ecdysteroid regulated protein, JH epoxide hydrolase, insulin receptor, methionine-rich storage protein 1, gloverin, hemolin, pxSerpin 3 and Toll receptor. The qRT-PCR method is far more stringent than deep sequencing in terms of assessing relative levels of expression for various genes and was required by reviewers of the associated scientific manuscript for publication of the deep sequencing data. The qRT-PCR results confirmed the data obtained from deep sequencing analysis showing similar trends in up- or down-regulation of host genes (Figure 59). For example, based on deep sequencing analysis gloverin, Toll receptor, and pxSerpin were upregulated 6.9, 2.5 and 2.2 fold (Table 9), respectively, and showed 5.5, 2.6 and 2.7 fold change in qRT-PCR analysis (Figure 59).

Since the samples analysed above were pools of RNA from various time points and it is known that expression of host genes may vary at different periods after parasitisation, we further isolated RNA from 2nd instar DBM larvae at 16, 24 and 48 hrs after parasitisation and analyzed them by qRT-PCR. For each time point, a mixture of 10 larvae was used. These were hemolin, gloverin and the ecdysteroid regulated protein. As expected, there were fluctuations in the expression levels of these genes following parasitisation (Figure 60). For example, gloverin expression was highly induced at 12 hrs after parasitisation and subsequently declined at 16 hrs and then further reduced to the same level as unparasitised larvae at 48 hrs post-parasitisation (Figure 60). Hemolin was only induced at 48 hrs after parasitisation. Expression of the ecdyesteroid regulated protein was initially declined at 12 hrs after parasitisation but increased at 16 hrs and subsequently declined at 48 hrs post-parasitisation (Figure 60).

Sequence ID	TSA Accession No.	Nt. Length	Fold change	Protein	Species	E value	Nt. ID (%)	Accession no.
Locus 2992	JL943792	517	11	Moricin-like peptide C2	Galleria mellonella	5.00E-12	75	ABQ42576.1
Locus 11864	JL943746	452	7.06	Serine proteinase inhibitor	Procambarus clarkii	5.00E-14	41	AAQ22771.1
Locus 13987	JL943753	281	6.97	Gloverin	Plutella xylostella	3.00E-49	100	ACM69342.1
Locus 42625	JL943821	487	6.71	Beta-1,3-glucan recognition protein 3	Helicoverpa armigera	5.00E-30	45	ACI32828.1
Locus 652	JL943855	803	6.25	Proline-rich protein	Galleria mellonella	6.00E-18	38	ACQ99193.1
Locus 10530	JL943744	1440	6.09	Transferrin	Plutella xylostella	0	99	BAF36818.1
Locus 19881	JL943772	503	4.96	Odorant binding protein	Heliothis virescens	1.00E-49	66	ACX53743.1
Locus 8118	JL943865	992	4.51	Serine proteinase	Samia cynthia ricini	6.00E-89	55	BAF43531.1
Locus 4070	JL943818	449	4.37	Cecropin E	Plutella xylostella	8.00E-17	100	BAF36816.1
Locus 6056	JL943850	650	4.3	Cecropin 1 (antibacterial peptide)	Plutella xylostella	1.00E-16	98	ADA13281.1
Locus 2740	JL943785	349	4.23	Thrombin inhibitor infestin	Triatoma infestans	7.00E-19	47	AAK57342.1
Locus 742	JL943860	1405	3.99	Lysozyme II	Artogeia rapae	4.00E-15	76	AAT94286.1
Locus 8845	JL943866	517	3.81	Peptidoglycan recognition protein	Plutella xylostella	2.00E-86	97	BAF36823.1
Locus 3377	JL943803	744	3.78	Peptidoglycan recognition protein S6	Bombyx mori	3.00E-58	61	NP_001036858.1
Locus 5206	JL943842	712	3.67	Hemolin	Plutella xylostella	7.00E-131	97	ACN69054.1
Locus 11896	JL943747	1453	3.28	Prophenoloxidase-activating proteinase 3	Plutella xylostella	0	93	BAF36824.1
Locus 4541	JL943828	843	3	Trypsin-like serine proteinase 1	Plutella xylostella	2.00E-37	42	ADK66277.1
Locus 3869	JL943816	1604	2.91	Bifunctional protein folD	Culex quinquefasciatus	2.00E-101	63	XP_001846734.1
Locus 30146	JL943795	236	2.91	Nucleotide excision repair protein	Bombyx mori	1.00E-28	71	NP_001177140.1
Locus 14548	JL943754	580	2.87	Beta-1,3-glucan recognition protein 2	Bombyx mori	5.00E-40	49	NP_001037450.1
Locus 15717	JL943757	333	2.73	Prophenoloxidase activating factor 3	Bombyx mori	3.00E-19	57	AAL31707.1
Locus 13921	JL943752	602	2.68	Serine protease 33	Mamestra configurata	2.00E-36	50	ACR15983.2
Locus 12724	JL943748	1288	2.51	Serine protease inhibitor 7	Bombyx mori	5.00E-94	46	NP_001139701.1
Locus 43519	JL943823	256	2.5	Ceramidase	Aedes aegypti	2.00E-21	62	XP_001658093.1
Locus 48995	JL943836	207	2.5	Toll receptor	Tribolium castaneum	2.00E-19	59	XP_971999.1
Locus 1006	JL943743	1154	2.41	Lipocalin	Bombus ignitus	1.00E-89	64	ADA82597.1
Locus 6114	JL943851	1293	2.38	Lysosomal acid lipase	Tribolium castaneum	1.00E-65	39	XP_972957.2
Locus 28994	JL943788	911	2.33	Pattern recognition serine proteinase	Manduca sexta	3.00E-87	51	AAR29602.1

Locus 20345	JL943774	322	2.26	Trypsin T6	Heliothis virescens	9 E-16	54	ABR88249.1
Locus 17873	JL943765	412	2.25	NADP+	Danio rerio	1.00E-56	76	NP_998058.1
Locus 7994	JL943864	1305	2.24	Serine protease inhibitor (Serpin 3)	Plutella xylostella	2.00E-99	50	BAF36821.1
Locus 2093	JL943776	2890	2.21	Apolipophorins	Manduca sexta	0	67	Q25490.1
Locus 20404	JL943775	251	2.19	Serine protease inhibitor (Serpin 13)	Bombyx mori	4.00E-14	49	NP_001139705.1
Locus 41604	JL943819	282	2.16	Broad-Complex isoform Z2	Bombyx mori	1.00E-30	98	BAD24051.1
Locus 35475	JL943806	363	2.15	Heat Shock Protein (HSP70)	Acyrthosiphon pisum	3.00E-12	44	XP_001950064.1
Locus 29819	JL943791	461	2.14	Beta-1,3-glucan recognition protein 2a	Helicoverpa armigera	1.00E-53	64	ACI32826.1
Locus 4518	JL943827	303	2.13	Serine protease 1	Lonomia obliqua	4.00E-22	51	AAV91432.2
Locus 39662	JL943817	299	2.12	1-phosphatidylinositol-4,5-bisphosphate	Bombyx mori	6.00E-45	86	NP_001165393.1
Locus 9824	JL943870	627	2.11	Peripheral-type benzodiazepine receptor	Bombyx mori	6.00E-34	57	NP_001040343.1
Locus 19848	JL943771	1136	2.1	Peroxidasin	Tribolium castaneum	1.00E-134	62	XP_968570.1
Locus 21658	JL943781	437	2.04	Hemolymph proteinase 8	Manduca sexta	4 E-49	71	AAV91006.1
Locus 620	JL943852	1032	-2	Heat Shock Protein (HSP90)	Plutella xylostella	8.00E-140	100	BAE48742.1
Locus 18755	JL943766	351	-2.06	Vasorin	Culex quinquefasciatus	1.00E-54	85	XP_001870087.1
Locus 15108	JL943755	615	-2.07	Arylalkylamine N-acetyltransferase	Antheraea pernyi	1.00E-29	38	ABD17803.1
Locus 19225	JL943768	253	-2.12	Flap endonuclease	Carukia barnesi	6.00E-25	83	ACY74444.1
Locus 29249	JL943789	213	-2.12	Putative lysozyme	Bombyx mori	4.00E-22	67	ADA67927.1
Locus 7618	JL943861	3056	-2.14	Fascin	Tribolium castaneum	0	79	XP_972494.1
Locus 13139	JL943751	701	-2.4	Hemocyte protease-1	Bombyx mori	6 E-75	60	BAG70409.1
Locus 11481	JL943873	364	-3.25	Trypsin	Helicoverpa armigera	5 E-16	43	ACB54939.1
Locus 24418	JL943783	211	-3.5	Black (DOPA-deC-like)	Papilio xuthus	1.00E-29	87	BAI87832.1
Locus 536	JL943843	527	-3.65	Catalase	Takifugu obscurus	1.00E-17	35	ABV24056.1
Locus 3343	JL943800	289	-3.78	Immune-related Hdd1	Hyphantria cunea	3.00E-11	39	AAD09279.1
Locus 13049	JL943750	452	-5.81	Putative defense protein Hdd11	Hyphantria cunea	8.00E-55	67	O96382.1

Table 9: A list of DBM immune related genes that were differentially transcribed after parasitisation by *D. semiclausum*. Fold changes were generated by comparing average read depth for each contig.

Sequence ID	TSA Accession No.	Nt. Length	Fold change	Protein	Species	E value	Nt. ID (%)	Accession no.
Locus 29717	JL943790	504	27.86	Endonuclease-reverse transcriptase	Bombyx mori	1 E-46	67	ADI61832.1
Locus 3567	JL943808	277	20.01	Glucose dehydrogenase precursor	Pediculus humanus corporis	1 E-15	52	XP_002429706.1
Locus 784	JL943863	1943	12.5	Methionine-rich storage protein 1	Plutella xylostella	0	100	BAF45385.1
Locus 50007	JL943839	234	8.31	Putative RecQ Helicase	Heliconius melpomene	1 E-11	63	CBH09254.1
Locus 3712	JL943813	1744	7.8	Methionine-rich storage protein 2	Plutella xylostella	0	100	BAF45386.1
Locus 1098	JL943745	724	4.4	Arylphorin-like hexamerin-2	Plutella xylostella	1 E-141	100	BAF32562.1
Locus 9922	JL943871	1790	4.31	44 kDa zymogen (serine protease)	Tenebrio molitor	9 E-61	35	BAG14262.1
Locus 2239	JL943782	2186	3.46	Methionine-rich storage protein	Spodoptera exigua	0	59	ABX55887.1
Locus 352	JL943805	1023	3.43	Arylphorin-like hexamerin-1	Plutella xylostella	2 E-172	89	BAF32561.1
Locus 5917	JL943849	2338	3.4	Phenylalanine hydroxylase	Papilio xuthus	0	88	BAE66652.1
Locus 42829	JL943822	273	3.33	Syntaxin	Culex quinquefasciatus	3 E-21	60	XP_001865470.1
Locus 1575	JL943758	1738	3.12	Phosphoribosylaminoimidazole carboxylase	Bombyx mori	0	90	NP_001040376.1
Locus 33387	JL943799	375	3.11	Insulin receptor	Bombyx mori	3 E-34	59	NP_001037011.1
Locus 47369	JL943832	347	3	Leucine-rich transmembrane protein	Pediculus humanus corporis	1 E-24	60	XP_002422869.1
Locus 7126	JL943859	1075	2.98	Sugar transporter 4	Bombyx mori	2 E-104	64	NP_001165395.1
Locus 35539	JL943807	592	2.55	Torso-like protein	Tribolium castaneum	2 E-31	38	NP_001107843.1
Locus 36082	JL943809	735	2.44	Reverse transcriptase	Aedes aegypti	3 E-36	39	AAZ15237.1
Locus 199	JL943773	1588	2.4	S-adenosyl-L-homocysteine hydrolase	Plutella xylostella	0	100	BAF36817.1
Locus 5556	JL943845	1186	2.33	Yellow-fa	Bombyx mori	4 E-141	69	NP_001037424.1
Locus 4588	JL943829	205	2.24	Endoprotease FURIN	Spodoptera frugiperda	4 E-28	87	CAA93116.1
Locus 4894	JL943835	861	2.24	Lipase	Helicoverpa armigera	3 E-50	54	ACB54943.1
Locus 4689	JL943830	2429	2.21	Cathepsin L precursor	Tribolium castaneum	0	62	NP_001164088.1
Locus 3008	JL943793	950	2.21	Hemolymph proteinase 5	Manduca sexta	2 E-	62	AAV91003.1

Locus 20931	JL943777	661	2.17	Gamma-glutamyl transferase	Bombyx mori	1 E-62	56	NP_001165385.1
Locus 21405	JL943780	705	2.14	Juvenile hormone binding protein	Manduca sexta	2 E-27	35	AAB25736.2
Locus 3797	JL943815	1653	2.13	Imaginal disk growth factor	Plutella xylostella	0	100	BAF36822.1
Locus 5088	JL943841	1476	2.12	Cathepsin B-like cysteine proteinase	Spodoptera exigua	1 E-146	81	ABK90823.1
Locus 1887	JL943767	1872	2.1	Cathepsin D isoform 1	Tribolium castaneum	7 E-165	73	XP_966517.1
Locus 47019	JL943831	207	2.09	DNA-binding protein Ewg putative	Pediculus humanus corporis	3 E-22	93	XP_002430412.1
Locus 16109	JL943872	515	2.08	Nesprin-1	Pediculus humanus corporis	3 E-26	36	XP_002427810.1
Locus 41758	JL943820	222	2.06	Neuroglian	Mythimna separata	4 E-29	78	BAI49425.1
Locus 6830	JL943856	427	2.04	Cytochrome P450	Plutella xylostella	2 E-67	96	ABW34440.1
Locus 17556	JL943762	1272	2.03	Arginase	Bombyx mori	9 E-144	72	BAH19308.1
Locus 25700	JL943784	286	-2.03	Cytochrome P450 monooxygenase	Helicoverpa zea	7 E-16	74	AAM54723.1
Locus 7042	JL943858	809	-2.05	Tyrosine transporter	Aedes aegypti	2 E-18	76	XP_001658764.1
Locus 4738	JL943833	1359	-2.07	Collagen	Bombyx mori	2 E-23	49	CAA83002.1
Locus 3369	JL943802	471	-2.09	Trypsin alkaline B	Manduca sexta	7 E-37	71	P35046.1
Locus 7004	JL943857	696	-2.13	Cuticular protein glycine-rich 20	Bombyx mori	3 E-15	52	NP_001166784.1
Locus 17043	JL943761	237	-2.13	Voltage & ligand gated potassium channel	Culex quinquefasciatus	2 E-15	71	XP_001853758.1
Locus 16717	JL943760	1585	-2.14	Multidrug resistance protein 2	Culex quinquefasciatus	1 E-93	41	XP_001866984.1
Locus 5571	JL943846	389	-2.19	Sugar transporter	Aedes aegypti	1 E-11	48	XP_001652873.1
Locus 13022	JL943749	216	-2.36	Ecdysis-triggering hormone	Manduca sexta	2 E-15	65	AAD45613.1
Locus 6441	JL943853	661	-2.43	Retinol dehydratase	Spodoptera frugiperda	1 E-53	58	AAC47136.1
Locus 15939	JL943759	279	-2.46	Cyclin-dependent kinase 2-like	Saccoglossus kowalevskii	3 E-23	68	XP_002740677.1
Locus 487	JL943834	1615	-2.56	Glucosinolate sulphatase	Plutella xylostella	0	64	CAD33828.1
Locus 6512	JL943854	484	-2.57	Phosphohistidine phosphatase	Bombyx mori	3 E-45	62	NP_001040265.1
Locus 7636	JL943862	454	-2.7	Reverse transcriptase	Ostrinia nubilalis	3 E-39	48	ABO45231.1
Locus 33235	JL943798	220	-2.74	Juvenile hormone epoxide hydrolase	Bombyx mori	5 E-18	64	NP_001159617.1
Locus 36575	JL943812	209	-2.83	Lipase	Bombyx mori	8 E-12	52	ADA67928.1

Locus 5577	JL943847	1813	-2.9	Chitinase	Plutella xylostella	0	100	ACU42267.1
Locus 4357	JL943824	1009	-3.21	Cuticular protein RR-1 motif 10	Bombyx mori	1 E-56	68	NP_001166738.1
Locus 21088	JL943778	247	-3.25	Carboxypeptidase M	Aedes aegypti	1 E-37	83	XP_001661307.1
Locus 2898	JL943787	485	-4.27	Acheron	Manduca sexta	1 E-68	88	AF443827_1
Locus 5445	JL943844	1708	-8.82	Urbain	Bombyx mori	4 E-24	37	NP_001139414.1
Locus 21299	JL943779	290	-15.5	37-kDa serine protease	Bombyx mori	6 E-41	81	NP_001128675.1
Locus 17795	JL943764	363	-24.01	Cuticle protein	Aedes aegypti	3 E-29	67.78	XP_001659461.1
Locus 8908	JL943867	625	-26.71	Ecdysteroid regulated protein	Manduca sexta	1 E-12	71	AAA29312.1

Table 10: Developmental and non-immune metabolism-related transcripts of DBM which were differentially expressed after *D. semiclausum* parasitisation. Fold changes were generated by comparing average read depth for each contig.

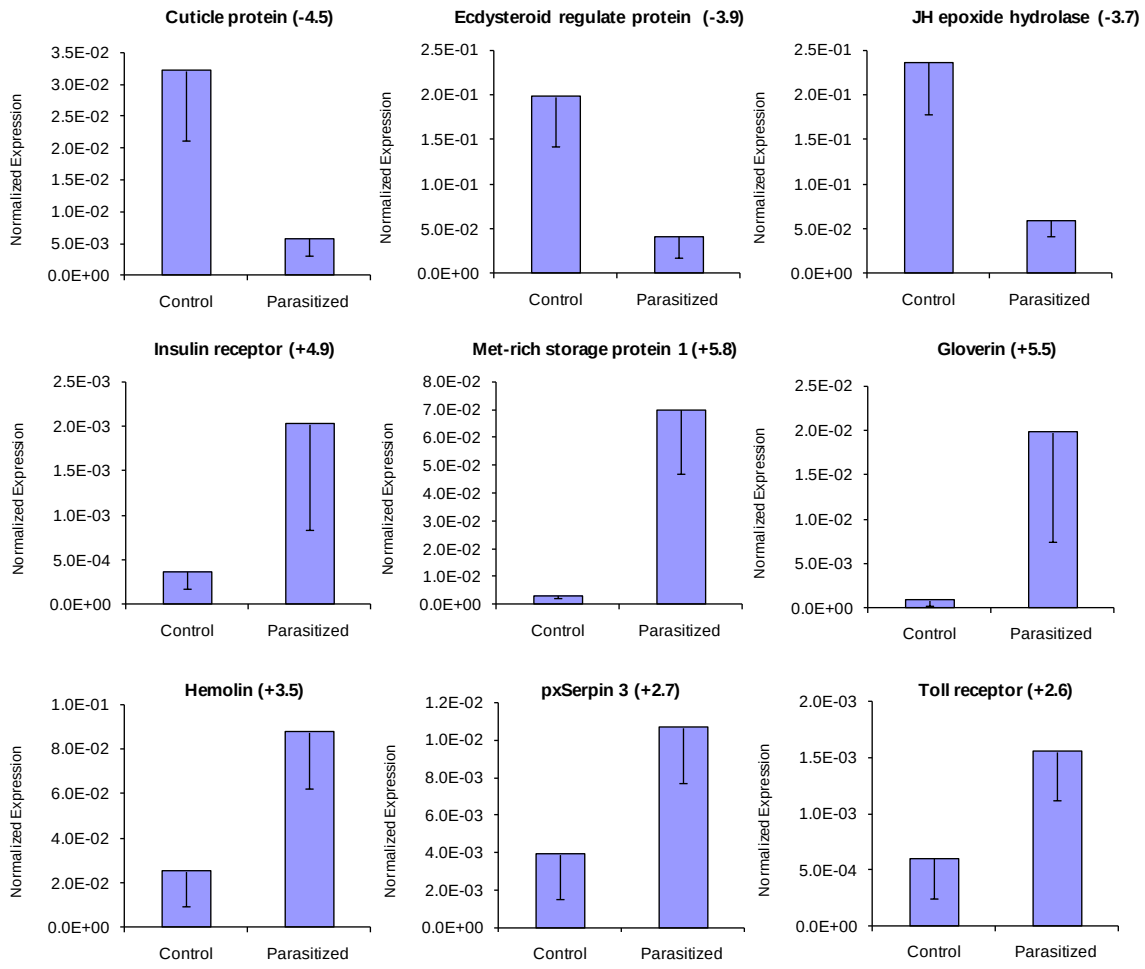

Figure 59: qRT-PCR analysis of 9 selected genes from DBM which showed differential expression after parasitisation based on deep sequencing analysis. The same RNA samples used for deep sequencing were used in the qRT-PCR analyses. Error bars indicate standard deviations of averages from three replicates. Fold changes are shown in brackets.

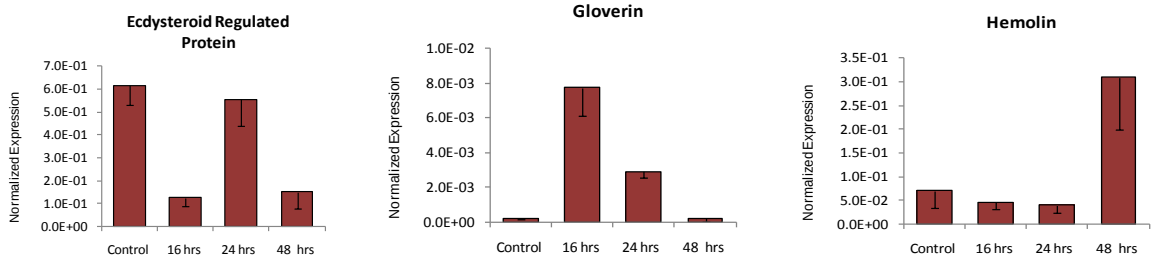

Figure 60: qRT-PCR analysis of expression levels of 3 selected genes in 2nd instar DBM larvae at three time points after parasitisation with *D. semiclausum* which showed differential expression after parasitisation based on deep sequencing analysis. Error bars indicate standard deviations of averages from three replicates.

Diadegma semiclausum ichnovirus (*Ds*IV) genes

*Ds*IV (and other polydnavirus) genes are divided into three groups based on whether they are expressed in the carrier wasp *Diadegma* (class I), the infected DBM larvae (class II) or both organisms (class III) (146). Among these genes, class II genes have received the greatest attention and have been studied more than other groups (147) as they are generally the genes that directly regulate parasitism and have deleterious effects on parasitised larvae. The genomes of some viruses, such as those found in the wasps *C. sonorensis, C. chlorideae, Hyposoter fugitivus, H. didymator, and Tranosema rostrale*, have been sequenced and resultant data are available on public databases (146,148,149). Six conserved gene families: repeat element, cysteine motif, viral innexin, viral ankyrin, N-family and the polar-residue-rich proteins (a newly defined putative family), have been reported in most IV genomes (146). This data was important as it allowed us to directly compare our sequences, which not only confirmed they are *Ds*IV genes (rather than wasp or DBM genes),but also provided us with some information as to the identity and putative function of the virus genes we detected in parasitised DBM.

In our analysis, 19 unique sequences were identified from five virus gene families including vankyrin, viral innexin, repeat elements, cysteine-rich motif, and polar residue rich protein families (Table 11). In addition, and importantly for potential biopesticide production, five other virus protein sequences of unknown function were identified in parasitised larvae, and showed more than 50% similarity with some parts of other IV genomes but no putative specific protein domain was detected in their sequences (Table 11). The online open reading frame finder tool at the NCBI website (www.ncbi.nlm.nih.gov/projects/gorf) was used for prediction of full-length sequences in *Ds*IV genes and only four of these genes are reported here as full-length (Table 11).

Presence of multiple sequences for each virus gene family is common in other viruses and we identified four sequences with vankyrin domain and two viral innexin transcripts, which showed high similarity with *H. fugitivus* virus innexins (Table 11). Repeat element domains were also identified in six sequences with lengths between 209-244 amino acids. Transcription levels (or gene expression values) were found to be different among different members of each gene family. Vankyrin 1 and repeat element 1 had the highest transcription levels in their groups and also among the other *Ds*IV genes (Figure 61).

Hierarchical cluster analysis of vankyrin gene sequences of all reported wasp virus vankyrins (protein sequences at NCBI) using a neighbour-joining algorithm, classified vankyrins from bracoviruses and ichnoviruses (such as *Ds*IV) into two major groups (Figure 62). All four *Ds*IV vankyrins that were identified in this study have high similarities with those from other ichnoviruses.

Protein	Length (nt)	Accession Number	Similarity (Protein/virus/Accession No.)	length (aa)	E value	Nt. ID %	Conserved Domains
Vankyrin 1	671*	JI257593	vankyrin-b17 (HfIV) AAS90270.1	170	3.56E-52	61	Yes
Vankyrin 2	519*	JI257594	vankyrin-d8.3 (HfIV) BAF45734.1	159	6 E-64	80	Yes
Vankyrin 3	257	JI257595	hypothetical protein 2 (HdIV) AAR99845.1	126	3.58E-23	61	Yes
Vankyrin 4	361	JI257596	vankyrin-b1(HfIV) AAX24120.1	167	2 E-39	76	Yes
Viral Innexin 1	1370	JI257597	viral innexin-b5.1 (HfIV) BAF45654.1	354	5 E-95	60	Yes
Viral Innexin 2	576	JI257598	viral innexin-c16 (HfIV) AAS58041.1	371	2 E-81	75	Yes
Repeat element 1	833	JI257599	repeat element protein 7 (HdIV) AAR89179.1	224	4.32E-73	67	Yes
Repeat element 2	697	JI257600	repeat element protein-d10.1 (HfIV) BAF45740.1	244	1.53E-72	64	Yes
Repeat element 3	947	JI257601	repeat element protein-c18.1 (HfIV) BAF45697.1	244	9.52E-94	71	Yes
Repeat element 4	859*	JI257602	repeat element protein-e2.3 (HfIV) BAF45758.1	209	3.40E-76	67	Yes
Repeat element 5	656	JI257603	repeat element protein (HdIV) AAO16959.1	225	1.21E-73	59	Yes
Repeat element 6	500	JI257604	repeat element protein-d11.2 (HfIV) BAF45744.1	244	1E-68	72	Yes
Cysteine rich motif	630	JI257605	cysteine motif gene-d9.1(HfIV) BAF45736.1	311	2.99E-55	64	Yes
Polar residue rich protein	671	JI257606	polar residue rich protein-b13.2 (HfIV) BAF45664.1	159	1.24E-12	42	No
Unknown Protein	256	JI257607	c7-2.1 (TrIV) BAF45599.1	119	2.90E-17	68	Yes
Unknown Protein	2143*	JI257608	c12.1 (HfIV) AAS68099.1	432	2E-107	50	No
Unknown Protein	418	JI257609	P12 (HdIV) AAS83461.1	106	6E-18	58	No
Unknown Protein	584	JI257610	c10.1 (HfIV) AAS90272.1	385	9.15E-50	51	No
Unknown Protein	208	JI257611	b5.3 (HfIV) BAF45655.1	115	9.57E-13	69	No

* Full length Hf: Hyposoter fugitivus Hd: Hyposoter didymator Tr: Tranosema rostrale

Table 11: *Diadegma semiclausum* ichnovirus transcripts which were detected in parasitised DBM larvae.

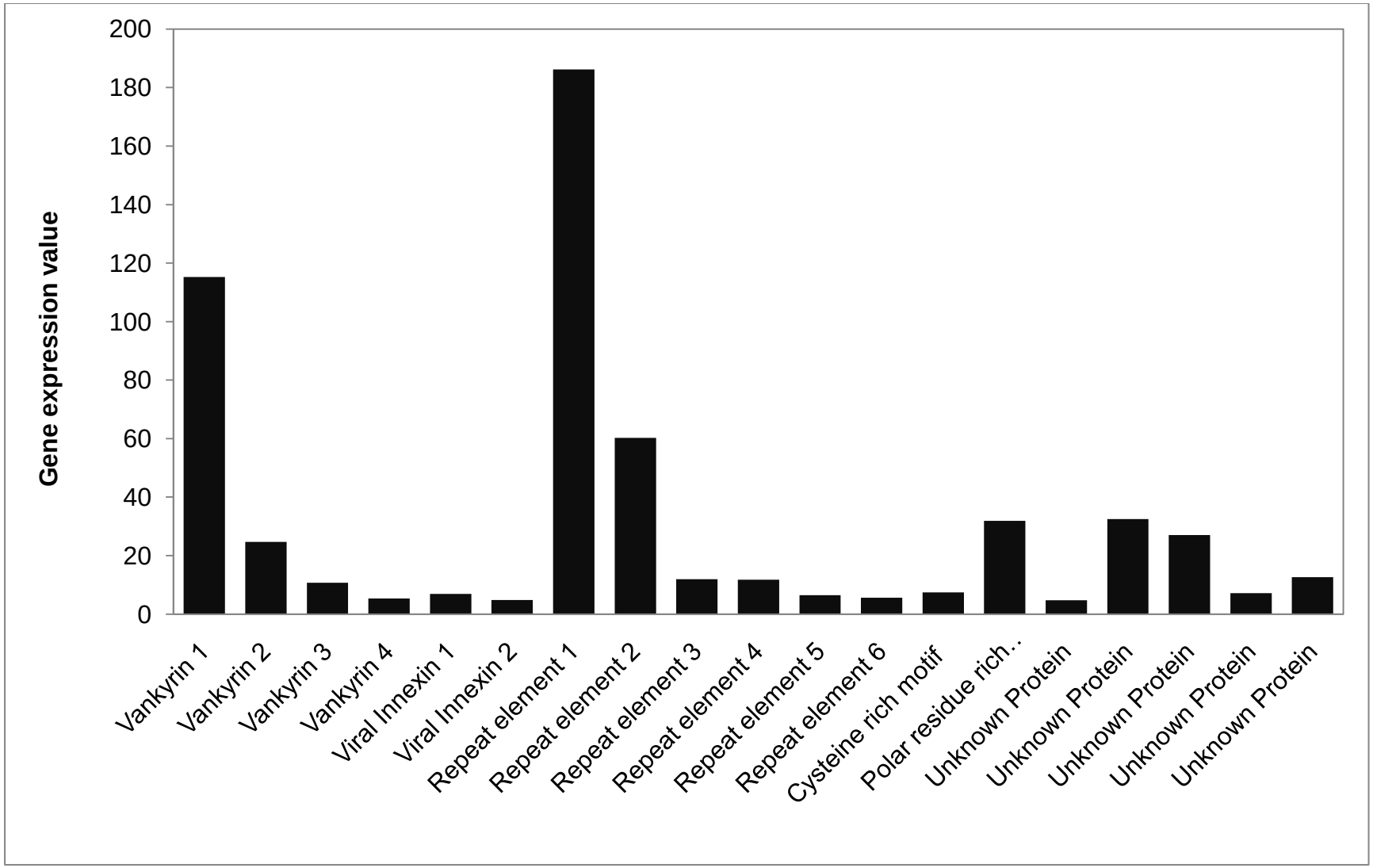

Figure 61: Relative gene expression values based on average read depth for all detected *D. semiclausum* ichnovirus genes. RPKM normalised values were used to generate the data.

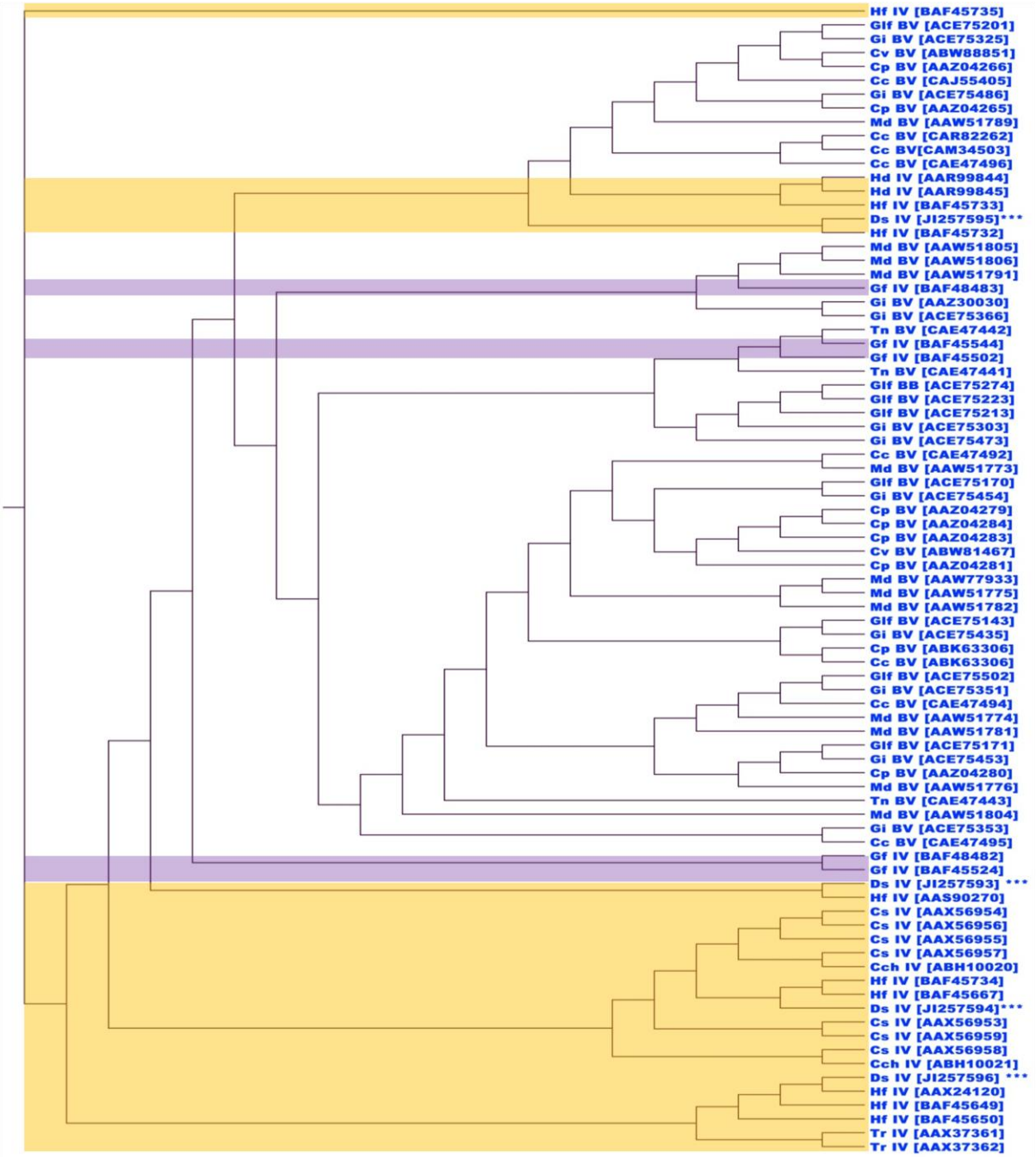

Figure 62: Hierarchical Cluster analysis of vankyrin gene sequences of all reported polydnavirus vankyrins using neighbour joining algorithm. The accession code for each vankyrin is mentioned in bracket. The yellow and purple backgrounds show the *Ichnovirus* (IV) and provisional group of banchine virus genes, respectively, and the rest are *Bracovirus* (BV) vankyrins.

Deep sequencing analysis of DBM immune genes and *Ds*IV genes: Laypersons' summary

As mentioned previously, deep sequencing is a relatively recent technological development which allows researchers to generate huge amounts of DNA sequence data, relatively quickly. The term "deep sequencing" refers to the ability to the capacity of the technology to produce DNA sequence data for the full repertoire of genes in complex samples, in this case parasitised and non-parasitised DBM larvae. Our deep sequencing experiments produced the following data:

- a list of DBM genes that are affected by parasitisation. This provides us with detailed fundamental information about how DBM immune system is responding to parasitisation will be important for developing immune-related controls for caterpillars and provides useful information for researchers globally. This can also be extrapolated to other caterpillar pests to some degree.

- a list of genes of the *Diadegma semiclausum* virus, which facilitate parasitisation through immune suppression of DBM. These genes, several of which are new to science, are immune-suppressive candidates for further characterisation.

This fundamental information will soon be published in *BMC Genomics* and will improve our understanding of how DBM immunity works, and how we can modulate it for pest management.

CHAPTER 5: CrV2 Protein From the *Cotesia rubecula* Bracovirus (results and discussion)

In this project we performed several experiments which allowed us to confirm, and subsequently publish data relating to, an *in vitro* interaction between a wasp virus protein that we discovered in 2004 (CrV2; see (50)) and an important cell-signalling protein, Gα. The CrV2 virus protein is produced by the braconid wasp, *Cotesia rubecula*, which is a parasitoid of another Brassica pest, the Cabbage white butterfly, *Pieris rapae*. In previous projects we had produced data showing a potential interaction which we confirmed with experiments in this project. In addition, we showed that the protein interacts with immune cells (haemocytes) in both DBM and Cabbage white butterfly and interestingly, appears to target a specific subclass of haemocyte. CrV2 may become a useful compound as it's interaction with Gα would represent a novel form of insect immune-suppression which is active against blood cells of two key Brassica pests.

In this chapter we provide results and discussion relating to the experiments performed in this project, with corresponding methods contained in Chapter 1. However, in order to place these data in an industry context and make all previous information regarding CrV2 available to industry, the complete final approved draft manuscript of the scientific publication that summarises what is known about Crv2 and its effects, is provided in Appendix A. We have removed from the manuscript, the methods performed as part of this project (which are in Chapter 1) and retained the complete results and discussion.

Confirmation of interaction of CrV2 with $G\alpha_o$

To confirm the specific interaction we previously observed via other methods (see (50) and/or Appendix A), $G\alpha_o$ was blotted onto a nitrocellulose membrane and was labelled by probing with recombinant CrV2, and then bound CrV2 was detected with anti-CrV2 (Figure 63). A range of results producing no detection indicated the blotted $G\alpha_o$ was only detectable due to prior CrV2 binding, *viz*: Gα was not detected when CrV2 was absent or when anti-CrV2 was not applied. Furthermore, CrV2 did not bind to bovine serum albumin under the same conditions.

Specific uptake of CrV2 by granuloctytes

Application of CrV2 to haemocytes showed that CrV2 was taken up from surrounding medium. Moreover, the recombinant protein was only associated with a specific type of haemocyte that once attached to the slide surface, display a smaller, more rounded morphology, typical of granulocytes (Figure 64). This suggests that CrV2 targets a particular immune function carried out by granulocytes, that may not occur in plasmatocytes. Infection with PDVs has previously been observed to have effects on a single haemocyte type. Interestingly, other researchers (150,151) reported that *Microplitis demolitor* bracovirus induced apoptosis specifically in granulocytes. However, to date our studies have not shown that the presence of CrV2 results in apoptosis and apoptosis has not been observed in the *Cotesia-Pieris* system.

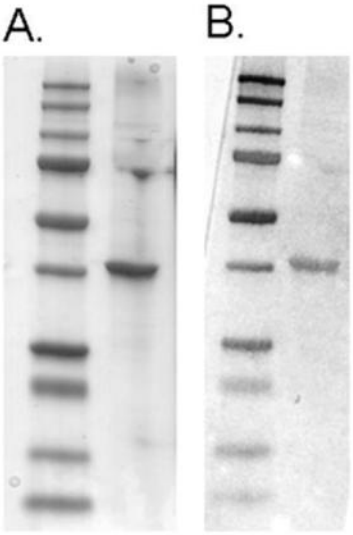

Figure 63: Far Western blot confirms $G\alpha_o$ interaction with CrV2. (A) Coomassie stained gel of $G\alpha_o$ (right lane) run by SDS-PAGE with molecular weight marker (Bio-Rad precision plus dual colour protein standard) in left lane. (B) Duplicate samples of (A) transferred to nitrocellulose and probed with CrV2. CrV2 binding was detected using rabbit anti-CrV2 and alkaline phosphatase conjugated secondary antibody. CrV2 bound to the band of $G\alpha_o$ but did not bind to BSA under the same conditions (data not shown). $G\alpha_o$ was not detected when probe CrV2 or anti-CrV2 was absent (data not shown).

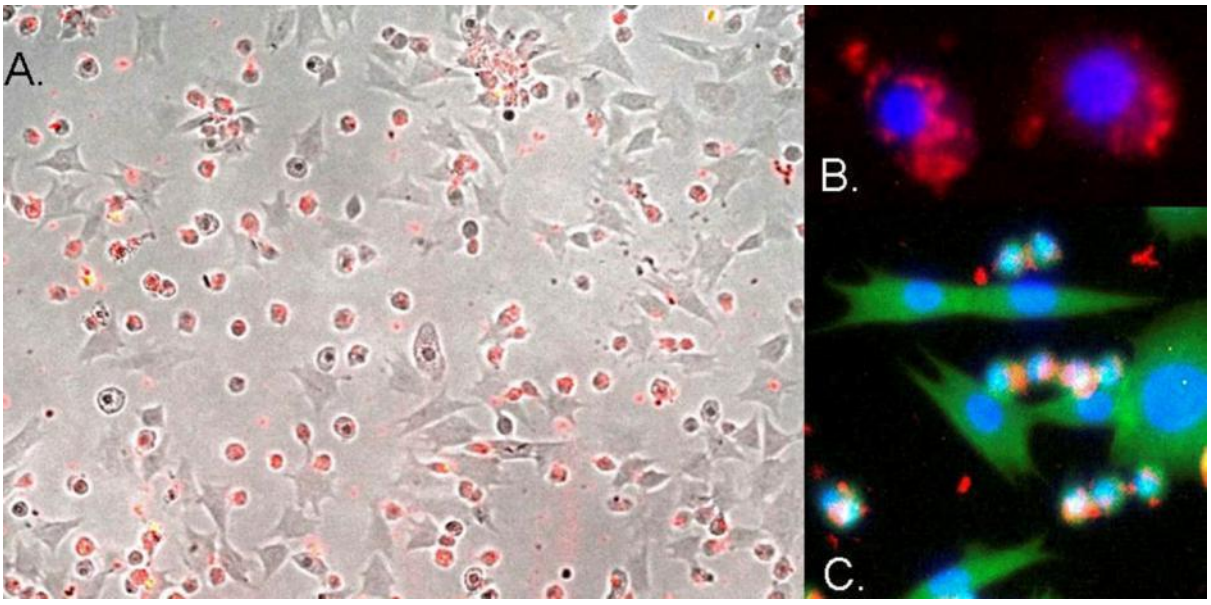

Figure 64: Uptake of CrV2 by specific *Pieris rapae* haemocytes. *Pieris* larvae were bled into medium saturated with PTU, the haemocytes were applied to the wells of a glass slide and allowed to adhere and spread. CrV2 in medium was then applied to the cells and incubated for 45 min. A) Merged image of brightfield and red fluorescence from TRITC secondary antibody bound to anti-CrV2 shows CrV2 associated with the small round haemocytes. B) Merged blue and red fluorescence images showing the nucleus (blue) stained with DAPI and CrV2 (red). C) Merged blue, red and green fluorescent image showing the nucleus (blue), CrV2 (red) and the cytoskeleton stained with FITC conjugated phalloidin (green).

CrV2 protein: Laypersons' summary

In this chapter we describe several experiments which allowed us to partly determine how the CrV2 protein functions to suppress immunity of Brassica pests. We know that the protein itself is produced by wasp viruses, in larvae of DBM (and also of Cabbage white butterfly in which we first discovered CrV2 in 2004; see (50)). Previously we had conducted experiments that indicated there was a very strong interaction between the CrV2 protein and an important cell signaling protein, Gα. In this project, we decided to investigate this interaction further. This led to confirmation of the interaction and evidence that the protein is taken up by a specific type of caterpillar blood cell (granulocytes). This provided enough evidence to publish this interaction (see Appendix A) and speculate on the immune-suppressive mode-of-action of CrV2, which appears to be novel.

Given the combined evidence for Gα involvement in the immune response of invertebrates, and the data we present here showing nanomolar affinity between the proteins, we hypothesise that CrV2 targets Gα subunits in specific immune cells (granulocytes) to disrupt Gα-associated immune-signalling by these cells. This would likely produce an abrogation of normal cellular immune processes such as exocytosis. This indicates that CrV2 may be a good candidate to investigate further as a biopesticide for Brassica caterpillars. Further work establishing the interaction in vivo and elucidation of the novel CrV2 mode-of-action will likely be useful in understanding the molecular signalling mechanisms in invertebrate immunology. Such knowledge will be useful for designing non-toxic, immune-related compounds for control of pest insects.

Technology Transfer

Given the fundamental scientific nature of this stage of the project, technology transfer amongst primary producers was not a key focus, although dissemination of key findings amongst primary producers is important. The key focus for this type of research is to gain scientific acceptance of the data and disseminate the information to other scientists, agrichemical companies, HAL strategists, and potential investors in the technology. This is primarily because of the technical nature of the data and the specific scientific and commercial expertise required to take the research further and to then develop compounds for commercial pest management. Indeed, basic science is required prior to commercialisation of any agrichemical.

In that sense the project has been quite successful in that we will have published two papers in international peer reviewed journals. The first of these described a potential mode-of-action for CrV2 protein which we showed could attack a specific type of caterpillar blood cell, *viz*:

Cooper, T., Bailey-Hill, K., Leifert, W.R., McMurchie, E.J., Asgari, S. and Glatz, R.V. (2011). Identification of an *in vitro* interaction between an insect immune-suppressor protein (CrV2) and Gα proteins. *The Journal of Biological Chemistry*, 286, 10466-10475.

The second of these papers is currently in press and reports on the deep sequencing data which provided much information about the immune function of DBM and how the Diadegma wasp suppresses DBM immunity, *viz*:

Etebari, K., Palfreyman, R., Schlipalius, D., Nielsen, L., Glatz, R. and Asgari, S. (2011). Deep sequencing-based transcriptome analysis of *Plutella xylostella* larvae parasitized by *Diadegma semiclausum*. *BMC Genomics*.

Both papers are important for driving Australian and global research on DBM and other vegetable pests.

In addition, there have been several industry-based reports on the project, which have provided information about progress to primary producers and others within industry and government, *viz*:

HAL Vegetable Industry Report 2008-2009. *Immune suppressors to manage diamondback moth (DBM)*; p40.
(SEE APPENDIX B for full article)

Brassica IPM National Newsletter, Issue 13, October 2009. *Investigation of immune suppressors of Diamond-back moth*; pp3-4.
(SEE APPENDIX C for full article)

Additionally, this project has been chosen as a feature story for the HAL Annual Report for 2011-2012.

Recommendations

The broad aim of this project was to provide fundamental scientific information how the DBM immune system functions, and the molecular basis for how DBM immunity is subverted by the parasitoid wasp, *Diadegma semiclausm.* This fundamental information is important as it will form the basis for future work investigating the use of immune-suppressive compounds for integrated control of Brassica pest caterpillars.

We found that a range of wasp venom and virus proteins are active in attacking immune cells in pest caterpillars, and further, we now have a good understanding of the how the immune system of DBM responds to parasitisation. These pieces of information effectively identify a pool of novel immune-suppressive bioactive compounds, and a pool of molecular targets within larval DBM, respectively. We have disseminated much of this information throughout the scientific community through international peer-reviewed journals.

At the outset of the project we had hoped to be able to directly recommend changes to pest management protocols on order to increase the efficicency of *D. semiclausum* in controlling DBM. However, changes to our experimental approach meant that we identified many more potential candidate bioactives than we initially thought we would, but that the degree of characterisation of the detailed mode-of-action of individual compounds is less than our original plans. Therefore, while we still think it possible with further knowledge, we are not able to recommend any refinement to management of *D. semiclausum* at this time.

In terms of recommendations for development of the novel compounds as commercial insecticides (and the relevant protocols for their use), we suggest that a further 12-24 months research should be undertaken prior to consultation with a commercial partner for assessment and development of these compounds. Research should focus on the following areas:

1. screening for remainder of the proteins
2. isolating new virus proteins for analysis
3. targeting partially characterised, promising proteins/peptides from this study for detailed functional studies
4. investigate CrV2 mode-of-action to assess development potential
5. investigate other methods of interfering with DBM immunity based on deep sequencing data

Acknowledgements

This project has been funded by HAL using the vegetable industry levy and matched funds from the Australian Government. The project was a collaboration between HAL, The South Australian Research and Development Institute (SARDI) and The University of Queensland.

Bibliography of Literature Cited

1. Talekar, N. S., and Shelton, A. M. (1993) *Annual Review of Entomology* **38**, 275-301
2. Endersby, N. M., Ridland, P. M., and Hoffmann, A. A. (2008) *Bulletin of Entomological Research* **98**, 145-157
3. Furlong, M. J., Spafford, H., Ridland, P. M., Endersby, N. M., Edwards, O. R., Baker, G. J., Keller, M. A., and Paull, C. A. (2008) *Australian Journal of Experimental Agriculture* **48**, 1494-1505
4. Gong, Y. J., Wang, C. L., Yang, Y. H., Wu, S. W., and Wu, Y. D. (2010) *Journal of Invertebrate Pathology* **104**, 90-96
5. Yang, J. C., Chu, Y. I., and Talekar, N. S. (1994) *Entomophaga* **39**, 397-406
6. Huang, F., Shi, M., Chen, Y. F., Cao, T. T., and Chen, X. X. (2008) *Microscopy Research and Technique* **71**, 676-683
7. Huang, F., Cao, T. T., Shi, M., Chen, Y. F., and Chen, X. X. (2008) *Insect Science* **15**, 237-243
8. Doi, S. F., Cai, D. Z., Li, X., and Chen, X. X. (2009) *Archives of Insect Biochemistry and Physiology* **70**, 30-43
9. Asgari, S. (2006) Archives of Insect Biochemistry and Physiology **61**, 146-156
10. Zhang, G. M., Schmidt, O., and Asgari, S. (2004) *J.Biol.Chem.* **279**, 41580-41585
11. Stoltz, D. B., Guzo, D., Belland, E. R., Lucarotti, C. J., and Mackinnon, E. A. (1988) *Journal of General Virology* **69**, 903-907
12. Colinet, D., Dubuffet, A., Cazes, D., Moreau, S., Drezen, J. M., and Poirie, M. (2009) *Developmental and comparative immunology* **33**, 681-689
13. Zhang, G., Schmidt, O., and Asgari, S. (2006) *Developmental and Comparative Immunology* **30**, 756-764
14. Uckan, F., Ergin, E., Rivers, D. B., and Gencer, N. (2006) *Archives of Insect Biochemistry and Physiology* **63**, 177-187
15. Ergin, E., Uckan, F., Rivers, D. B., and Sak, O. (2006) *Archives of Insect Biochemistry and Physiology* **61**, 87-97
16. Marris, G. C., Bell, H. A., Naylor, J. M., and Edwards, J. P. (1999) *Entomologia Experimentalis Et Applicata* **93**, 291-298
17. Dani, M. P., Richards, E. H., Isaac, R. E., and Edwards, J. P. (2003) *Journal of Insect Physiology* **49**, 945-954
18. Parkinson, N. M., Conyers, C. M., Keen, J. N., MacNicoll, A. D., Smith, I., and Weaver, R. J. (2003) *Comparative Biochemistry and Physiology C-Toxicology & Pharmacology* **134**, 513-520
19. Parkinson, N., Richards, E. H., Conyers, C., Smith, I., and Edwards, J. P. (2002) *Insect Biochemistry and Molecular Biology* **32**, 729-735
20. Richards, E. H., and Dani, M. P. (2008) *Journal of Insect Physiology* **54**, 1041-1049
21. Doucet, D., and Cusson, M. (1996) *Entomologia Experimentalis Et Applicata* **81**, 21-30
22. Doucet, D., and Cusson, M. (1996) Comparative Biochemistry and Physiology a-Physiology **114**, 311-317
23. Webb, B. A., and Summers, M. D. (1990) Proceedings of the National Academy of Sciences of the United States of America **87**, 4961-4965
24. Webb, B. A., and Luckhart, S. (1994) *Archives of Insect Biochemistry and Physiology* **26**, 147-163
25. Rahman, M. M., Roberts, H. L. S., Sarjan, M., Asgari, S., and Schmidt, O. (2004) *Proceedings of the National Academy of Sciences of the United States of America* **101**, 2696-2699

26. Wiese, M. D., Chataway, T. K., Davies, N. W., Milne, R. W., Brown, S. G. A., Gal, W. P., and Heddle, R. J. (2006) *Toxicon* **47**, 208-217
27. Nielsen, H., Engelbrecht, J., Brunak, S., and vonHeijne, G. (1997) *Protein engineering* **10**, 1-6
28. Bendtsen, J. D., Nielsen, H., von Heijne, G., and Brunak, S. (2004) *Journal of Molecular Biology* **340**, 783-795
29. Bendtsen, J. D., Jensen, L. J., Blom, N., von Heijne, G., and Brunak, S. (2004) *Protein Engineering Design and Selection* **17**, 349-356
30. Gasteiger, E., Hoogland, C., Gattiker, A., Duvaud, S. e., Wilkins, M. R., Appel, R. D., and Bairoch, A. (2005) Protein Identification and Analysis Tools on the ExPASy Server. in *The Proteomics Protocols Handbook* (Walker, J. M. ed.), Humana Press. pp 571-607
31. Southey, B. R., Amare, A., Zimmerman, T. A., Rodriguez-Zas, S. L., and Sweedler, J. V. (2006) *Nucleic Acids Research* **34**, W267-W272
32. Schultz, J., Milpetz, F., Bork, P., and Ponting, C. P. (1998) *Proceedings of the National Academy of Sciences* **95**, 5857-5864
33. Letunic, I., Doerks, T., and Bork, P. (2009) *Nucleic Acids Research* **37**, D229-D232
34. Zhang, Y. (2008) *Bmc Bioinformatics* **9**
35. Roy, A., Kucukural, A., and Zhang, Y. *Nature Protocols* **5**, 725-738
36. Shi, J., Blundell, T. L., and Mizuguchi, K. (2001) *Journal of Molecular Biology* **310**, 243-257
37. Kelley, L. A., and Sternberg, M. J. E. (2009) *Nature Protocols* **4**, 363-371
38. Horton, P., Park, K.-J., Obayashi, T., Fujita, N., Harada, H., Adams-Collier, C. J., and Nakai, K. (2007) *Nucleic Acids Research* **35**, W585-W587
39. Ceroni, A., Passerini, A., Vullo, A., and Frasconi, P. (2006) *Nucleic Acids Research* **34**, W177-W181
40. Marsella, L., Sirocco, F., Trovato, A., Seno, F., and Tosatto, S. C. E. (2009) *Bioinformatics* **25**, i289-i295
41. Dettloff, M., Kaiser, B., and Wiesner, A. (2001) *Journal of Insect Physiology* **47**, 789-797
42. Pettersen, E. F., Goddard, T. D., Huang, C. C., Couch, G. S., Greenblatt, D. M., Meng, E. C., and Ferrin, T. E. (2004) *Journal of Computational Chemistry* **25**, 1605-1612
43. Bio, C. CLC genomics workbench [http://www.clcbio.com].
44. Schulz, M., and Zerbino, D. Oases: a transcriptome assembler for very short reads [http://www.ebi.ac.uk/~zerbino/oases].
45. Li, H., and Durbin, R. (2009) *Bioinformatics* **25**, 1754-1760
46. Li, H., Handsaker, B., Wysoker, A., Fennell, T., Ruan, J., Homer, N., Marth, G., Abecasis, G., Durbin, R., and Genome Project Data, P. (2009) *Bioinformatics* **25**, 2078-2079
47. Altschul, S. F., Madden, T. L., Schaffer, A. A., Zhang, J. H., Zhang, Z., Miller, W., and Lipman, D. J. (1997) *Nucleic Acids Research* **25**, 3389-3402
48. Conesa, A., and Gotz, S. (2008) *International Journal of Plant Genomics* **2008**, 619832
49. Hunter, S., Apweiler, R., Attwood, T. K., Bairoch, A., Bateman, A., Binns, D., Bork, P., Das, U., Daugherty, L., Duquenne, L., Finn, R. D., Gough, J., Haft, D., Hulo, N., Kahn, D., Kelly, E., Laugraud, A., Letunic, I., Lonsdale, D., Lopez, R., Madera, M., Maslen, J., McAnulla, C., McDowall, J., Mistry, J., Mitchell, A., Mulder, N., Natale, D., Orengo, C., Quinn, A. F., Selengut, J. D., Sigrist, C. J. A., Thimma, M., Thomas, P. D., Valentin, F., Wilson, D., Wu, C. H., and Yeats, C. (2009) *Nucleic Acids Research* **37**, D211-D215
50. Cooper, T., Bailey-Hill, K., Leifert, W., McMurchie, E., Asgari, S., and Glatz, R. (2011) *The Journal of Biological Chemistry* **286**, 10466-10475
51. Glatz, R., Schmidt, O., and Asgari, S. (2004) *Journal of General Virology* **85**, 2873-2882
52. Uckan, F., Sinan, S., Savasci, S., and Ergin, E. (2004) *Annals of the Entomological Society of America* **97**, 775-780

53. Vincent, B., Kaeslin, M., Roth, T., Heller, M., Poulain, J., Cousserans, F., Schaller, J., Poirie, M., Lanzrein, B., Drezen, J. M., and Moreau, S. J. M. (2010) *Bmc Genomics* **11**
54. Crawford, A. M., Brauning, R., Smolenski, G., Ferguson, C., Barton, D., Wheeler, T. T., and McCulloch, A. (2008) *Insect Molecular Biology* **17**, 313-324
55. Okada, M., Taguchi, K., Maekawa, S., Fukami, K., and Yagisawa, H. (2010) *Neuroscience Letters* **472**, 188-193
56. Shinzawa, K., and Tsujimoto, Y. (2003) *Journal of Cell Biology* **163**, 1219-1230
57. Rivers, D. B., Dani, M. P., and Richards, E. H. (2009) *Archives of Insect Biochemistry and Physiology* **71**, 173-190
58. Rivers, D. B., Crawley, T., and Bauser, H. (2005) *Journal of Insect Physiology* **51**, 149-160
59. Leluk, J., Schmidt, J., and Jones, D. (1989) *Toxicon* **27**, 105-114
60. Rholam, M., and Fahy, C. (2009) *Cellular and Molecular Life Sciences* **66**, 2075-2091
61. Buscaglia, C. A., Alfonso, J., Campetella, O., and Frasch, A. C. C. (1999) *Blood* **93**, 2025-2032
62. Jones, D., Sawicki, G., and Wozniak, M. (1992) *Journal of Biological Chemistry* **267**, 14871-14878
63. Kobe, B., and Kajava, A. V. (2000) *Trends in Biochemical Sciences* **25**, 509-515
64. Wang, L., Zhou, M., Lynch, L., Chen, T. B., Walker, B., and Shaw, C. (2009) *Biochimie* **91**, 613-619
65. Bernard, C., Corzo, G., Adachi-Akahane, S., Foures, G., Kanemaru, K., Furukawa, Y., Nakajima, T., and Darbon, H. (2004) *Proteins-Structure Function and Genetics* **54**, 195-205
66. Corzo, G., Adachi-Akahane, S., Nagao, T., Kusui, Y., and Nakajima, T. (2001) *FEBS letters* **499**, 256-261
67. Kaplan, N., Morpurgo, N., and Linial, M. (2007) *Journal of Molecular Biology* **369**, 553-566
68. Shi, L., Li, B., and Paskewitz, S. M. (2006) *Insect Molecular Biology* **15**, 313-320
69. Daquinag, A. C., Sato, T., Koda, H., Takao, T., Fukuda, M., Shimonishi, Y., and Tsukamoto, T. (1999) *Biochemistry (John Wiley & Sons)* **38**, 2179-2188
70. Tedford, H. W., Gilles, N., Menez, A., Doering, C. J., Zamponi, G. W., and King, G. F. (2004) *Journal of Biological Chemistry* **279**, 44133-44140
71. Tedford, H. W., Fletcher, J. I., and King, G. F. (2001) *Journal of Biological Chemistry* **276**, 26568-26576
72. Asgari, S., Zareie, R., Zhang, G. M., and Schmidt, O. (2003) *Arch.Insect Biochem.Physiol.* **53**, 92-100
73. Andersen, A. S., Hansen, P. H., Schaffer, L., and Kristensen, C. (2000) *Journal of Biological Chemistry* **275**, 16948-16953
74. Szeto, T. H., Wang, X. H., Smith, R., Connor, M., Christie, M. J., Nicholson, G. M., and King, G. F. (2000) *Toxicon* **38**, 429-442
75. Zhu, J. Y., Ye, G. Y., and Hu, C. (2008) *Toxicon* **51**, 1391-1399
76. Tang, B. L. (2001) International Journal of Biochemistry & Cell Biology **33**, 33-44
77. Ote, M., Mita, K., Kawasaki, H., Kobayashi, M., and Shimada, T. (2005) *Archives of Insect Biochemistry and Physiology* **59**, 91-98
78. Masuda, S., Ohta, T., Kaji, K., Fox, J. W., Hayashi, H., and Araki, S. (2000) *Biochemical and biophysical research communications* **278**, 197-204
79. Masuda, S., Maeda, H., Miao, J. Y., Hayashi, H., and Araki, S. (2007) *Endothelium-Journal of Endothelial Cell Research* **14**, 89-96
80. Stirnimann, C. U., Petsalaki, E., Russell, R. B., and Muller, C. W. (2010) *Trends in Biochemical Sciences* **35**, 565-574

81. Ron, D., Chen, C. H., Caldwell, J., Jamieson, L., Orr, E., and Mochlyrosen, D. (1994) *Proceedings of the National Academy of Sciences of the United States of America* **91**, 839-843
82. Cox, E. A., Bennin, D., Doan, A. T., O'Toole, T., and Huttenlocher, A. (2003) *Molecular biology of the cell* **14**, 658-669
83. Kiely, P. A., O'Gorman, D., Luong, K., Ron, D., and O'Connor, R. (2006) *Molecular and Cellular Biology* **26**, 4041-4051
84. Dell, E. J., Connor, J., Chen, S. H., Stebbins, E. G., Skiba, N. P., Mochly-Rosen, D., and Hamm, H. E. (2002) *Journal of Biological Chemistry* **277**, 49888-49895
85. Gomez-Arreaza, A., Acosta, H., Barros-Alvarez, X., Concepcion, J. L., Albericio, F., and Avilan, L. (2011) *Experimental Parasitology* **127**, 752-761
86. Cuervo, P., De Jesus, J. B., Saboia-Vahia, L., Mendonca-Lima, L., Domont, G. B., and Cupolillo, E. (2009) *Journal of Proteomics* **73**, 79-92
87. Udekwu, K., Parrish, N., Ankomah, P., Baquero, F., and Levin, B. (2009) *Journal of Antimicrobial Chemotherapy* **63**, 745-757
88. Dowson, C., Johnson, A., Cercenado, E., and George, R. (1994) *Antimicrobial Agents and Chemotherapy* **38**, 49-53
89. Lv, P., Xiong, J., Chen, J., Wang, K., Mao, W., and Zhu, H. (2010) *Journal of Enzyme Inhibition and Medicinal Chemistry* **25**, 590-595
90. Rahbar, M., Mehrgan, H., and Hadji-nejad, S. (2010) *Basic and Clinical Pharmacology and Toxicology* **107**, 676-679
91. Giacometti, A., Cirioni, O., Kamysz, W., D'Amato, G., Silvestri, C., Prete, M., Licci, A., Lukasiak, J., and Scalise, G. (2005) *Journal of Antimicrobial Chemotherapy* **55**, 272-274
92. Lawrence, L., Danese, P., DeVito, J., Franceschi, F., and Sutcliffe, J. (2008) *Antimicrobial Agents and Chemotherapy* **52**, 1653-1662
93. Fass, R., and Barnishan, J. (1979) *Antimicrobial Agents and Chemotherapy* **16**, 622-624
94. Rasheed, J., Anderson, G., Yigit, H., Queenan, A., Domenech-Sanchez, A., Swenson, J., Biddle, J., Ferraro, M., Jacoby, G., and Tenover, F. (2000) *Antimicrobial Agents and Chemotherapy* **44**, 2382-2388
95. Punpanich, W., Tantichattanon, W., Wongwatcharapaiboon, S., and Treeratweeraphong, V. (2008) *Journal of the Medical Asscoaition of Thailand* **91, Supplement 3**, S21-S27
96. Bisignano, G., Tomaino, A., Cascio, R., Crisafi, G., Uccella, N., and Saija, A. (1999) *Journal of Pharmacy and Pharmacology* **51**, 971-974
97. Haag, R. (1986) *Infection* **14**, 38-43
98. David, J. P., Coissac, E., Melodelima, C., Poupardin, R., Riaz, M. A., Chandor-Proust, A., and Reynaud, S. (2010) *BMC Genomics* **11**
99. Mu, Y. N., Ding, F., Cui, P., Ao, J. Q., Hu, S. N., and Chen, X. H. (2010) *Bmc Genomics* **11**, 506
100. Xiang, L., He, D., Dong, W., Zhang, Y., and Shao, J. (2010) *BMC Genomics* **11**
101. Bae, S., and Kim, Y. (2004) Comparative Biochemistry and Physiology a-Molecular & Integrative Physiology **138**, 39-44
102. Shelby, K. S., Cui, L., and Webb, B. A. (1998) *Insect Molecular Biology* **7**, 265-272
103. Barandoc, K. P., and Kim, Y. (2010) Comparative Biochemistry and Physiology B-Biochemistry & Molecular Biology **156**, 129-136
104. Nicolas, E., Nappi, A. J., and Lemaitre, B. *Developmental & Comparative Immunology* **20**, 175-181
105. Eum, J. H., Seo, Y. R., Yoe, S. M., Kang, S. W., and Han, S. S. (2007) *Developmental and Comparative Immunology* **31**, 1107-1120
106. Barandoc, K. P., Kim, J., and Kim, Y. (2010) *Journal of Microbiology* **48**, 117-123

107. Abdel-Latief, M., and Hilker, M. (2008) *Insect Biochemistry and Molecular Biology* **38**, 136-145
108. Kim, J., and Kim, Y. (2010) *Journal of Asia-Pacific Entomology* **13**, 313-318
109. Song, K. H., Jung, M. K., Eum, J. H., Hwang, I. C., and Han, S. S. (2008) *Journal of Insect Physiology* **54**, 1271-1280
110. Beck, M., Theopold, U., and Schmidt, O. (2000) *Journal of Insect Physiology* **46**, 1275-1283
111. Rai, S., Aggarwal, K. K., Mitra, B., Das, T. K., and Babu, C. R. (2010) *Peptides* **31**, 474-481
112. Aguilar, R., Jedlicka, A. E., Mintz, M., Mahairaki, V., Scott, A. L., and Dimopoulos, G. (2005) *Insect Biochemistry and Molecular Biology* **35**, 709-719
113. Schlenke, T. A., Morales, J., Govind, S., and Clark, A. G. (2007) *Plos Pathogens* **3**, 1486-1501
114. Barat-Houari, M., Hilliou, F., Jousset, F. X., Sofer, L., Deleury, E., Rocher, J., Ravallec, M., Galibert, L., Delobel, P., Feyereisen, R., Fournier, P., and Volkoff, A. N. (2006) *BMC Genomics* **7**, 1-20
115. Provost, B., Jouan, V., Hilliou, F., Delobel, P., Bernardo, P., Ravallec, M., Cousserans, F., Wajnberg, E., Darboux, I., Fournier, P., Strand, M. R., and Volkoff, A.-N. (2011) *Insect Biochemistry and Molecular Biology* **41**, 582-591
116. Wertheim, B., Kraaijeveld, A. R., Schuster, E., Blanc, E., Hopkins, M., Pletcher, S. D., Strand, M. R., Partridge, L., and Godfray, H. C. J. (2005) *Genome Biology* **6**, R94
117. Govind, S. (2008) *Insect Science* **15**, 29-43
118. Antonova, Y., Alvarez, K. S., Kim, Y. J., Kokoza, V., and Raikhel, A. S. (2009) *Insect Biochemistry and Molecular Biology* **39**, 303-314
119. Shrestha, S., Kim, H. H., and Kim, Y. (2009) *Journal of Asia-Pacific Entomology* **12**, 277-283
120. Thoetkiattikul, H., Beck, M. H., and Strand, M. R. (2005) *Proceedings of the National Academy of Sciences of the United States of America* **102**, 11426-11431
121. Tian, S. P., Zhang, J. H., and Wang, C. Z. (2007) *Journal of Insect Physiology* **53**, 699-707
122. Fath-Goodin, A., Kroemer, J. A., and Webb, B. A. (2009) *Insect Molecular Biology* **18**, 497-506
123. Takeda, T., Nakamatsu, Y., and Tanaka, T. (2006) *Pesticide Biochemistry and Physiology* **86**, 15-22
124. Asgari, S. (2007) Endoparasitoid venom proteins as modulators of host immunity and development. in *Recent advances in the biochemistry, toxicity and mode of action of parasitic wasp venom* (Rivers, D., and Yoder, J. eds.), Research Signpost, Kerala. pp 57-73
125. Pennacchio, F., and Strand, M. R. (2006) *Annual Review of Entomology* **51**, 233-258
126. Li, X., Cui, L., Bai, S., and Yuan, G. (2005) *Journal of Henan Agricultural University* **39**, 308-311
127. Dover, B. A., Davies, D. H., Strand, M. R., Gray, R. S., Keeley, L. L., and Vinson, S. B. (1987) *Journal of Insect Physiology* **33**, 333-338
128. Kwon, B., Song, S., Choi, J. Y., Je, Y. H., and Kim, Y. (2010) *Journal of Insect Physiology* **56**, 650-658
129. Soller, M., and Lanzrein, B. (1996) *Journal of Insect Physiology* **42**, 471-481
130. Webb, B. A., and Dahlman, D. L. (1985) *Archives of Insect Biochemistry and Physiology* **2**, 131-143
131. Lee, S., and Kim, Y. (2004) *Journal of Asia-Pacific Entomology* **7**, 283-287
132. Li, S., Falabella, P., Kuriachan, I., Vinson, S. B., Borst, D. W., Malva, C., and Pennacchio, F. (2003) *Journal of Insect Physiology* **49**, 1021-1030
133. Pfister-Wilhelm, R., and Lanzrein, B. (2009) *Journal of Insect Physiology* **55**, 707-715

134. Schafellner, C., Marktl, R. C., and Schopf, A. (2007) *Journal of Insect Physiology* **53**, 858-868
135. Zhu, J. Y., Ye, G. Y., Dong, S. Z., Fang, Q., and Hu, C. (2009) *Archives of Insect Biochemistry and Physiology* **71**, 45-53
136. Meszaros, M., and Morton, D. B. (1994) *Developmental Biology* **162**, 618-630
137. Dahlman, D. L., Coar, D. L., Koller, C. N., and Neary, T. J. (1990) *Archives of Insect Biochemistry and Physiology* **13**, 29-39
138. Gelman, D. B., Reed, D. A., and Beckage, N. E. (1998) *Journal of Insect Physiology* **44**, 833-843
139. Pruijssers, A. J., Falabella, P., Eum, J. H., Pennacchio, F., Brown, M. R., and Strand, M. R. (2009) *Journal of Experimental Biology* **212**, 2998-3006
140. Strand, M. R., Dover, B. A., and Johnson, J. A. (1990) *Archives of Insect Biochemistry and Physiology* **13**, 41-51
141. Touhara, K., and Prestwich, G. D. (1993) *Journal of Biological Chemistry* **268**, 19604-19609
142. Dover, B. A., Menon, A., Brown, R. C., and Strand, M. R. (1995) *Journal of Insect Physiology* **41**, 809-817
143. Nalini, M., and Kim, Y. (2007) *Journal of Insect Physiology* **53**, 1283-1292
144. Shelby, K. S., and Webb, B. A. (1994) *Journal of General Virology* **75**, 2285-2292
145. Shelby, K. S., and Webb, B. A. (1997) *Insect Biochemistry and Molecular Biology* **27**, 263-270
146. Tanaka, K., Lapointe, R., Barney, W. E., Makkay, A. M., Stoltz, D., Cusson, M., and Webb, B. A. (2007) *Virology* **363**, 26-35
147. Strand, M. R. (2010) Polydnaviruses. in *Insect Virology* (Asgari, S., and Janson, K. eds.), Caister Academic Press, Norfolk. pp 171-197
148. Lapointe, R., Tanaka, K., Barney, W. E., Whitfield, J. B., Banks, J. C., Beliveau, C., Stoltz, D., Webb, B. A., and Cusson, M. (2007) *Journal of Virology* **81**, 6491-6501
149. Webb, B. A., Strand, M. R., Dickey, S. E., Beck, M. H., Hilgarth, R. S., Barney, W. E., Kadash, K., Kroemer, J. A., Lindstrom, K. G., Rattanadechakul, W., Shelby, K. S., Thoetkiattikul, H., Turnbull, M. W., and Witherell, R. A. (2006) *Virology* **347**, 160-174
150. Strand, M. R., and Pech, L. L. (1995) *Journal of General Virology* **76**, 283-291
151. Lentschat, A., Karahashi, H., Michelsen, K. S., Thomas, L. S., Vogel, S. N., and Arditi, M. (2005) *The Journal of Immunology* **174**, 4252-4261

APPENDIX A

Final draft of manuscript of data relating to CrV2 protein, *viz*: Cooper, T., Bailey-Hill, K., Leifert, W.R., McMurchie, E.J., Asgari, S. and Glatz, R.V. (2011). Identification of an *in vitro* interaction between an insect immune-suppressor protein (CrV2) and Gα proteins. *The Journal of Biological Chemistry*, 286, 10466-10475.

Identification of an *in vitro* interaction between an insect immune-suppressor protein (CrV2) and Gα proteins

Tamara H. Cooper[1,2], Kelly Bailey-Hill[1,2], Wayne R. Leifert[2,3], Edward J. McMurchie[2], Sassan Asgari[4] and Richard V. Glatz[1,2¶]

From South Australian Research and Development Institute (SARDI), Entomology, Waite Road, Urrbrae, South Australia, 5064, Australia[1], Division of Molecular and Health Technologies, Commonwealth Scientific and Industrial Research Organisation (CSIRO), Kintore Avenue, Adelaide, South Australia, 5000, Australia[2], Division of Human Nutrition, Commonwealth Scientific and Industrial Research Organisation (CSIRO), Kintore Avenue, Adelaide, South Australia, 5000, Australia[3] and School of Biological Sciences, The University of Queensland, St Lucia, Queensland, 4072[4],

Running head: *In vitro* interaction of CrV2 with Gα

Address correspondence to: Richard Glatz. GPO Box 397, Adelaide, South Australia, 5001. Telephone: +618 8303 9539, Fax: +618 8303 9542, Email: richard.glatz@sa.gov.au

The protein CrV2 is encoded by a polydnavirus integrated into the genome of the endoparasitoid *Cotesia rubecula* (Hymenoptera: Braconidae: Microgastrinae) and is expressed in host larvae with other gene products of the PDV to allow successful development of the parasitoid. CrV2 expression has previously been associated with immune suppression although the molecular basis for this was not known. Here we have used Time-resolved Förster Resonance Energy Transfer (TR-FRET) to demonstrate high-affinity binding of CrV2 to Gα-subunits (but not the Gβγ dimer) of heterotrimeric G-proteins. Signals up to 5-fold above background were generated and an apparent dissociation constant of 6.2 nM calculated. Protease treatment abolished the TR-FRET signal and the presence of unlabelled CrV2 or Gα proteins also reduced the TR-FRET signal. The activation state of the Gα subunit was altered with aluminium fluoride and this decreased the affinity of the interaction with CrV2. It was also demonstrated that CrV2 preferentially bound to *Drosophila* $G\alpha_o$ compared to rat $G\alpha_{i1}$. In addition, three CrV2 homologs were detected in sequences derived from polydnaviruses from *Cotesia plutellae* and *C. congregata* (including the immune-related early-expressed transcript, EP2). These data suggest a potential mode-of-action of immune suppressors not previously reported, which in addition to furthering our understanding of insect immunity, may have practical benefits such as facilitating development of novel controls for pest insect species.

Polydnaviruses (PDVs) are endogenous particles that are produced by some parasitoid wasps and injected, along with the wasp egg(s), into the hemocoel of host insects causing a range of developmental and immune effects that allow the parasitoid to successfully develop (1-4). Members of the Polydnaviridae are divided into two paraphyletic groups; bracoviruses (BVs; genus *Bracovirus*) and ichnoviruses (genus *Ichnovirus*) which occur in some members of the wasp families, Braconidae and

Ichneumonidae, respectively (5). Recent evidence suggests that these genera should perhaps be placed into separate virus families, as there is good evidence that *Bracovirus* and *Ichnovirus* derived from different ancestral viruses (6,7). PDVs are replicated only in the ovaries of female wasps and are not known to affect the wasp (8). PDVs are highly unusual in that individual particles only contain a sub-set of the expressed genes and do not contain any genes for virus structure/replication. Therefore, the virus is only able to be transmitted vertically (between wasp generations) through the integration of the PDV genome into wasp chromosomes (8-10). Indeed, it was the analysis of non-packaged PDV genes (such as capsid proteins) that allowed the different ancestral viruses to be differentiated. Prior to this, a range of encapsidated PDV genes and/or gene families, were postulated as being immune-suppressive, targeting cellular and humoral (cell-free) aspects of the innate insect immune system (4). Proteins encoded by these genes include protein tyrosine phosphatases (11), viral ankyrins (vankyrins) (12,13), host translation inhibitory factors (14,15), EGF-like proteins (16), CrV1 homologs (17-19), EP1-like proteins (20), the H4 histone (21) and C-type lectins (22-25). Other PDV proteins are also thought to target insect immunity but as yet, their class and potential mode-of-action are yet to be elucidated. CrV2, expressed by the *Cotesia rubecula* bracovirus (*Cr*BV) is an example of such a protein. CrV2 is expressed by *Cr*BV only in the larvae of two closely related butterflies (*Pieris* spp.) and is secreted into the hemolymph. It was thought to be temporally associated with short term, subtle immune dysfunction in hemocyte cells that take up the secreted protein, although the molecular basis for its effects is not yet understood (26). The protein does not cause toxic effects on the cells which recover their immune function once significant expression of CrV2 and (and other early-expressed proteins) is reduced. Here we present data that infer a specific, high-affinity interaction between CrV2 and invertebrate/mammalian Gα-subunits of heterotrimeric G-proteins, which are important cell-signalling proteins, indirectly implicated in vertebrate and invertebrate immune function (see Discussion and (27-32)).

Heterotrimeric G-proteins consist of 3 subunits, the Gα subunit and a dimer of Gβ and Gγ (Gβγ). There are a variety of subtypes for each G-protein class. The Gα-subunit binds guanine nucleotides and exchanges GDP for GTP upon activation of the G-protein coupled receptor (GPCR) with which the G-protein is usually associated. Nucleotide exchange causes conformation changes such that the Gα subunit and the Gβγ dimer interact with downstream effectors including various enzymes and ion channels that alter cellular metabolism (33). We previously developed a TR-FRET (Time-resolved Förster Resonance Energy Transfer) assay utilising a terbium-chelate donor and Alexa546 acceptor, to demonstrate interactions of the Gα subunit with the Gβγ dimer and the regulator of G-protein signalling 4 (RGS4) (34). The assay was recently adapted by others to monitor the effect of allosteric modulators of RGS4 in altering RGS4:Gα affinity, and further developed into a high-throughput screen for other such modulators (35). Generally, TR-FRET uses a lanthanide donor fluorophore (such as terbium or europium) in combination with an appropriate acceptor (with an excitation spectrum overlapping the donor emission spectrum). When the fluorophores are in close proximity (<100 angstroms), energy transfer occurs between them and acceptor emission is measured to determine binding kinetics (36). Using a lanthanide donor increases the signal:noise ratio when the long-lived luminescence (characteristic of lanthanides) is exploited with time-gated measurements that eliminate short-lived background signals. Lanthanides also exhibit other favourable properties including multiple emission peaks, a large Stokes shift and non-polarised emission (37,38).

As part of validating the original TR-FRET assay, we determined that the CrV2 protein appeared to specifically interact with mammalian Gα subunits. Here, we adapt our TR-FRET assay to demonstrate a high affinity (nanomolar) interaction of acceptor-labelled CrV2 with mammalian and insect donor-labelled Gα. We also demonstrate that recombinant CrV2 is taken up by a specific hemocyte morphotype from larval *Pieris rapae*, which are key immune cells, where it could potentially interact with cellular proteins such as Gα. These results are intriguing as they suggest that insect hemocyte immune function could be regulated through G-protein signalling pathways and that some PDVs subvert host immunity by producing proteins that interact with Gα to alter immune signalling. This mode-of-action for immune suppression has not previously been reported and its elucidation has the potential to facilitate the development of novel insect controls.

Experimental Procedures

All chemicals and reagents were of analytical grade and purchased from Sigma Aldrich unless otherwise stated. All buffers were made in milli-Q water.

Production and purification of recombinant CrV2 and G-protein subunits. To produce CrV2 used in cell and Far-western blot experiments, PCR was used to generate full CrV2 constructs containing the N-terminal signal peptide with a His-tag incorporated at the 3' end, and *Not*I and *Kpn*I restriction enzyme sites at the 5' and 3' ends, respectively. The forward primer sequence was 5'gcg gcc gca tgt tgt cta caa agc3' and the reverse primer sequence was 5'ggt acc tta gtg atg gtg atg gtg atg ggg atg atc tcg agc cct3'. PCR products were produced with proof-reading polymerase and cloned into pCR®-Blunt (Invitrogen) to allow subsequent restriction of the cloned products for insertion into pFastBac1 (Invitrogen). Recombinant baculovirus was then generated using the Bac-to-Bac system (Invitrogen) as per the manufacturer's instructions. *Sf*9 cells at 2 x10^6 cells/ml were infected with amplified virus at an MOI ~2 for 48-72 hours in suspension at 27˚C with shaking. Cells were harvested by centrifugation and expression confirmed by Western blot. The media containing secreted CrV2 was stored at -20˚C, or -80˚C for longer term storage.

To produce purified recombinant CrV2 for TR-FRET experiments, the coding sequence without the first 21 N-terminal amino acids which contain the secretory signal peptide, was cloned into pQE30 (Qiagen) and transformed into M15[pREP4] *Escherichia coli* as per Glatz *et al*. (2004) (26). Expression of recombinant CrV2 was induced in 400 ml bacterial cultures in YT Broth (8 g/L tryptone, 5 g/L yeast extract, 2.5 g/L NaCl, pH 7.0) as per manufacturers instructions. Induced bacterial cells were pelleted by centrifugation and stored at -80°C. Cells were later resuspended in 10 ml of TBP buffer (50 mM Tris pH 8, 10 mM β-mercaptoethanol, 0.02 mg/ml phenylmethanesulphonylfluoride, 0.03 mg/ml benzamidine). Lysozyme was added to a final concentration of 0.2 mg/ml and gently mixed at 4°C for 30 min. $MgCl_2$ was then added to a final concentration of 5 mM followed by DNaseI to a concentration of 0.01 mg/ml. Mixing was continued for a further 30 min. Twenty percent (w/v) cholate solution (50 mM NaHEPES pH 8.0, 3 mM $MgCl_2$, 50 mM NaCl and 200 g/L cholic acid (Na^+)) was added to give a final cholate concentration of 1% (v/v). The preparation was then gently stirred (1 h at 4°C) before ultra-centrifugation in a Beckman Coulter Optima™ LE-80K at 100 000 x g for 40 min. Ni-NTA agarose beads (800 µl; Qiagen) in TBP (50%) were added to the supernatant and incubated on ice for 30 min with occasional stirring. Supernatants were then applied to gravity-fed columns. Columns were then washed with 20 ml of TBP containing 100 mM NaCl followed by washing with 5 ml TBP containing 100 mM NaCl and 10 mM imidazole. All washing procedures were carried out at 4°C. His-tagged CrV2 was eluted from the column in 400 µl fractions using TBP containing 100 mM NaCl and 250 mM imidazole. Elution fractions were run on a polyacrylamide gel

and stained using Coomassie blue. Elutions containing CrV2 were identified and fractions pooled. Protein concentration was determined according to Bradford (39) or laser densitometry, before aliquoting and storage at -80 °C.

G-protein subunits were produced from 1-2 litres of *Sf*9 cells infected with the desired recombinant baculovirus. Recombinant full-length *Drosophila* $G\alpha_o$ (isoform I)-expressing baculovirus was produced using the Bac-to-Bac expression system as described by the manufacturer (Invitrogen). Cell culture, virus amplifications and infections, as well as the purification of G-protein subunits using Ni-NTA agarose beads and fluorescent labelling of G-proteins or CrV2 with cysteine reactive Alexa Fluor 546 C_5-maleimide (Invitrogen) or CS124-DTPA-EMCH:Tb (Invitrogen), was performed as described by Leifert *et al*. (2006) (34).

Antibody labelling of CrV2 in hemocytes in vitro. Larval *Pieris rapae* were surface sterilized in ice-cold 70% ethanol for a few minutes and then kept on ice until they were bled from a severed proleg directly into an ice-chilled 1.5 ml microcentrifuge tube containing ~200 µL of Sf900II medium (Invitrogen) saturated with phenylthiourea (PTU, which inhibits melanisation reactions). Hemocytes were aliquoted into wells of a printed glass slide and incubated at room temperature until cells attached and spreading was observed. Obviously spread cells were considered to be a plasmatocyte morphotype and attached cells that retained a rounded, apparently unspread, conformation were considered as a granulocyte morphotype. Insect cell-culture medium containing secreted, baculovirus-expressed CrV2 was applied to the hemocyte-containing slides and incubated for the desired time. Medium was then removed and cells fixed in 4% paraformaldehyde for 15 min, permeabilized with 0.1% TritonX-100 for 4 min and washed in TBST (8.8 g/L NaCl, 0.2 g/L KCl, 3 g/L Trizma, 500 µL/L Tween-20 detergent). Anti-CrV2 polyclonal rabbit antibodies (see (26)) in TBST (1:500) were added to the glass slide and incubated for 1.5-2 h at room temperature. Cells were washed with TBST and flurophore-conjugated anti-rabbit antibody (1:200-250) with 1:50 dilution of FITC-Phalloidin (0.1 mg/ml) in TBST, were applied to slides for 1 h at RT in darkness. Cells were then washed with TBST and stained with 1:10 000 dilution (1 µg/ml) of DAPI for 5 min. Cells were then washed with TBST and PBS, a coverslip was applied, and the coverslip sealed with nail varnish.

TR-FRET assays. The interaction between Alexa546 (Alexa)- and CS124-DTPA-EMCH:Tb (Tb)-labelled proteins was measured using TR-FRET as described in Leifert *et al*. 2006 (34). Briefly, these experiments were conducted in black 96-well plates. 20x working solutions of proteins were made in TMN buffer (50 mM Tris pH 7.6, 100 mM NaCl, 10 mM $MgCl_2$). Five microlitres of each was then applied to opposite sides of the well such that mixing did not occur. Other indicated components such as Proteinase K could also be added in this manner where required. TMN buffer was then added to give a final assay volume of 100 µl and the reaction initiated by mixing of all components. TR-FRET was then measured using a Victor3 multilabel plate reader (Perkin Elmer) using an excitation wavelength of 340 nm and a delay of 50 µs, before measuring the emission at 572 nm for 900 µs. Measurements could be ceased so that unlabelled proteins or buffer could be added and then measurements resumed.

[35S]GTPγS binding assay. 40 nM of purified Gα-subunit or CrV2 was mixed with 1 nM [^{35}S]GTPγS in a final volume of 100 µL of TMN buffer and incubated in a shaking water bath for 90 min at 27°C. Twenty five microlitres in triplicate, were then filtered through glass microfiber 1 µm filter papers (GFCs; Filtech) and unbound [^{35}S]GTPγS removed by washing with 3 x 4 ml of TMN buffer. The filters were then dried and the amount of bound [^{35}S]GTPγS was measured by scintillation counting for 60 s in pico pro vials with 4 ml of Ultima Gold™

scintillation cocktail (Perkin Elmer) using a Wallac 1410 liquid scintillation counter.

Far-western assay. Purified *Drosophila* $G\alpha_o$ and bovine serum albumin were subjected to SDS-PAGE on an "any kD" TGX gel (Bio-Rad) using a non-reducing sample buffer. Proteins were transferred onto a Hybond-C nitrocellulose membrane (GE healthcare life sciences) at 100 V for 1 hr. Membranes were blocked with 5% skim milk powder in TBS buffer (8.8 g/L NaCl, 0.2g/L KCl, 3 g/L Trizma) for > 2 hr. Membranes were then probed with CrV2 in Sf900II medium or conditioned medium overnight. Membranes were then washed with TBST buffer (see above) and probed with rabbit anti-CrV2 (1:10 000) in blocking solution for 2 hr. Following washing with TBST, membranes were probed with alkaline phosphatase-conjugated goat anti-rabbit IgG (1:20 000) in blocking solution for 2 hr. Membranes were washed with TBST and developed using 5-bromo-4-chloro-3'-indoyphosphate p-toluidine salt, and nitro-blue tetrazolium chloride, to detect any CrV2 bound to $G\alpha_o$.

TR-FRET data analyses. Data were analysed using Prism™ 4.00 (GraphPad software Inc., San Diego CA, USA). Data are presented as mean ± SEM where n is equal or greater than 3. Where n=2, data is presented as the mean and error bars represent the range of the duplicates. If error bars are not visible they are small and therefore hidden by the symbols.

Amino acid sequence analyses. The CrV2 amino acid sequence was subjected to protein Blast, (http://blast.ncbi.nlm.nih.gov/Blast.cgi?CMD=Web&PAGE_TYPE=BlastHome) in order to detect any similar protein sequences. Three similar sequences were detected. ClustalW2 software (http://www.ebi.ac.uk/Tools/clustalw2/index.html) was then used to align the amino acid sequences of the four similar proteins, and to produce a simple phylogenetic tree of the four protein sequences. Protein BLAST was also used to determine the amino acid identity between the two experimental Gα subunits used here, i.e. rat $G\alpha_{i1}$ (GenBank accession no. NP_037277) and *Drosophila melanogaster* $G\alpha_o$ isoform I (GenBank accession no. AAS64873).

Results

Identification of CrV2 homologs. CrV2 amino acid sequence was subjected to protein Blast, resulting in detection of three similar amino acid sequences, which are putative homologs (Fig. 1). One sequence (EPL-7) is a hypothetical protein determined from the genome sequence of *Cotesia plutellae* bracovirus (*Cp*BV). The other two proteins are derived from the *Cotesia congregata* bracovirus (*Cc*BV); One of these encodes the early expressed, immune suppression-related transcript, EP2 (40), and the second is a hypothetical protein CcBV_31.9 derived from the total *Cc*BV genome sequence. ClustalW2 software was used to align the amino acid sequences of the four proteins.

Uptake of CrV2 by hemocytes. Application of hemocytes to the wells of a glass slide results in adherent cells attaching to the slide surface. A sub-population of cells are then observed to spread while other cells remain more rounded. These cells are considered as plasmatocytes and granulocytes, respectively. CrV2 was only detected in association with the unspread, rounded cells following incubation of all hemocytes with CrV2 (Fig. 2). These results suggest that CrV2 is likely to modulate some function of granulocytes while not directly affecting plasmatocytes. However, apart from the uptake of CrV2, the effect on granulocytes produced no other phenotype observable under our conditions.

Interaction of CrV2 with $G\alpha_{i1}$ measured by TR-FRET. Recombinant bacterially-expressed CrV2 was successfully purified using Ni-NTA chromatography and the protein labelled with the fluor Alexa546. G-protein subunits were expressed in *Sf*9 cells and also purified using Ni-NTA chromatography. These terbium-labelled (or unlabelled) G-proteins were functional in receiving signals from appropriate GPCRs in a reconstituted system as shown by Leifert *et al.* (2006) (34). Purified CrV2 labelled with

Alexa546 (CrV2:Alexa) as the acceptor for TR-FRET, was mixed with purified $G\alpha_{i1}$ labelled with CS124-DTPA-EMCH:Tb ($G\alpha_{i1}$:Tb) as the fluorescent donor exhibiting long-lived luminescence. Upon mixing of the two labelled proteins and excitation of terbium at 340 nm, an increase in gated emission of Alexa546 (acceptor) fluorescence at 572 nm, occurred with time. Signals up to 5-fold greater than the background could be achieved and the signal increased upon addition of increasing amounts of CrV2:Alexa (Fig. 3A). Background fluorescence was generated by a low amount of $G\alpha_{i1}$:Tb emission in the 572 nm channel, while background contributions from Alexa546 and other buffer components were negligible since typical auto-fluorescence had decayed during the 50 μs delay (after excitation) before the emission signal was measured. When increasing concentrations of CrV2:Alexa were added to 10 nM $G\alpha_{i1}$:Tb, saturation was achieved at approx. 25 nM CrV2:Alexa and an apparent dissociation constant (*K*d) of 6.2 nM was produced (Fig. 3B). This indicated that a high affinity interaction was occurring between CrV2:Alexa and $G\alpha_{i1}$:Tb, which was comparable to the affinity between the Gα subunit and the Gβγ dimer (2 nM) measured using the same technique (34). To show the TR-FRET signal was attributable to a specific protein-protein interaction, Proteinase K, a broad spectrum serine protease that cleaves peptide bonds at the carboxylic sides of aliphatic, aromatic or hydrophobic amino acids, was used to digest the proteins. This reduced the TR-FRET signal (Fig. 3C) and suggested that generation of the TR-FRET signal was due to a specific interaction between complete CrV2 and $G\alpha_{i1}$ proteins, which were destroyed by protease digestion.

The addition of an excess of unlabelled binding partners including $G\alpha_{i1}$ or CrV2 (Fig. 4A and 4B, respectively) rapidly decreased the TR-FRET signal while with the addition of buffer, the signal remained steady. This further showed that a specific interaction between the proteins was occurring (i.e. reduced TR-FRET was not the result of increased assay volume) resulting in a significant TR-FRET signal since unlabelled CrV2 or Gα appeared to compete for binding to labelled binding partners. $G\beta_4\gamma_2$ could also inhibit the association of Gα:Tb with CrV2:Alexa (Fig. 4C) and this was particularly interesting since assuming that CrV2 does not bind to Gβγ, this could suggest that Gβγ and CrV2 have overlapping binding sites on the $G\alpha_{i1}$ subunit and/or disrupts the binding of the other. To gain an insight as to whether CrV2 could also be associating with the Gβγ dimer, CrV2:Alexa was mixed with $G\beta_4\gamma_2$ labelled with terbium (Gβγ:Tb). However, this failed to produce a substantial TR-FRET signal compared to that generated by CrV2 and $G\alpha_{i1}$, or $G\alpha_{i1}$ and Gβγ (Fig. 5). Although the labelling efficiency of the Gβγ subunits with terbium may differ from Gα, the similar level of background terbium luminescence suggested that the amount of terbium present was not significantly less and did not result in the lack of TR-FRET signal. This was further established by the strong TR-FRET signal generated from the interaction of Gβγ:Tb with $G\alpha_{i1}$:Alexa. The activation state of the Gα subunit could also modulate the interaction with CrV2. The addition of excess GDP (or GTPγS; not shown) produced similar association curves over time while the addition of aluminium fluoride (AlF_3) by adding 10 mM NaF and 30 μM $AlCl_3$, appeared to decrease the maximum fluorescence achieved (Fig. 6).

Because insect Gα subunits would likely be the target for CrV2 *in vivo*, and show relatively little variation between different organisms and Gα subclasses, we used the TR-FRET assay to compare the CrV2:Gα interaction using *Drosophila* $G\alpha_o$. Protein Blast showed that there is 69% amino acid identity between the two experimental Gα proteins, rat $G\alpha_{i1}$ and *Drosophila* $G\alpha_o$ isoform I. Recombinant baculovirus-expressed *Drosophila* $G\alpha_o$ was purified (Fig. 7A) and shown to be similarly functional in binding [^{35}S]GTPγS as rat $G\alpha_{i1}$, while CrV2 did not bind significant amounts of [^{35}S]GTPγS (Fig.7B). This was a good indication that a functional *Drosophila* $G\alpha_o$ subunit had been expressed and purified from *Sf*9 cells. Fig. 7C shows that when

increasing concentrations of purified unlabelled Gα-subunits were added to the TR-FRET assay of CrV2:$G\alpha_{i1}$ interactions, *Drosophila* $G\alpha_o$ competed for binding to CrV2:Alexa at lower concentrations than unlabelled mammalian $G\alpha_{i1}$, with an IC_{50} of 41 nM compared to 241 nM. This indicated that *Drosophila* $G\alpha_o$ had a higher affinity for CrV2 than mammalian $G\alpha_{i1}$ and was the preferred binding partner of the two tested subunits.

Interaction of CrV2 with Gαo confirmed by Far Western blot. To confirm the specific interaction observed by TR-FRET, $G\alpha_o$ was blotted onto a nitrocellulose membrane and was labelled by probing with recombinant CrV2, and then bound CrV2 was detected with anti-CrV2 (Fig. 8). A range of results producing no detection indicated the blotted $G\alpha_o$ was only detectable due to prior CrV2 binding, *viz*: Gα was not detected when CrV2 was absent or when anti-CrV2 was not applied. Furthermore, CrV2 did not bind to bovine serum albumin under the same conditions.

Discussion

CrV2 homologs. The detection of CrV2 homologs in the genomic sequences of *Cc*BV and *Cp*BV, indicates that there is a family of CrV2-related proteins that are expressed by *Cotesia*-associated PDVs (Fig. 1). Two of the proteins (EPL-7 and CcBV_31.9) are hypothetical, their sequences having been directly translated from total virus genome sequences. The third is the confirmed transcript EP2, which like CrV2 transcripts, was detected soon after parasitisation and thought to be immune-suppressive (26,40). Relative to the hypothetical EPL-7 protein, the other homologs have two conserved deletions occurring within the first 100 amino acids of the respective proteins.

Each of the four homologs have identifiable, highly conserved secretion signals (containing a high proportion of hydrophiobic amino acids) at their N-termini, and are predicted to be glycosylated; secreted CrV2 is also detected in large amounts in the hemolymph of parasitised larvae (26,40). It is therefore likely that like CrV2, all of the homologs would be secreted from infected cells. CrV2 protein was also detectable at 24 hours post-parasitization (by antibody staining of hemocytes, and Western analyses of tissues and serum from parasitised larvae). This is in contrast to the CrV2 transcript, which had reduced so as to be undetectable by Northern hybridization as early as 12 hours post-parasitisation (26,41). The large amount of hemocyte-related CrV2 protein at a time where high-level expression is not detected and corresponding (transient) loss of hemocyte immune function, both suggested that these key immune cells are the target for CrV2 (26).

CrV2 was also shown to exist as a trimer in the hemolymph of infected larvae and a C-terminal coiled-coil region (starting approximately at amino acid 270) was predicted to be responsible for the trimeric structure (26). This region is again well conserved, with a large percentage of "redundant" amino acid substitutions occurring between the homologs in this region, indicating that each protein forms polymeric structures in the hemolymph. Therefore, the key functional region is likely to lie within the highly conserved central parts of the amino acid sequence. This could be assessed by generating mutants with targeted amino acid substitutions in that region.

Specific uptake of CrV2 by granuloctytes. Application of CrV2 to hemocytes showed that CrV2 was taken up from surrounding medium. Moreover, the recombinant protein was only associated with a specific type of hemocyte that once attached to the slide surface, display a smaller, more rounded morphology, typical of granulocytes. This suggests that CrV2 targets a particular immune function carried out by granulocytes, that may not occur in plasmatocytes. Infection with PDVs has previously been observed to have effects on a single hemocyte type. Interestingly, Strand and Pech (1995) (42) reported that *Microplitis demolitor* bracovirus induced apoptosis specifically in granulocytes.

However, to date our studies have not shown that the presence of CrV2 results in apoptosis and apoptosis has not been observed in the *Cotesia-Pieris* system.

A specific in vitro interaction between CrV2 and Gα. In this study, we used an established *in vitro* TR-FRET assay (34,35) to identify a novel interaction between the G-protein subunit Gα, and CrV2. We demonstrated that CrV2 binds to Gα subunits from rat and *Drosophila*, with nanomolar affinity (*K*d = 6.2 nM). Far-western analysis also confirmed the presence of a specific interaction with *Drosophila* $G\alpha_o$. There are relatively few proven/proposed Gα-binding proteins and these proteins generally have affinities in the nM range. For example, the TR-FRET assay used here was previously applied to calculate *K*d values of 2.4 nM and 14.6 nM for the interaction of $G\alpha_{i1}$ with Gβγ and RGS4, respectively (34). Other assays have produced comparable results, The mammalian Gβγ:$G\alpha_{i1}$ interaction was shown to have a *K*d of 3 nM using flow cytometry (43). A regulator of G-protein signalling, RGS4 was shown to interact with GTP-activated Gq protein with a *K*d of < 1 nM (44). Ozaki *et al.* (2005) (31) used Surface Plasmon Resonance on immobilised bovine G-protein to calculate *K*d values for the invertebrate proteins tachyplesin and mastoparan (both discussed below), of 880 nM and 220 nM, respectively. Therefore, the high affinity of the CrV2-Gα interaction (*K*d = 6.2 nM for rat $G\alpha_{i1}$) is highly unlikely to occur through chance alone and suggests that the interaction between Gα and CrV2 could also occur *in vivo* as part of immune suppression by *Cr*BV.

A specific interaction is also supported by the finding that the CrV2:Gα interaction can be modulated by AlF_3, which changes the conformation of the Gα subunit to mimic the "transition state" (45,46). This is similar to the association of Gα with Gβγ whereby AlF_3 causes dissociation of the subunits and a decrease in TR-FRET signal and is in contrast to the result seen with RGS4 where an increase in TR-FRET signal with Gα was achieved in the presence of AlF_3 (34). The decrease in signal generated by the interaction of Gα with CrV2, upon the addition of AlF_3 could be a result of the inability of CrV2 to bind to Gα subunits in the transition state or alternatively, a conformational change in the bound CrV2:Gα complex resulting in the donor and acceptor labels being moved further apart and decreasing FRET efficiency (resulting in a lower signal). The fact that AlF_3 does not return the signal to background level could indicate that conformational change or a decrease in affinity is more likely than a complete loss of interaction. The physiological importance of these data is unclear because although commonly employed for this purpose within published literature, the presence of AlF_3 'mimics' an *in vivo* Gα activation state; actual AlF_3-activated Gα proteins do not occur *in vivo*.

It also appears that the binding site of CrV2 could overlap with that of Gβγ since Gβγ can compete with CrV2 for binding to Gα. This may also in part explain the effect of AlF_3 in decreasing the interaction between CrV2 and Gα since AlF_3 changes the conformation of Gα in switch regions known to be important for Gβγ binding (45,46). The fact that CrV2 binds to Gα-subunits from rat and *Drosophila* is not particularly surprising as the two experimental proteins showed a high level of amino acid identity (69%). Analyses of partial Gα amino acid sequences from lepidopteran cell lines has shown that $G\alpha_q$ and $G\alpha_i$ subtypes identical between tested lepidopteran species, were between 88-98% identical to other invertebrates and 88-90% identical to known mammalian subunits (47). Similarly to CrV2, invertebrate proteins mastoparan (from *Vespa* spp. wasps) and tachyplesin (from the horseshoe crab, *Tachypleus tridentatus*), are also known to bind to mammalian G-proteins even though they interact with homologous invertebrate proteins *in vivo* (31,48). CrV2 had a higher affinity for the *Drosophila* protein (Fig. 6c), which could be due to an evolved preference for $G\alpha_o$ rather than $G\alpha_{i1}$ or the invertebrate origin of the protein rather than the mammalian.

Regardless of the reasons for CrV2 interaction with mammalian Gα and the preference for the tested *Drosophila* subunit, these data suggest that is likely physiological importance in the CrV2 interaction with Gα-subunits in insects. However, the specific metabolic consequences of the interaction between CrV2 and $G\alpha_{i1}$ requires further investigation.

G-protein relationship with invertebrate immunity – why would CrV2 target Gα? Most work on G-protein coupled receptors, G-proteins and their associated signal transduction pathways have been conducted in mammalian organisms. In mammals, G-proteins regulate various effectors including enzymes and ion channels to mediate processes in most bodily systems including the nervous, circulatory and immune systems (49). G-proteins are also known to be important signalling molecules in invertebrates but as yet, specific immune-associated biochemical pathways and protein interactions have not been elucidated. However, there is a range of evidence that has indirectly linked invertebrate immunity and G-protein signalling. For example, in the mollusc *Mytilus galloprovinicialis*, corticotrophin-releasing hormone GPCR subtypes are involved with mediating cell shape changes in immunocytes through G-protein pathways (50). Exocytotic responses that release defence related molecules from the intracellular stores of hemocytes are an important part of the immune response of invertebrates in detection of pathogens. The invertebrate *Styela plicata*, induces the release of such molecules through a G-protein pathway where pharmacological reagents known to inhibit G-proteins and tubulin microtubule assembly, decreased the release of C3-like proteins (51). Exocytosis has also been shown to be regulated by G-protein subunits including $G\alpha_i$, $G\alpha_o$, and Gβγ subunits (52,53) and immune pathways are induced by activating adenylate cyclases to produce cyclic AMP (cAMP, or phospholipases to produce IP_3 and diacylglycerol, and cause release of divalent cations to activate protein kinases (27,32), all of which are classical downstream effects of G-proteins. A specific example is data showing that cAMP levels are related to the immune responses of hemocytes in larval lepidopteran insects (29).

There are also other examples of proteins from invertebrates that interact with G-proteins to apparently modulate immune responses. Tachyplesin (discussed above) is a major granular component of hemocytes of the horseshoe crab) and is an antimicrobial peptide with broad spectrum activity against both Gram positive and negative bacteria (30). Moreover, tachyplesin has been found to induce hemocyte exocytosis in a positive feedback mechanism to amplify the immune response to an infection through a G-protein signalling pathway and was also demonstrated to interact directly with a bovine G-protein with a *K*d of 0.88 µM (31,54), which is relatively low in affinity compared to the CrV2 interactions we propose here. A similar process is likely to occur in other invertebrates but as yet, tachyplesin homologs have not been discovered. Tachyplesin shares a number of structural similarities with the wasp venom protein, mastoparan (see above), that has also been found to regulate cellular responses by inducing exocytosis of substances from mammalian cells such as histamine from rat mast cells, serotonin from platelets, catecholamines from chromaffin cells and prolactin from the anterior pituitary (48). As mentioned previously, mastoparan was shown to directly interact with bovine G-proteins (31) and also to increase the GTPase activity and rate of nucleotide exchange to purified bovine $G\alpha_o$ independently of a GPCR (48). Interestingly, mastoparan was also associated with G-protein dysfunction leading to decreased expression of genes associated with LPS-induced (i.e. bacteria-induced) responses of mammalian endothelial and immune cells (28). This is interesting as it represents another example of a wasp-derived protein that interacts with G-proteins from a wide variety of organisms and is associated indirectly with immune regulation.

Concluding remarks. Here we have provided evidence that CrV2 accumulates in a specific type of hemocyte where it would be expected to modulate immune functions. The existence of CrV2 homologs also suggests that CrV2 has an important role in modulating host physiology that is conserved amongst a number of braconid species. We have also shown an *in vitro* interaction at physiologically relevant concentrations of CrV2 with Gα subunits. Although there is indirect evidence that G-proteins are involved in cellular immune cascades in invertebrates, there have not been reports of potentially immune suppressive proteins that interact with G-proteins or their signalling cascades. We therefore propose that CrV2 provides further evidence of the involvement of Gα in insect immune-signalling, and that the interaction between CrV2 and Gα could represent a novel mode-of-action for immune-suppression by PDVs, which are known to express a range of immune-suppressive proteins in parasitised insects (1, 3).

Given this combined evidence for Gα involvement in the immune response of invertebrates, and the data we present here showing nanomolar affinity between the proteins, we hypothesise that CrV2 targets Gα subunits in specific immune cells (granulocytes) to disrupt Gα-associated immune-signalling by these cells. This would likely produce an abrogation of normal immune processes such as exocytosis. Further work establishing the interaction *in vivo* and elucidation of the novel CrV2 mode-of-action will likely be useful in understanding the molecular signalling mechanisms in invertebrate immunology. Such knowledge will be useful for designing non-toxic, immune-related compounds for control of pest insects.

References

1. Webb, B. A., and Strand, M. R. (2005) In *Comprehensive Molecular Insect Science* (Gilbert, L. I., Latrou, K., and Gill, S. S. eds.), Elsevier, San Diego, California. pp 260-323
2. Beckage, N. E., and Gelman, D. B. (2004) *Annu. Rev. Entomol.* **49**, 299-330
3. Kroemer, J. A., and Webb, B. A. (2004) *Annu. Rev. Entomol.* **49**, 431-456
4. Glatz, R. V., Asgari, S., and Schmidt, O. (2004) *Trends Microbiol.* **12**, 545-554
5. Webb, B. A., Beckage, N. E., Hayakawa, Y., Lanzrein, B., Stoltz, D. B., Strand, M. R., and Summers, M. D. (2005) In *8th Report of the International Committee on Taxonomy of Viruses* (Fauquet, C. M., Mayo, M. A., Maniloff, J., Desselberger, U., and Ball, L. A. eds.), Elsevier Academic Press, San Diego, California. pp 255-267
6. Bezier, A., Annaheim, M., Herbiniere, J., Wetterwald, C., Gyapay, G., Bernard-Samain, S., Wincker, P., Roditi, I., Heller, M., Belghazi, M., Pfister-Wilhelm, R., Periquet, G., Dupuy, C., Huguet, E., Volkoff, A.-N., Lanzrein, B., and Drezen, J.-M. (2009) *Science* **323**, 926-930
7. Volkoff, A.-N., Jouan, V., Urbach, S., Samain, S., Bergoin, M., Wincker, P., Demettre, E., Cousserans, F., Provost, B., Coulibaly, F., Legeai, F., Beliveau, C., Cusson, M., Gyapay, G., and Drezen, J.-M. (2010) *PLoS Pathog.* **6**, e1000923. doi:1000910.1001371/journal.ppat.1000923
8. Beckage, N. E. (1998) *Bioscience* **48**, 305-311
9. Stoltz, D. B. (1990) *J. Gen. Virol.* **71**, 1051-1056
10. Stoltz, D. B. (1993) In *Parasites and Pathogens of Insects.* (Beckage, N. E., Thompson, S. N., and Federici, B. A. eds.), Academic Press, New York. pp 80-101
11. Ibrahim, A. M. A., and Kim, Y. (2008) *Naturwissenschaften* **95**, 25-32
12. Kroemer, J. A., and Webb, B. A. (2006) *J. Virol.* **80**, 12219-12228
13. Shi, M., Chen, Y.-F., Huang, F., Liu, P.-C., Zhou, X.-P., and Chen, X. X. (2008) *Virology* **375**, 374-382
14. Barandoc, K. P., and Kim, Y. (2009) *Comp. Biochem. Phys. D* **4**, 218-226
15. Nalini, M., and Kim, Y. (2007) *J. Insect Physiol.* **53**, 1283-1292
16. Beck, M. H., and Strand, M. R. (2007) *Proc. Natl. Acad. Sci. U. S. A.* **104**, 19267-19272
17. Asgari, S., Schmidt, O., and Theopold, U. (1997) *J. Gen. Virol.* **78**, 3061-3070
18. Gitau, C. W., Gundersen-Rindal, D., Predroni, M., Mbugi, P. J., and Dupas, S. (2007) *J. Insect Physiol.* **53**, 676-684
19. Labropoulou, V., Douris, V., Stefanou, D., Magrioti, C., Swevers, L., and Latrou, K. (2008) *Cell. Microbiol.* **10**, 2118-2128
20. Kwon, B., and Kim, Y. (2008) *Dev. Comp. Immunol.* **32**, 932-942
21. Gad, W., and Kim, Y. (2008) *J. Gen. Virol.* **89**, 931-938
22. Glatz, R., Schmidt, O., and Asgari, S. (2003) *J. Biol. Chem.* **278**, 19743-19750
23. Lee, S., Nalini, M., and Kim, Y. (2008) *Comp. Biochem. Phys. A* **149**, 351-361

24. Nalini, M., Choi, J. Y., Je, Y. H., Hwang, I., and Kim, Y. (2008) *J. Insect Physiol.* **54**, 1125-1131

25. Teramoto, T., and Tanaka, T. (2003) *J. Insect. Physiol*. **49**, 463-471

26. Glatz, R., Schmidt, O., and Asgari, S. (2004) *J. General Virol.* **85**, 2873-2882

27. Cytrynska, M., Zdybicka-Barabas, A., and Jakubowicz, T. (2006) *J. Insect Physiol.* **52**, 744-753

28. Lentschat, A., Karahashi, H., Michelsen, K. S., Thomas, L. S., Vogel, S. N., and Arditi, M. (2005) *J. Immunol.* **174**, 4252-4261

29. Marin, D., Dunphy, G. B., and Mandato, C. A. (2005) *J. Insect Physiol.* **51**, 575-586

30. Nakamura, T., Furunaka, H., Miyata, T., Tokunaga, F., Muta, T., Iwanaga, S., Niwa, M., Takao, T., and Shimonishi, Y. (1988) *J. Biol. Chem.* **263**, 16709-16713

31. Ozaki, A., Ariki, S., and Kawabata, S. (2005) *FEBS J.* **272**, 3863-3871

32. Solon, E., Gupta, A. P., and Gaugler, R. (1996) *Dev. Com.p Immunol.* **20**, 307-321

33. Oldham, W. M., and Hamm, H. E. (2008) *Nat. Rev. Mol. Cell. Biol.* **9**, 60-71

34. Leifert, W. R., Bailey, K., Cooper, T. H., Aloia, A. L., Glatz, R. V., and McMurchie, E. J. (2006) *Anal. Biochem.* **355**, 201-212

35. Blazer, L. L., Roman, D. L., Chung, A., Larsen, M. J., Greedy, B. M., Husbands, S. M., and Neubig, R. R. (2010) *Mol. Pharmacol.* **78**, 524-533

36. Selvin, P. R. (2002) *Annu. Rev. Bioph. Biom.* **31**, 275-302

37. Nishioka, T., Yuan, J., and Matsumoto, K. (2007) In *BioMEMS and Biomedical Nanotechnology*, Vol. III (Ferrari, M., Ozkan, M., and Heller, M. J. eds.), Springer US. pp 437-446

38. Roda, A., Guardigli, M., Michelini, E., and Mirasoli, M. (2009) *Anal Bioanal Chem* **393**, 109-123

39. Bradford, M. (1976) *Anal. Biochem.* **72**, 248-254

40. Harwood, S. H., and Beckage, N. E. (1994) *Insect Biochem. Mol. Biol.* **24**, 685-698

41. Asgari, S., Hellers, M., and Schmidt, O. (1996) *J. Gen. Virol*. **77**, 2653-2662

42. Strand, M. R., and Pech, L. L. (1995) *J. Gen.Virol.* **76**, 283-291

43. Sarvazyan, N. A., Remmers, A. E., and Neubig, R. R. (1998) *J. Biol. Chem.* **273**, 7934-7940

44. Dowal, L., Elliot, J., Popov, S., Wilkie, T. M., and Scarlata, S. (2001) *Biochemistry-US* **40**, 414-421

45. Wall, M. A., Posner, B. A., and Sprang, S. R. (1998) *Structure* **6**, 1169-1183

46. Sondek, J., Lambright, D. G., Noel, J. P., Hamm, H. E., and Sigler, P. B. (1994) *Nature* **372**, 276-279

47. Knight, P. J. K., and Grigliatti, T. A. (2004) *Arch. Insect. Biochem.* **57**, 142-150

48. Higashijima, T., Uzu, S., Nakajima, T., and Ross, E. M. (1988) *J Biol Chem* **263**, 6491-6494

49. Offermanns, S. (2003) *Prog. Biophys. Mol. Bio.* **83**, 101-130

50. Malagoli, D., Franchini, A., and Ottaviani, E. (2000) *Peptides* **21**, 175-182

51. Raftos, D. A., Fabbro, M., and Nair, S. V. (2004) *Dev. Comp. Immunol*. **28**, 181-190

52. Lang, J., Nishimoto, I., Okamoto, T., Regazzi, R., Kiraly, C., Weller, U., and Wollheim, C. B. (1995) *EMBO J.* **14**, 3635-3644

53. Blackmer, T., Larsen, E. C., Bartleson, C., Kowalchyk, J. A., Yoon, E. J., Preininger, A. M., Alford, S., Hamm, H. E., and Martin, T. F. J. (2005) *Nat. Neurosci.* **8**, 421-425

54. Kurata, S., Ariki, S., and Kawabata, S. (2006) *Immunobiology* **211**, 237-249

FOOTNOTES

We thank Prof. Rick Neubig (University of Michigan) for the provision of His-Gα_{i1}, His-Gγ_2, Gα_{i1} and Gγ_2 baculoviruses and Prof. James Garrison, (University of Virginia) for the provision of Gβ_4/Gβ_1 baculovirus stocks. This work was supported by the OzNano2Life research initiative of the Australian Department of Education, Science and Technology, CSIRO's Emerging Science Area for Nanotechnology funding Scheme, an Australian Research Council grant (F09943013), a University of Queensland grant to S. Asgari, and a Horticulture Australia Ltd. Grant (VG08048) to R. Glatz.

FIGURE LEGENDS

Fig. 1. A CrV2 gene-family exists in *Cotesia*-associated bracoviruses. ClustalW2 software was used to align CrV2 against 3 putative homologs detected via protein Blast. Amino acid numbers are presented at the end of each line of sequence. Proteins are as follows: EPL-7 = hypothetical protein from *Cp*BV genome sequence (GenBank accession no. ABK63352), CrV2 = CrV2 expressed by *Cr*BV (GenBank accession no. AY631272), EP2 = EP2 expressed by *Cc*BV (GenBank accession no. AJ632305), CcBV_31.9 = putative protein from *Cc*BV genome sequence (GenBank accession no. YP184881). The alignment is presented in order of increasing size of the first deletion common to three genes, but absent from hypothetical EPL-7 protein. There is another conserved deletion downstream of the first, (relative to hypothetical EPL-7 protein) in the central region of the protein. The high level of conservation indicates that the four genes are homologous. Consensus symbols follow convention of ClustalW2 software: * = complete conservation, : = conserved substitution, . = semi-conserved substitutions.

Fig. 2. Uptake of CrV2 by specific *Pieris rapae* hemocytes. *Pieris* larvae were bled into media saturated with PTU, the hemocytes were applied to the wells of a glass slide and allowed to adhere and spread. CrV2 in media was then applied to the cells and incubated for 45 min. A) Merged image of brightfield and red fluorescence from TRITC secondary antibody bound to anti-CrV2 shows CrV2 associated with the small round hemocytes. B) Merged blue and red fluorescence images showing the nucleus (blue) stained with DAPI and CrV2 (red). C) Merged blue, red and green fluorescent image showing the nucleus (blue), CrV2 (red) and the cytoskeleton stained with FITC conjugated phalloidin (green).

Fig.3. CrV2:Alexa association with Gα_{i1}:Tb increases TR-FRET to saturation while treatment with proteinase K abolishes TR-FRET.
TR-FRET measurements were taken using a Victor3 plate reader set for time-resolved fluorescence with the following parameters: λ_{ex} 340 nm, λ_{em} 572 nm, 50 µs delay and 900 µs counting duration. (A) 10 nM Gα_{i1}:Tb (■) was mixed with 20 nM (▲), 40 nM (●) or 100 nM (◆)

CrV2:Alexa. Data shown are mean (n=2). (B) 10 nM $G\alpha_{i1}$:Tb was mixed with increasing concentrations (0-40 nM) of CrV2:Alexa and TR-FRET measured following 10 min incubation. The background from 10 nM Gαi1:Tb has been deducted and an apparent dissociation constant (*K*d) of 6.2 nM was calculated. Data shown are mean ± SEM (n=3). (C) 10 nM $G\alpha_{i1}$:Tb was mixed with 20 nM CrV2:Alexa ± 0.1 mg/ml proteinase K. After an incubation period of 30 min at 37 ºC, TR-FRET measurements were taken. Data shown are mean ± SEM (n=3) of the ratio of acceptor emission: donor emission.

Fig. 4. Unlabelled binding partners compete with $G\alpha_{i1}$:Tb for binding to CrV2:Alexa.
TR-FRET measurements were taken with the following parameters: λ_{ex} 340 nm, λ_{em} 572 nm, 50 µs delay and 900 µs counting duration. (A) Unlabelled $G\alpha_{i1}$ competes for binding to CrV2:Alexa reducing the TR-FRET signal. (B) Unlabelled CrV2 competes for binding to $G\alpha_{i1}$:Tb reducing the TR-FRET signal. For (A) and (B) 10 nM $G\alpha_{i1}$:Tb was mixed with 20 nM CrV2:Alexa in 100 µl of TMN buffer. At 5 min, 2 µM of unlabelled $G\alpha_{i1}$ or 70 nM of unlabelled CrV2 (■) or an equivalent volume of TMN buffer (▲) was added and TR-FRET measurements over the shown time period. Backgrounds of 10 nM $G\alpha_{i1}$:Tb with buffer added at 5 min (●) and 10 nM $G\alpha_{i1}$:Tb + the indicated unlabelled protein (◆) are shown. Data shown are mean (n=2). (C) $G\beta_4\gamma_2$ inhibits CrV2:Alexa association with $G\alpha_{i1}$:Tb. 10 nM $G\alpha_{i1}$:Tb was mixed with 20 nM CrV2:Alexa with or without 240 nM $G\beta_4\gamma_2$ in 100 µl of TMN buffer. Backgrounds of $G\alpha_{i1}$:Tb and $G\alpha_{i1}$:Tb + $G\beta_4\gamma_2$ have been deducted as appropriate. Data shown are mean (n=2).

Fig. 5. CrV2:Alexa interacts only minimally with Gβγ:Tb.
10 nM Gβγ:Tb was mixed with 20 nM CrV2:Alexa or 10 nM $G\alpha_{i1}$:Alexa to a final volume of 100 µl with TMN buffer. TR-FRET measurements were taken with the following parameters: λ_{ex} 340 nm, λ_{em} 572 nm, 50 µs delay and 900 µs counting duration over the shown time period. Data shown are mean (n=2).

Fig. 6. Alteration of the activation state of $G\alpha_{i1}$ using aluminium fluoride decreases the interaction with CrV2. 10 nM $G\alpha_{i1}$:Tb was mixed with 20 nM CrV2:Alexa with excess amounts of GDP (2.5 µM) or aluminium fluoride produced by the addition of NaF (10 mM) and $AlCl_3$ (30 µM). TR-FRET measurements were immediately taken with the following parameters: λ_{ex} 340 nm, λ_{em} 572 nm, 50 µs delay and 900 µs counting duration. Background of $G\alpha_{i1}$:Tb with GDP or aluminium fluoride has been deducted. Data shown are mean ± SEM (n=3).

Fig. 7. *Drosophila* $G\alpha_o$ purified from *Sf*9 cells, binds to [^{35}S]GTPγS and competes for binding to CrV2. (A) Polyacrylamide gel showing eluted fractions of *Drosophila* $G\alpha_o$ from 1.7 litres of infected cells purified using Ni-NTA chromatography. (B) 40 nM of Gα or CrV2 was mixed with 1 nM [^{35}S]GTPγS in a final volume of 100 µl of TMN buffer and incubated in a shaking water bath for 90 min at 27°C. 25 µl was then filtered through GFC filters and unbound [^{35}S]GTPγS removed by washing with TMN buffer. The amount of bound [^{35}S]GTPγS was then measured by scintillation counting. Data shown are mean ± SEM (n=6) of filter triplicates of 2 experiments. (C) CrV2:Alexa binds preferentially to *Drosophila* $G\alpha_o$ when 20 nM CrV2:Alexa was mixed with 20 nM mammalian $G\alpha_{i1}$:Tb and doses (0-900 nM) of unlabelled *Drosophila* $G\alpha_o$ (■) or mammalian $G\alpha_{i1}$ (▼) were added to compete with labelled proteins. TR-FRET measurements were taken with the following parameters: λ_{ex} 340 nm, λ_{em} 572 nm, 50 µs delay and 900 µs counting duration over the shown time period. Data shown are mean ± SEM (n=3).

Fig. 8. Far Western blot confirms $G\alpha_o$ interaction with CrV2. (A) Coomassie stained gel of $G\alpha_o$ (right lane) run by SDS-PAGE with molecular weight marker (Bio-Rad precision plus dual colour protein standard) in left lane. (B) Duplicate samples of (A) transferred to nitrocellulose and probed with CrV2. CrV2 binding was detected using rabbit anti-CrV2 and alkaline phosphatase conjugated secondary antibody. CrV2 bound to the band of $G\alpha_o$ but did not bind to BSA under the same conditions (data not shown). $G\alpha_o$ was not detected when probe CrV2 or anti-CrV2 was absent (data not shown).

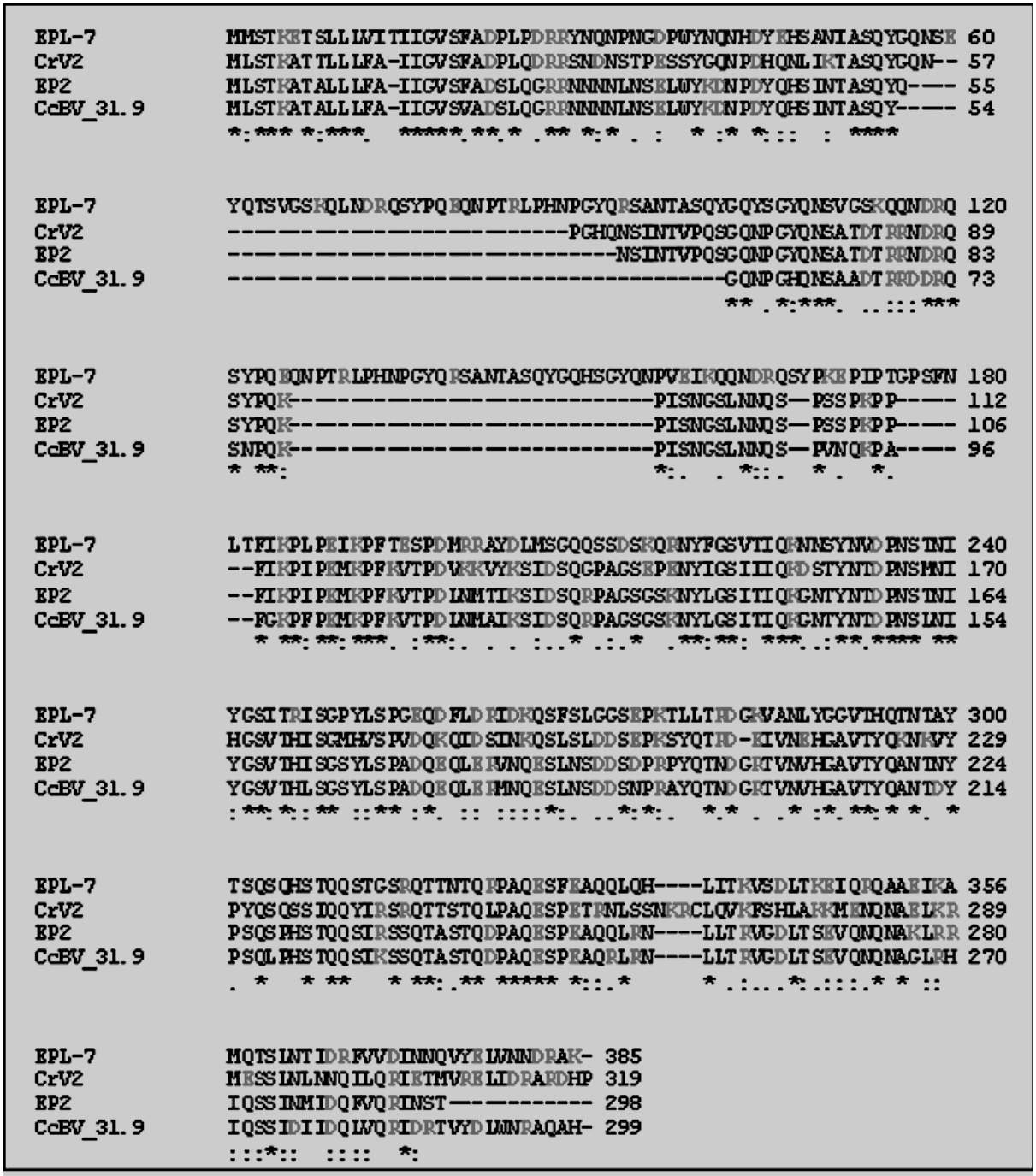
EPL-7 MMSTKETSLLLVITIIGVSFADPLPDRRYNQNPNGDPWYNQNHDYKHSANIASQYGQNSE 60
CrV2 MLSTKATTLLLFA-IIGVSFADPLQDRRSNDNSTPESSYGQNPDHQNLIKTASQYGQN-- 57
EP2 MLSTKATALLLFA-IIGVSFADSLQGRRNNNNLNSELWYKDNPDYQHSINTASQYQ---- 55
CcBV_31.9 MLSTKATALLLFA-IIGVSVADSLQGRRNNNNLNSELWYKDNPDYQHSINTASQY----- 54
EPL-7 YQTSVGSKQLNDRQSYPQEQNPTRLPHNPGYQRSANTASQYGQYSGYQNSVGSKQQNDRQ 120
CrV2 ----------PGHQNSINTVPQSGQNPGYQNSATDTRRNDRQ 89
EP2 ----------NSINTVPQSGQNPGYQNSATDTRRNDRQ 83
CcBV_31.9 ----------GQNPGHQNSAADTRRDDRQ 73
EPL-7 SYPQEQNPTRLPHNPGYQRSANTASQYGQHSGYQNPVKIKQQNDRQSYPKEPIPTGPSFN 180
CrV2 SYPQK----------PISNGSLNNQS—PSSPKPP----- 112
EP2 SYPQK----------PISNGSLNNQS—PSSPKPP----- 106
CcBV_31.9 SNPQK----------PISNGSLNNQS—PVNQKPA----- 96
EPL-7 LTFIKPLPEIKPFTESPDMRRAYDLMSGQQSSDSKQRNYPGSVTIQRNNSYNVDRNSTNI 240
CrV2 --FIKPIPKMKPFKVTPDVKKVYKSIDSQGPAGSEPENYIGSIIIQKDSTYNTDRNSMNI 170
EP2 --FIKPIPKMKPFKVTPDLNMTIKSIDSQRPAGSGSKNYLGSITIQKGNTYNTDRNSTNI 164
CcBV_31.9 --FGKPFPKMKPFKVTPDLNMAIKSIDSQRPAGSGSKNYLGSITIQKGNTYNTDRNSLNI 154
EPL-7 YGSITRISGPYLSPGEQDFLDRIDRQSFSLGGSEPKTLLTRDGKVANLYGGVIHQTNTAY 300
CrV2 HGSVTHISGMHVSPVDQKQIDSINKQSLSLDDSEPKSYQTRD-KIVNEHGAVTYQKNKVY 229
EP2 YGSVTHISGSYLSPADQEQLERVNQESLNSDDSDPRPYQTNDGKTVNVHGAVTYQANTNY 224
CcBV_31.9 YGSVTHLSGSYLSPADQEQLERMNQESLNSDDSNPRAYQTNDGKTVNVHGAVTYQANTDY 214
EPL-7 TSQSQHSTQQSTGSRQTTNTQRPAQESFEAQQLQH----LITKVSDLTKEIQRQAAEIKA 356
CrV2 PYQSQSSIQQYIRSRQTTSTQLPAQESPETRNLSSNKRCLQVKFSHLAKKMKNQNAELKR 289
EP2 PSQSPHSTQQSIRSSQTASTQDPAQESPEAQQLRN----LLTKVGDLTSEVQNQNAKLRR 280
CcBV_31.9 PSQLPHSTQQSIKSSQTASTQDPAQESPEAQRLRN----LLTKVGDLTSEVQNQNAGLRH 270
EPL-7 MQTSINTIDRFVVDINNQVYEIVNNDRAK- 385
CrV2 MESSINLNNQILQRIETMVRELIDRARDHP 319
EP2 IQSSINMIDQFVQRINST---------- 298
CcBV_31.9 IQSSIDIIDQIVQRIDRTVYDLVNRAQAH- 299

Figure 1

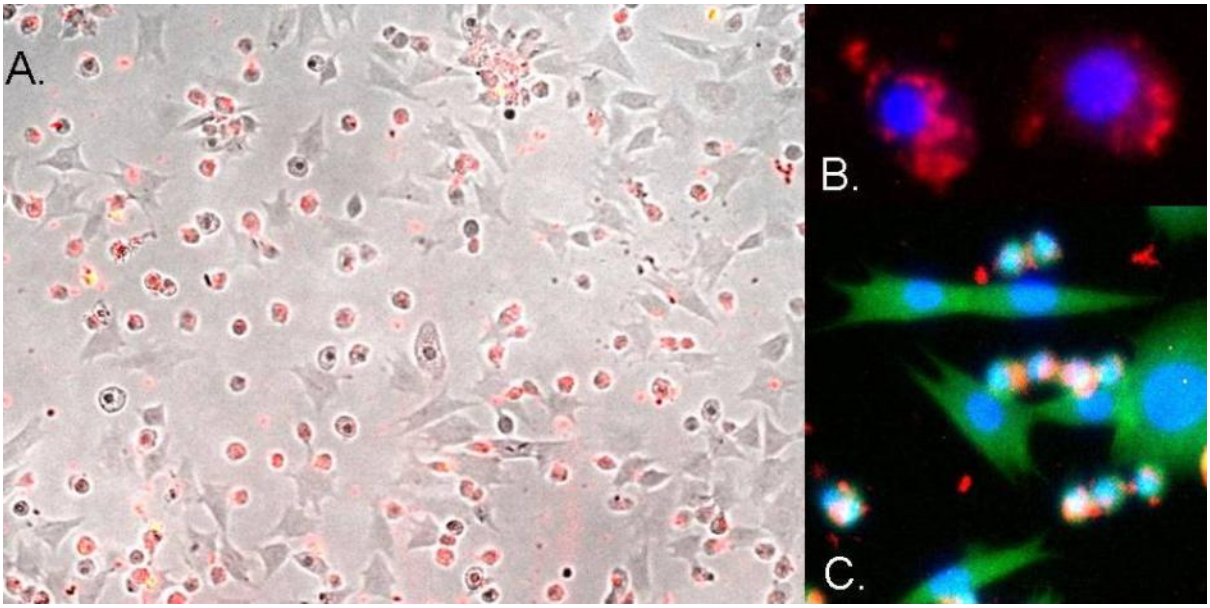

Figure 2

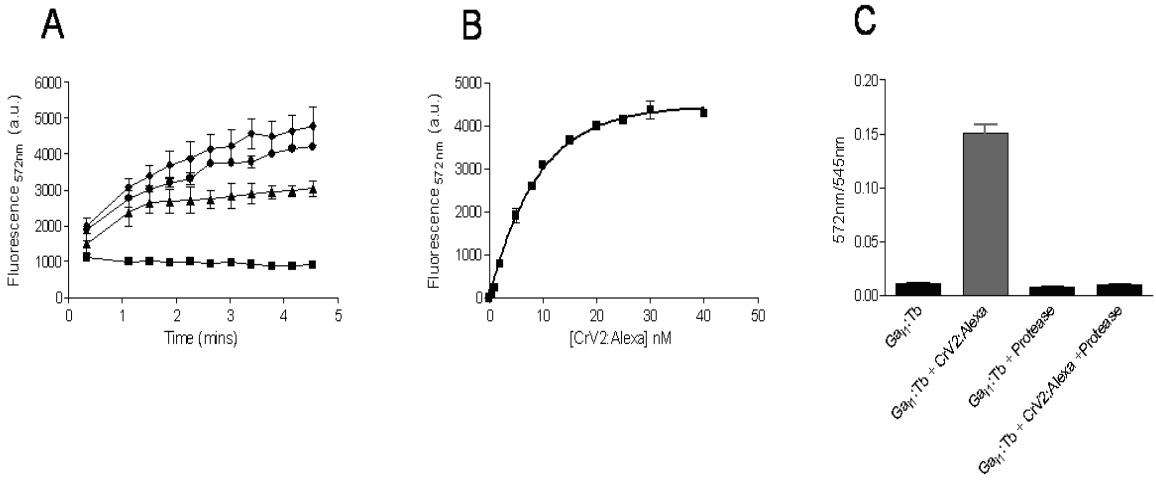

Figure 3

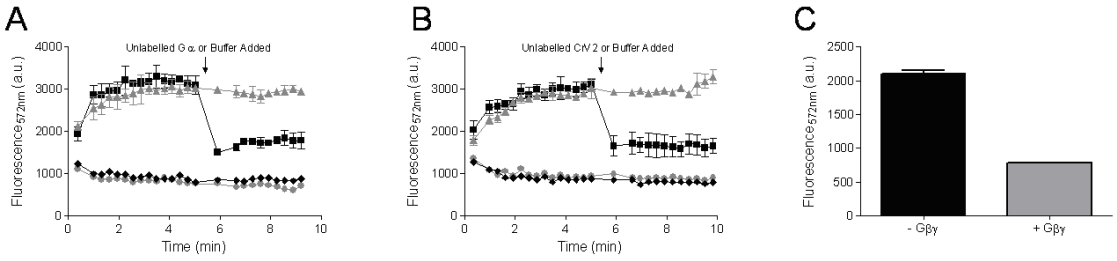

Figure 4

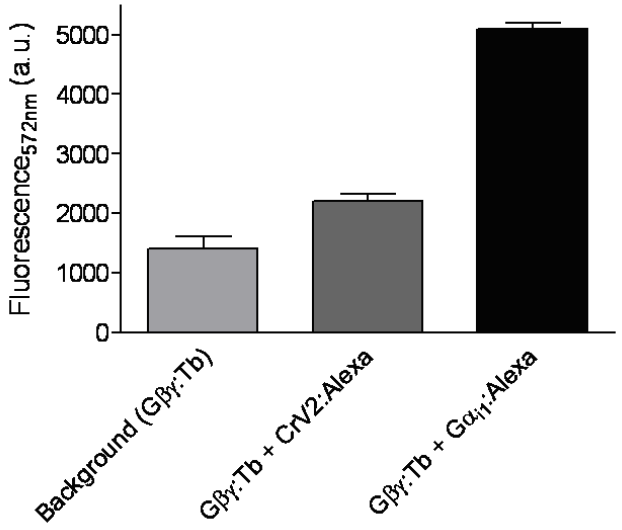

Figure 5

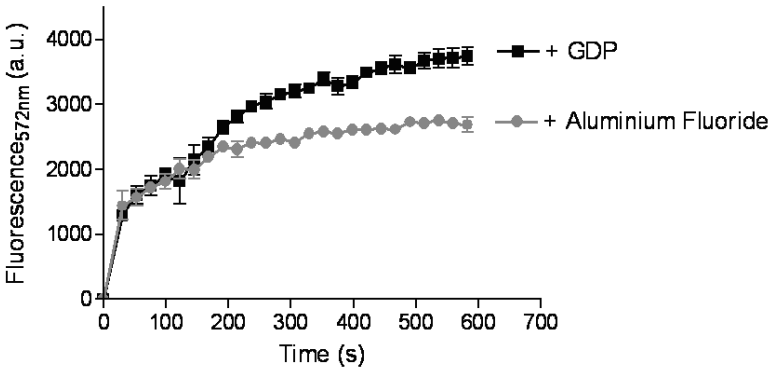

Figure 6

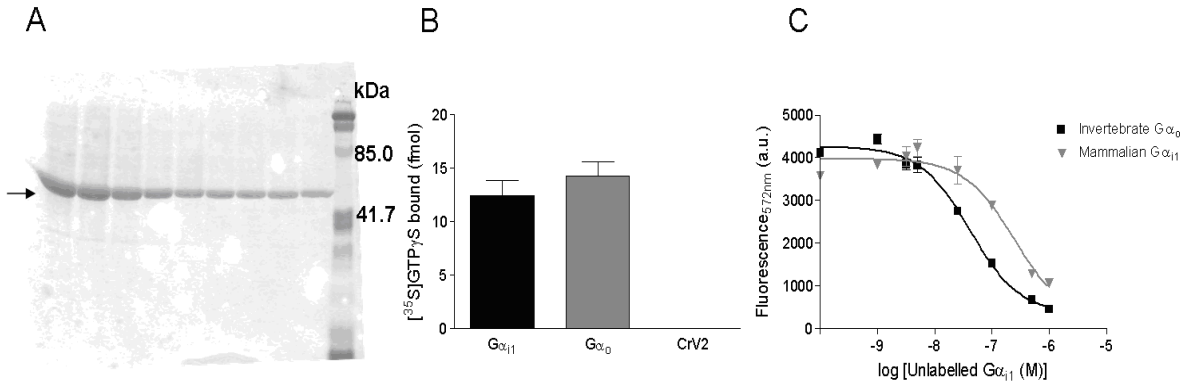

Figure 7

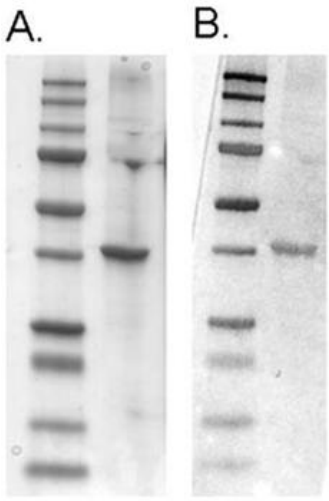

Figure 8

APPENDIX B

HAL Vegetable Industry Report 2008-2009. *Immune suppressors to manage diamondback moth (DBM).*

Immune suppressors to manage diamondback moth (DBM)

Suppressing immunity is the latest strategy being researched in the quest to control Diamondback moth (DBM) in Australia, as an alternative to the poisoning strategy of current pesticides. DBM is the main pest of brassica species and has already developed resistance to a range of insecticides.

Immune-suppressing compounds are expected to be present in the venom of *Diadegma semiclausum*, a beneficial parasitoid wasp that is an important biological control agent of DBM.

D. semiclausum deposits its egg into a DBM larva along with its venom, which plays a role in suppressing the immune responses of the parasitised DBM and manipulating other aspects of DBM physiology.

In the first six months of the project several genes believed to produce venom proteins have been identified. The next steps are to prove that these genes produce venom proteins and manufacture the individual proteins for analysis of their function.

Project VG08048

For more information contact:
Richard Glatz, SARDI
T 08 8303 9539
E richard.glatz@sa.gov.au

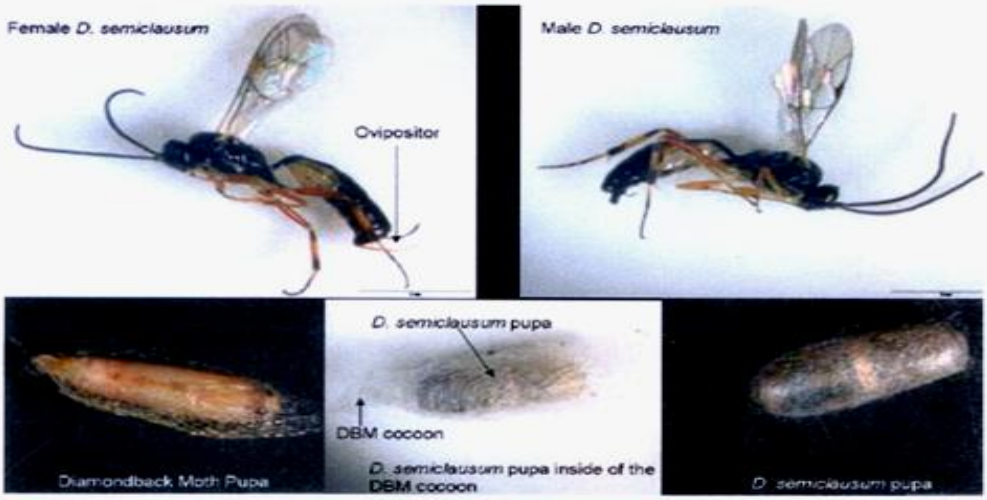

The parasitic wasp *Diadegma semiclausum* attacks the key pest of Brassica vegetables. Top: adult *Diadegma* wasps. Bottom: pupae of DBM and *D. semiclausum*.

Reproductive organs of adult female Diadegma semiclausum wasps. Venom (made of various proteins) is produced in cells of the venom glands and secreted into the venom sac where it is stored. The ovaries (containing wasp eggs) are seen at the right of the picture. When the female wasp lays an egg into a Diamondback moth (DBM) larva, venom is also injected along with the egg. The venom proteins are thought to suppress DBM immunity thus preventing the wasp egg from being destroyed by the DBM immune system.

40

APPENDIX C

Brassica IPM National Newsletter, Issue 13, October 2009.

***Investigation of immune suppressors of Diamond-back moth*.**

INVESTIGATION OF IMMUNE SUPPRESSORS OF DIAMOND-BACK MOTH (DBM)

Dr Tamara Cooper and Dr Richard Glatz (SARDI)

Postdoctoral fellow Dr Tamara Cooper from (SARDI) is conducting research under the supervision of Dr. Richard Glatz (SARDI) and Dr. Sassan Asgari (University of Queensland). The research is aimed at understanding the properties of parasitoid (wasp) venom and the potential benefits it may have to help control insect pests

The wasp parasitoid Diadegma semiclausum (Ichneumonidae) is an important biological control agent of Diamondback moth (DBM), Plutella xylostella (L.). Successful parasitism of DBM by D. semiclausum results in the wasp egg being injected (oviposited) into the larvae. This egg hatches and the developing wasp larvae consumes the DBM larvae from the inside out. It then pupates and emerges as a mature wasp (Figure 1). Adults are distinctive and their pupae can be distinguished from DBM pupae as they have rounded ends (bullet shaped), often inside of the more loosely woven DBM cocoon that have pointed ends (Figure 1).

When D. semiclausum oviposits its egg into a DBM larvae it also injects virus particles (polydnavirus) and venom. The parasitoid polydnavirus and venom work to mediate successful development of the wasp larvae inside the DBM host by suppressing host immune responses and manipulating host physiology and development. The venom from D. semiclausum is expected to contain a number of proteins that are secreted from the venom gland and stored in the venom sac (Figure 2) until oviposition.

A number of molecular biology techniques will be used to identify the proteins in D. semiclausum venom. The first part of the project involves identifying the DNA that encodes the venom proteins which can then be isolated and manipulated so that larger amount of the resulting venom proteins can be produced in bacteria. The proteins produced from this DNA are confirmed as being present in the venom in part, by using antibodies that have been raised against the venom in a rabbit. The next step is to use the purified proteins for further experiments to determine their function. This step will help to characterise the identified venom proteins with regard to their individual effects on DBM and the molecular pathways through which they act.

Ultimately, this research could lead to the identification of protein molecules with new insecticidal activity that could be applied to manage horticultural pests such as DBM, and or molecules that could have useful pharmaceutical properties. Understanding the mechanisms of venom action may also lead to the identification of new target sites for insecticides within DBM. The success of venom in mediating parasitism may mean that using such target sites will make it harder for DBM to develop resistance. It is anticipated that a number of the findings from this project will be directly relevant to and could be adapted for other moth pests.

This project titled "Investigation of Immune Suppressors of DBM" is a joint research effort between the South Australian Research and Development Institute (SARDI) and University of Queensland (UQ) and is funded by Horticulture Australia Ltd.

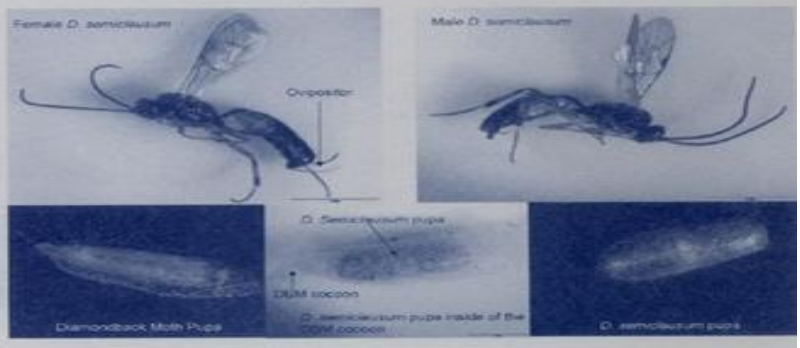

Figure 1: D. semiclausum adults and comparison of a DBM pupa with a D. semiclausum pupa

INVESTIGATION OF IMMUNE SUPPRESSORS OF DIAMOND-BACK MOTH (DBM) *continued*

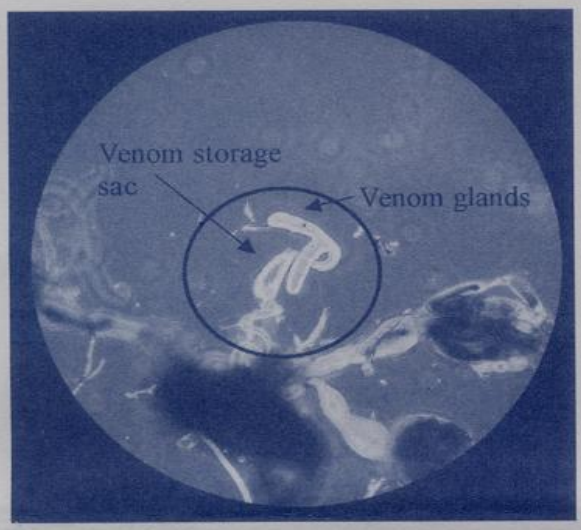

Figure 2: Reproductive organs of adult female Diadegma semiclausum wasps. (photo by Dr. Sassan Asgari, collaborator, University of Queensland). Venom (made of various proteins) is produced in cells of the venom glands and secreted into the venom sac where it is stored. The ovaries (containing wasp eggs) are seen at the right of the picture. When the female wasp lays an egg into a (DBM) larva, venom is also injected along with the egg. The venom proteins are thought to suppress DBM immunity thus preventing the wasp egg from being destroyed by the DBM immune system.

Scientists working on the project "Identification of immune-suppressors of Diamond-back moth (DBM)". From left: Dr Richard Glatz (Project Leader; SARDI), Dr Sassan Asgari (Expert Collaborator; University of Queensland) and Dr Tamara Cooper (Principle Investigator; SARDI).